Evaluation of Global Climate Models for Use in Energy Analysis

Grant Buster,[1] Slater Podgorny,[1] Laura Vimmerstedt,[1] Brandon Benton,[1] and Nicholas D. Lybarger[2]

1 National Renewable Energy Laboratory
2 U.S. National Science Foundation National Center for Atmospheric Research

NREL is a national laboratory of the U.S. Department of Energy
Office of Energy Efficiency & Renewable Energy
Operated by the Alliance for Sustainable Energy, LLC

This report is available at no cost from the National Renewable Energy Laboratory (NREL) at www.nrel.gov/publications.

Contract No. DE-AC36-08GO28308

Technical Report
NREL/TP-6A20-90166
August 2024

Evaluation of Global Climate Models for Use in Energy Analysis

Grant Buster,[1] Slater Podgorny,[1] Laura Vimmerstedt,[1] Brandon Benton,[1] and Nicholas D. Lybarger[2]

1 National Renewable Energy Laboratory
2 U.S. National Science Foundation National Center for Atmospheric Research

Suggested Citation
Buster, Grant, Slater Podgorny, Laura Vimmerstedt, Brandon Benton, and Nicholas D. Lybarger. 2024. *Evaluation of Global Climate Models for Use in Energy Analysis*. Golden, CO: National Renewable Energy Laboratory. NREL/TP-6A20-90166. https://www.nrel.gov/docs/fy24osti/90166.pdf.

NREL is a national laboratory of the U.S. Department of Energy
Office of Energy Efficiency & Renewable Energy
Operated by the Alliance for Sustainable Energy, LLC

This report is available at no cost from the National Renewable Energy Laboratory (NREL) at www.nrel.gov/publications.

Contract No. DE-AC36-08GO28308

Technical Report
NREL/TP-6A20-90166
August 2024

National Renewable Energy Laboratory
15013 Denver West Parkway
Golden, CO 80401
303-275-3000 • www.nrel.gov

NOTICE

This work was authored [in part] by the National Renewable Energy Laboratory, operated by Alliance for Sustainable Energy, LLC, for the U.S. Department of Energy (DOE) under Contract No. DE-AC36-08GO28308. Funding provided by the DOE Office of Energy Efficiency and Renewable Energy (EERE), the DOE Office of Electricity (OE), the DOE Office of Fossil Energy and Carbon Management (FECM), and the DOE Office of Cybersecurity, Energy Security, and Emergency Response (CESER). The views expressed herein do not necessarily represent the views of the DOE or the U.S. Government.

Cover Photos by Dennis Schroeder: (clockwise, left to right) NREL 51934, NREL 45897, NREL 42160, NREL 45891, NREL 48097, NREL 46526.

Table of Contents

List of Figures

List of Tables

1 Abstract

The interplay between energy, climate, and weather is becoming more complex due to increasing contributions of renewable energy generation, energy storage, electrified end uses, and the increasing frequency of extreme weather events. Energy system analyses commonly rely on meteorological inputs to estimate renewable energy generation and energy demand; however, these inputs rarely represent the estimated impacts of future climate change. Climate models and publicly available climate change datasets can be used for this purpose, but the selection of inputs from the myriad of available models and datasets is a nuanced and subjective process. In this work, we assess datasets from various global climate models (GCMs) from the Coupled Model Intercomparison Project Phase 6 (CMIP6). We present evaluations of their skills with respect to the historical climate and comparisons of their future projections of climate change for two climate change scenarios. We present the results for different climatic and energy system regions and include interactive figures in the accompanying software repository. Previous work has presented similar GCM evaluations, but none have presented variables and metrics specifically intended for comprehensive energy systems analysis including impacts on energy demand, thermal cooling, hydropower, water availability, solar energy generation, and wind energy generation. We focus on GCM output meteorological variables that directly affect these energy system components including the representation of extreme values that can drive grid resilience events. The objective of this work is not to recommend the best climate model and dataset for a given analysis, but instead to provide a reference to facilitate the selection of climate models and scenarios in subsequent work.

2 Introduction

Energy system analyses commonly use historical weather datasets as input to energy generation and demand models (Brinkman et al. 2021; Carvallo et al. 2023; Stenclik et al. 2021; Sharp et al. 2023). Recently, more work has started to incorporate the impacts of climate change on these inputs (Bloomfield et al. 2016; Yalew et al. 2020; Craig et al. 2018). GCMs and their associated publicly-available datasets from CMIP6 are a valuable resource for estimating the impacts of climate change (Eyring et al., 2016). However, there are a myriad of unique GCMs developed by climate research institutions around the world. Each GCM is unique in its physical and parametric formulations, its skill in representing historical climate in different geographies, and its sensitivity to anthropogenic greenhouse gas emissions (Flato et al., 2013). For example, a given GCM may represent a variable in the historical climate with great precision but may be greatly biased in several other variables (further discussed in Section 4). To further complicate the topic, CMIP6 includes several possible climate change scenarios that attempt to characterize deeply uncertain human factors related to the developmental progress of civilization and our continued emissions. Scenarios have been developed that project decreases in emissions by mid-century, and others that project emissions decreasing only near the end of the century (Riahi et al., 2017). Experts and quantitative models alike have perspectives on which scenarios are more likely (Hausfather & Peters 2020), but we cannot know with certainty which future we will experience.

Prior work studying climate change in applied impact studies has handled these nuances through the following process: 1) compare data from various GCMs with historical reference datasets to identify those that best represent historical climate 2) select one or more GCMs with good

historical skill and climate change scenarios that encompass a range of possible climate futures, 3) downscale the low-resolution GCM data for applied studies (when required by high-resolution applications), and 4) perform the subsequent applied analysis using domain-specific models (Kao et al., 2022; Ralston Fonseca et al., 2021). The comparison and selection of inputs from GCMs and climate scenarios (steps #1 and #2) is a nuanced process that commonly includes the quantitative comparison of GCM datasets using a few selected metrics over a focused region of interest (Parding et al., 2020; Ashfaq et al., 2022; Chhin et al., 2018). However, the selection of GCMs, climate scenarios, and comparative metrics are ultimately subjective decisions and represent value judgements in a challenging analytical process with no objectively best methodology. Further, the impacts of climate change are being studied in an increasingly wide range of applications and this comparison and selection process is often very specific to a given application.

This report focuses on supporting the GCM comparison and selection process specifically for energy applications in the Contiguous United States (CONUS). Previous work has presented similar GCM evaluations, but none have presented variables and metrics specifically intended for comprehensive energy systems analysis including impacts on energy demand, thermal cooling, hydropower, water availability, solar energy generation, and wind energy generation (Parding et al., 2020; Ashfaq et al., 2022; Martinez & Iglesias, 2022). Those that have focused on some aspect of energy impacts have typically focused on one variable or another such as climate impacts to hydropower or wind energy (Martinez & Iglesias, 2022), but none have presented metrics for variables that represent the full energy generation and demand system. This report is intended to fill that gap and facilitate more informed selections of climate change inputs for comprehensive energy analyses.

This report is structured as follows. Section 3 details the datasets used in this report and the methods used for GCM evaluation; Section 4 presents and discusses the results of the GCM skill evaluation and the comparison of their projections for the Contiguous United States (CONUS); Section 5 concludes the report; The appendices present similar results to Section 4 but for specific subregions within the larger CONUS domain.

3 Data and Methods

This report leverages publicly available climate change projections from GCMs in the CMIP6 archive and historical data from reference and reanalysis datasets. First, we explore the available datasets associated with each GCM in the CMIP6 archive and determine which datasets are viable for energy systems analysis.

For the purposes of this work, we look for GCM datasets that are of current state-of-the-art spatiotemporal resolution (e.g., 100km daily), that contain all variables necessary to model energy generation and demand (e.g., temperature, humidity, precipitation, wind speed, and solar irradiance), and that have public records in the CMIP6 archive for several key simulations. Note that different downscaling methodologies (e.g., dynamical downscaling with regional climate models, RCMs) may require variables other than those presented here. However, we still focus on this subset because they have direct impacts on the energy system.

For this work, we selected the CMIP6 historical simulation that is intended to represent the historical and current climate, and two Shared Socioeconomic Pathways (SSPs): SSP2 4.5, and SSP5 8.5. Note that these SSPs have corresponding Relative Concentration Pathway (RCP) scenarios from CMIP5. We selected the first variant from each GCM except for CESM2 and CESM2-WACCM which had other variants with more complete data availability. For the comparison of future projections, we select data from SSP2 4.5 and SSP5 8.5. We select these two scenarios because of the extensive use of these scenarios in prior climate impacts analysis (Craig et al., 2020; Kao et al., 2022; Ralston Fonseca et al., 2021; Martinez & Iglesias 2022). SSP2 4.5 is typically described as a "middle-of-the-road" emissions scenario where trends generally follow a dynamics-as-usual scenario, while SSP5 8.5 is an aggressive high-growth and high fossil fuel future with the most overall emissions of any scenario (Riahi et al., 2017).

To inform energy system analyses in which decisions on energy infrastructure are being made today and in the coming several decades, we focus on projections from the historical climate through mid-century (e.g., through 2059). Despite the significantly different emission trajectories in SSP2 4.5 and SSP5 8.5, the two scenarios vary only slightly by mid-century (as shown in Section 4) with a more dramatic bifurcation occurring in the latter half of the century.

After surveying 33 GCMs with data in CMIP6, we select 13 GCMs that have publicly available data that meet the above criteria. A summary of this process, the GCMs evaluated, and the GCMs selected is presented in Table 1 below.

GCMs that did not meet the criteria for this work may have additional variables and scenarios available from different data archives. These GCMs may be useful for climate impact studies, but based on their datasets available in the CMIP6 archive they were not used in this work.

Table 1. Summary of GCMs surveyed and used in this report.

GCM Name	Used	Notes and Reference
AWI-CM-1-1-MR	No	Historical simulation does not include irradiance, precipitation, or humidity (Semmler et al., 2019).
ACCESS-CM2	No	SSP data is low spatial resolution (Dix et al., 2019).
BCC-CSM2-MR	No	Does not include humidity (Xin et al., 2019).
CAMS-CSM1-0	No	Does not include humidity (Rong et al., 2019).
CanESM5	No	No data at desired spatiotemporal resolution (Swart et al., 2019)
CESM2	Yes	Used variant r4i1p1f1. Other variants (r1i1p1f1, r2i1p1f1, and r3i1p1f1) do not include daily min/max temperatures (Danabasoglu, 2019a).
CESM2-WACCM	Yes	Used variant r3i1p1f1. Other variants (r1i1p1f1 and r2i1p1f1) do not include daily min/max temperatures (Danabasoglu, 2019b).
CMCC-CM2-SR5	No	Does not include daily min/max temperatures (Lovato et al., 2020).
CMCC-ESM2	No	Does not include geopotential height (Lovato et al., 2021)
CNRM-ESM2-1	No	Does not include any relevant variables at desired spatiotemporal resolution (Voldoire, 2019).

GCM Name	Used	Notes and Reference
E3SM-1-0	No	SSP data at desired spatiotemporal resolution does not include irradiance, windspeeds, and humidity (Bader et al., 2022a).
E3SM-1-1	No	SSP data is at a monthly frequency (Bader et al., 2020).
E3SM-1-1-ECA	No	SSP data at desired spatiotemporal resolution does not include irradiance, windspeeds, and humidity (Bader et al., 2022b).
E3SM-2-0	No	No data for SSP5 8.5 (E3SM Project, DOE, 2022)
E3SM-2-0-NAARRM	No	No data for SSP5 8.5 (Tang et al., 2023)
EC-Earth3	Yes	(EC-Earth Consortium, 2019a)
EC-Earth3-CC	Yes	(EC-Earth Consortium, 2021b)
EC-Earth3-Veg	Yes	(EC-Earth Consortium, 2019b)
EC-Earth3-Veg-LR	No	No data at desired spatiotemporal resolution (EC-Earth Consortium, 2020)
FGOALS-f3-L	No	SSP data is at monthly frequency (Yu, 2019).
GFDL-CM4	Yes	(Guo et al., 2018)
GFDL-ESM4	Yes	(John et al., 2018)
HadGEM3-GC31-MM	No	No data for SSP2 4.5 and incomplete timeseries with less than 365 days per year (Jackson, 2020)
INM-CM4-8	Yes	(Volodin et al., 2019a)
INM-CM5-0	Yes	(Volodin et al., 2019b)
IPSL-CM6A-LR	No	No data at desired spatiotemporal resolution (Boucher et al., 2019).
KACE-1-0-G	No	SSP data is at low spatial resolution (Byun et al., 2019).
MIROC6	No	No data at desired spatiotemporal resolution (Shiogama et al., 2019).
MPI-ESM1-2-HR	Yes	(Schupfner et al., 2019)
MPI-ESM1-2-LR	No	SSP data is at low spatial resolution (Wieners et al., 2019).
MRI-ESM2-0	Yes	(Yukimoto et al., 2019)
NorESM2-MM	Yes	(Bentsen et al., 2019)
TaiESM1	Yes	(Lee et al., 2020)

For each variable, we select a historical reference dataset that can be used to evaluate the historical skill of the GCMs. We choose datasets that are publicly available, have at least a 20-year historical record, and have been used extensively in previous energy system studies. We leverage the European Centre for Medium-Range Weather Forecasts Reanalysis v5 (ERA5), Daymet, and the National Solar Radiation Database (NSRDB) (Copernicus Climate Change Service, 2017; Thornton et al., 2021; Sengupta et al., 2018). The variables analyzed and their corresponding historical reference datasets are detailed in Table 2 below.

The three historical reference datasets used in this work are all at finer spatial and temporal resolutions than the GCM data being evaluated. We perform a geospatial mapping to aggregate high-resolution historical pixels to their nearest low-resolution GCM pixel. This creates a sub-

grid mapping (e.g., similar to a sudoku grid) without overlap or duplication of the high-resolution pixels. A simple averaging or min/max operation is performed on the temporal axis to aggregate sub-daily data to the GCM daily values.

Table 2. Summary of variables analyzed along with historical baseline datasets.

Variable	Abbreviation	Historical Reference Dataset	Resolution	Temporal Extent	Reference
Air Temperature (2-meter)	T2M	ERA5	31-km hourly	1980-2019	Copernicus Climate Change Service, 2017
Relative Humidity (2-meter)	RH2M	ERA5	31-km hourly	1980-2019	Copernicus Climate Change Service, 2017
Precipitation	PR	Daymet	4-km daily	1980-2019	Thornton et al., 2021
Global Horizontal Irradiance	GHI	NSRDB	4-km 30-minute	2000-2019	Sengupta et al., 2018
Windspeed (100-meter)	WS 100m	ERA5	31-km hourly	1980-2019	Copernicus Climate Change Service, 2017

For the historical skill evaluation, we use 40-year records for each historical reference dataset from 1980 to 2019 inclusive, except for irradiance where we use 20 years from 2000 to 2019 from the NSRDB. We use the corresponding years of the historical GCM simulations which end in 2014, and the additional five years from 2015 to 2019 of data from the SSP5 8.5 simulation. These five years from the SSP simulation were used for the historical skill evaluation in order to match the GCM year range to the historical reference years. This is a somewhat arbitrary decision, and a similar analysis could be performed using data until the most recent year or using non-overlapping years from only the historical GCM simulation. We expect that the evaluation is insensitive to these choices due to the selection of a sufficiently long historical record (multiple decades) and the expectation that the first five years of any SSP simulation from 2014 to 2019 will still be representative of the current climate.

For wind speed variables, we interpolate or extrapolate the zonal and meridional wind components based on what is available from the source datasets. For the historical ERA5 wind data, the 100-meter winds are saved as output datasets and are used directly. For GCM data, when only 2D surface wind variables are available, we use the power law with exponent 0.2 to extrapolate to hub heights (US Department of Commerce 2020; Touma 1977). This approach was used for four GCMs that did not have 3D vertical wind profiles available: EC-Earth3-CC, EC-Earth3-Veg, GFDL-CM4, and GFDL-ESM4. When 3D vertical wind profiles are available, we linearly interpolate to the nominal hub heights. Note that the vertical spacing of the wind profile in GCM data from CMIP6 is very coarse, often on the order of 1 to 2 km (more vertical levels may be available to download from different data archives). This is insufficient to properly

resolve the near-surface boundary layer phenomena in which a wind turbine operates. Linear interpolation will not create a realistic boundary layer vertical wind speed profile and the data is too coarse to fit a realistic power law profile. Downstream applications of this data will benefit from an initial bias correction of the interpolated GCM data before downscaling the data to achieve a realistic representation of wind meteorology for energy applications.

It should be noted that several GCMs used here (CESM2, CESM2-WACCM, and MRI-ESM-2.0) have missing wind speed values where the vertical pressure levels increase above low surface pressures at high-elevation grid cells such as in the Rocky Mountains. For MRI-ESM-2.0, we use the 2D surface wind data to gap-fill the missing wind values in the 3D data. 2D surface winds are not available for CESM2 and CESM2-WACCM so we calculate hub-height winds by linearly extrapolating from higher vertical levels. Table 3 shows that this adversely affects the wind speed distributions, and caution should be taken if applying these models and data to wind energy studies. Note that CMIP6 models may have more complete data records, including near-surface winds, at their respective modeling centers' website, but we only used data from the Earth System Grid Federation (ESGF), as this is the central repository for all CMIP6 data. For example, the CESM2 models appear to have more complete data records with near-surface winds available via the National Center for Atmospheric Research Climate Data Gateway, but we only use the model data uploaded to ESGF for this work.

For the historical skill evaluation, we select several metrics that are intended to evaluate the skill with which the various GCMs represent the historical climate including extremes. One metric we select is the mean-centered Kolmogorov-Smirnov (KS) statistical test, which has been used previously in GCM evaluations and which is a concise metric for evaluating the similarity of higher-order statistical moments in probability distributions (Martinez & Iglesias 2022). Because the mean-centered KS test explicitly removes bias from the evaluation, we also present a bias metric for each variable. For most variables we use the 50^{th} percentile (P50) bias, which is the 50^{th} percentile of the GCM data minus the 50^{th} percentile of the historical values. For variables that represent the extremes of the variables (e.g., maximum daily temperature), we present the 5^{th} or 95^{th} percentile bias (P5 and P95). Because of the tendency for GCMs to produce days with very low precipitation instead of completely dry days (e.g., the “drizzle problem”, Polade et al., 2014), the mean-centered KS test of precipitation tends to evaluate the performance of the GCM in low-precipitation days. For this reason, we do not mean-center the precipitation distributions before running the KS test, and we also fix the rate of dry days between historical and future distributions. Common quantile mapping bias correction methods would perform the same adjustment on the historical dry day frequency (Cannon et al., 2015).

Lastly, because pixel-by-pixel metrics like the KS statistic and mean bias do not capture large-scale climate trends and sensitivity to climate processes like the El Niño Southern Oscillation (ENSO), we include a composite process metric based on Figure 5 of Lybarger et al., 2024. This is an aggregation of several climate process metrics including seasonal amplitudes, trends of change from 1901-2014, spatial correlations, and ENSO sensitivities (for the full list of process metrics, see Table 2 in Lybarger et al., 2024). The process metric is based on a combination of global and CONUS data, but not on any of the other subregions that we consider here. Nevertheless, we include this metric in the skill assessment for each subregion because of the importance of these large-scale climate processes in local climate impacts.

When presenting the historical skill assessments such as in Table 3, we order the GCMs according to their average skill. For each metric, we normalize the values from 0 to 1 with 0 being the best performing model. We then weight each metric such that each physical variable is considered equal in relation to each other. That is, the six temperature metrics each get multiplied by 1/6, the two metrics for relative humidity (we ignore min and max humidity in the rankings), precipitation, GHI, and windspeed each get multiplied by 1/2, and the process metric gets multiplied by 1. We then sum the normalized and weighted metrics for each GCM and then sort the GCMs by these values.

This ranking helps illustrate those GCMs that represent historical meteorology with high overall skill. However, this may not be the only result to consider when selecting GCMs, as historical skill does not guarantee a specific behavior with respect to the model's projections of change. This is further discussed in Section 4.

In comparing the projections of GCMs, we use a centered moving average to represent the overall trend of change and to reduce the effects of interannual variability on the projections. We select a 20-year moving average such that the datum from a GCM in 2030 in Figure 1 is a mean value of the data from 2020 to 2039. Note that we only use data from 1980 to 2059, so data before 1990 and after 2050 is not presented in subsequent figures because a full 20-year average cannot be calculated. The only exception to this is irradiance data where we select a 10-year moving average so that the trends present in the 20-year NSRDB historical record can be seen. Trends are centered at zero for the historical time period so that trends from various GCMs can be compared against each other and against the historical baseline data. This is essentially a simple "delta" bias correction method to enable comparison across GCMs. More advanced bias correction methods (e.g., quantile delta mapping) may be used prior to downscaling and would manipulate some of these results.

Because of the impactful nature of extreme events on both human health and the energy system, we also present comparisons of how GCMs represent extreme temperature events, drought years, and their variability over time. To do this, we use a minimum/maximum data reduction over a 10-year moving window similar to the centered moving average for trend calculations. For example, the maximum temperature value from a GCM in 2030 in Figure 2 is the maximum daily temperature event from 2025 through 2034 (i.e., the hottest single day peak temperature). Similarly, the minimum annual rainfall value from a GCM in 2030 in Figure 6 is the year with the smallest total annual rainfall from 2025 through 2034 (i.e., the worst drought year). Note that we plot all data at 5-year intervals, so some neighboring pairs of points have the same value if their extreme event falls in the overlapping period. All extreme values are centered on the mean value of the historical time period so that events from various GCMs can be compared against each other. Similarly to the bias correction of the trends, more advanced bias correction methods (e.g., quantile delta mapping) may be used prior to downscaling and would manipulate some of these results.

The spatial extent selected for this work is the CONUS with subregions presented in the appendices. All variables are averaged over the full spatial extent with even spatial weighting before the calculation of any metrics. For example, a P95 value of daily maximum temperature is the 95th percentile of the area-averaged maximum daily temperatures.

4 Results and Discussion

A summary of GCM skill in representing the historical climate is illustrated in Table 3, with a comparison of trends illustrated in Figure 1 through Figure 8 below. These results are CONUS-wide averages. The appendices to this report present regional results.

From these results, we can clearly see that some models (e.g., EC-Earth3-CC and TaiESM1) have better historical skill across more metrics than other models (e.g., INM-CM4-8). We can also confirm previous results that show models from the same institute tend to perform similarly (Ashfaq et al., 2022). For example, INM-CM4-8 and INM-CM5-0 both tend to show strong positive bias in maximum daily temperatures, strong negative bias in 100-m windspeed, and poor representation of temperature, humidity, precipitation, and windspeed distributions. In contrast, EC-Earth3, EC-Earth3-CC, and EC-Earth3-Veg all tend to have excellent representations of daily maximum temperatures, humidity distributions, precipitation, and windspeeds. However, as shown in these results, no climate model performs best on all metrics, and any given climate model may perform well on one metric while having significant bias in other metrics or other regions.

Perhaps equally important to the comparison of historical skill is the comparison of future projections of climate change. It has been previously found that GCMs with similarly high historical skill can have a range of future projections as large as a set of GCMs selected at random. This suggests that there is little relationship between the quality of the model-simulated historical meteorology and the quality of the model that determines the anthropogenic climate change signal (Pierce et al., 2009). For example, GFDL-CM4 and GFDL-ESM4 both have similar skill in representing windspeed distributions, with low KS statistics and similar negative bias values. However, GFDL-ESM4 projects very little change in wind resource (1% decrease in windspeed by midcentury in SSP5 8.5), while GFDL-CM4 projects the largest decrease in wind resource for any GCM (5% decrease in windspeed by midcentury in SSP5 8.5).

Sensitivity to emissions also varies across models, with some models (e.g., MPI-ESM1-2-HR and MRI-ESM2-0) showing less than a 0.4°C difference between mean temperature changes in SSP2 4.5 and SSP5 8.5 and other models (e.g., CESM2 and TaiESM1) showing differences greater than 1°C between the same climate change scenarios (differences between scenarios are calculated from the changes between the reference period 1980-2020 to mid-century 2050-2059). This confirms previous reports that even among the most historically accurate models the range of emissions response can be quite large (Coquard et al., 2004).

With respect to the two climate change scenarios, SSP5 8.5 has the highest radiative forcing of any climate scenario, but SSP2 4.5 and SSP5 8.5 show relatively similar projections through typical energy system planning horizons (e.g., through midcentury). Figure 1 shows SSP5 8.5 representing only slightly worse warming than SSP2 4.5 and there is significant overlap in projections between the variety of selected GCMs. For this reason, it has even been explicitly recommended by state planning agencies that SSP5 8.5 should be used when considering impacts by mid-century (California Governor's Office of Planning and Research, 2017).

The decision of which climate scenario to use in an applied climate impacts study is a contentious one. SSP5 8.5 and RCP 8.5 are widely studied in the literature (Miara et al., 2019;

Craig et al., 2020; Kao et al., 2022; Szinai et al., 2023), but are also widely criticized (Hausfather, 2019; Hausfather & Peters, 2020). Pielke & Ritchie, 2021 criticize SSP5 8.5 as too extreme and argue that it is often misused as a "business as usual" scenario when it is an implausible representation of the future that leads to skewed perceptions of climate risk. In a contrasting view, Schwalm et al., 2020 argue that the 8.5 scenario matches historical emissions from 2005-2020 within 1% and also that the 8.5 scenario is the most realistic until midcentury under current and stated policies. Schwalm et al., 2020 also note that RCP 8.5 is valuable for modeling physical climate risks (as opposed to emission trajectories) because of the lack of carbon cycle feedbacks in climate models (e.g., permafrost thaw, changes in soil carbon dynamics, increased forest fires, and pest spread).

Several studies have also analyzed the likelihood of respective climate scenarios using Integrated Assessment Models (IAMs). Capellán-Pérez et al., 2016 used the IAM “GCAM-MAGICC” to estimate that RCP 6.0 had the highest likelihood, and that there is relatively low, but significant, probability of reaching RCP 8.5 or mitigating climate change via RCP 4.5. Huard et al., 2022 analyzed five different IAMs and showed that SSP2 4.5 was most likely in three out of the five IAMs, and second most likely in the remaining two IAMs. Huard et al., 2022 also notes that SSP5 8.5 remains reasonably likely in all five IAMs until around 2060 at which time the likelihood decreases significantly.

We include both SSP2 4.5 and SSP5 8.5 here because of their extensive use in the literature but recommend that applied studies make their scenario selection based on the best information available to them.

It has been reported previously that natural variability and differences between GCMs tend to dominate climate uncertainty through midcentury while the uncertainty from emissions scenario grows after midcentury and dominates towards the end of the century (Wootten et al., 2017; Hawkins and Sutton 2009). Uncertainty from downscaling methods can also be important although this tends to vary by region, experiment, and metric, and can be sensitive to how the downscaling method manipulates extreme metrics (Wootten et al., 2017; Kao et al., 2022; Rastogi et al., 2022).

Regarding climate change impacts to renewable energy resources, there is much heterogeneity across regions and GCMs. For hydro resources, we generally see an increase in mean precipitation corresponding to the increase in temperature. This is seen across CONUS (Figure 5) and in most of the North American Electric Reliability Corporation (NERC) sub regions (Appendices A through F). The largest uncertainty in this trend is shown in the Texas Reliability Entity (Texas RE, Figure 50) and the Western Electricity Coordinating Council (WECC, Figure 59) which have changes in mean precipitation ranging from approximately -10 to +20% for Texas and -5 to +12% for WECC depending on the GCM and scenario. Previous work has focused on understanding how these potential changes in precipitation lead to impacts on hydropower. These studies have reported reduced summertime hydropower resource in California and the Pacific Northwest and reduced annual hydropower resource across the South with medium agreement among studies (Craig et al., 2018). For more detailed evaluations of climate impacts to hydropower, the continued report series on the “Effects of Climate Change on Federal Hydropower” by Kao et al., 2022 is an invaluable resource.

For climate impacts to wind resources, there have been several reports on the potential for decreased wind resources across CONUS (Martinez & Iglesias 2022; Martinez & Iglesias 2024; Craig et al., 2018; Karnauskas et al, 2018), although there is disagreement in this trend between GCMs (Figure 7) and in different reports (Pryor & Barthelmie 2011; Craig et al., 2018). In the data from CMIP6, several GCMs do indeed project significant decreases in wind resource in otherwise high-wind regions such as the Midwest Reliability Organization (MRO, Figure 16).

Solar resources have perhaps the least obvious climate change impact, with changes across CONUS ranging from -2 to +2.5% without substantial agreement on the direction of change (Figure 8). Although some studies suggest dramatic regional changes, most regions do not have agreement in the direction of change between GCM-RCM pairs (Craig et al., 2018).

There are many other effects of climate change that we do not attempt to quantify here. For example, although GCMs are intended to represent large-scale changes in climate, localized population- or capacity-weighted metrics may be more meaningful for energy analysis. We also do not disaggregate the data for seasonal impacts, which could affect energy systems more dramatically than annual averages might suggest. Finally, we focus here on raw GCM output variables, but non-linear transforms to variables like wet-bulb temperature, wind energy generation, water availability for thermal cooling, or hydropower resources may be more relevant for downstream applications. Nevertheless, we expect these results to provide a useful starting point for selecting GCMs for applied climate impacts research.

Table 3. Summary of historical GCM skill using KS statistic and bias metrics for CONUS. Values for a given metric in each row are ranked from best to worst historical skill (dark blue to dark red).

	TaiESM1	EC-Earth3-CC	GFDL-CM4	EC-Earth3-Veg	MPI-ESM1-2-HR	EC-Earth3	NorESM2-MM	CESM2	GFDL-ESM4	CESM2-WACCM	MRI-ESM2-0	INM-CM5-0	INM-CM4-8
T2M KS	0.04	0.05	0.05	0.05	0.06	0.06	0.06	0.05	0.05	0.05	0.06	0.05	0.06
T2M Bias P50 (°C)	0.29	-1.04	-2.28	-1.30	-0.73	-1.88	1.38	1.92	-2.41	1.89	-1.15	0.12	0.84
T2M Max KS	0.05	0.05	0.05	0.06	0.06	0.06	0.07	0.07	0.06	0.06	0.07	0.07	0.09
T2M Max Bias P95 (°C)	1.04	0.22	-1.46	0.08	0.07	-0.45	3.13	2.97	-1.04	-3.48	-0.88	2.55	4.03
T2M Min KS	0.04	0.05	0.05	0.05	0.06	0.06	0.06	0.07	0.05	0.09	0.06	0.06	0.06
T2M Min Bias P5 (°C)	-1.74	-2.43	-1.39	-2.57	-0.83	-3.83	0.90	3.01	-0.48	7.53	2.27	1.78	2.39
RH2M KS	0.08	0.07	0.07	0.07	0.13	0.07	0.10	0.09	0.13	0.09	0.09	0.13	0.15
RH2M Bias P50 (%)	7.5	9.2	12.8	8.7	7.9	10.1	-12.6	-8.9	18.3	-8.7	10.2	2.4	-2.8
RH2M Max KS		0.09	0.14	0.09	0.21	0.09					0.19	0.23	0.25
RH2M Max Bias P95 (%)		1.76	7.43	1.68	10.95	1.80					3.76	5.62	5.31
RH2M Min KS		0.09	0.09	0.09	0.12	0.09					0.10	0.11	0.11
RH2M Min Bias P5 (%)		7.8	4.7	6.7	5.9	9.6					13.8	-11.0	-15.4
PR KS	0.10	0.09	0.10	0.09	0.07	0.09	0.08	0.09	0.12	0.09	0.12	0.16	0.14
PR Bias P50 (%)	1.67	2.75	4.60	2.47	1.53	2.77	0.43	1.73	7.52	1.99	6.77	13.21	10.28
GHI KS	0.04	0.05	0.03	0.05	0.04	0.05	0.04	0.04	0.04	0.04	0.04	0.03	0.04
GHI Bias P50 (%)	-0.30	0.60	-2.12	3.01	0.42	1.82	10.72	5.79	-6.41	5.09	6.33	4.82	7.81
WS 100m KS	0.08	0.09	0.07	0.09	0.14	0.09	0.14	0.27	0.08	0.27	0.14	0.19	0.20
WS 100m Bias P50 (%)	-17.4	-1.2	-16.1	-0.8	-2.9	-16.4	7.3	45.2	-19.6	45.3	-27.9	-56.5	-56.1
Process Skill	0.29	0.05	0.06	0.06	0.09	0.06	0.04	0.20	0.14	0.16	0.34	0.82	0.85

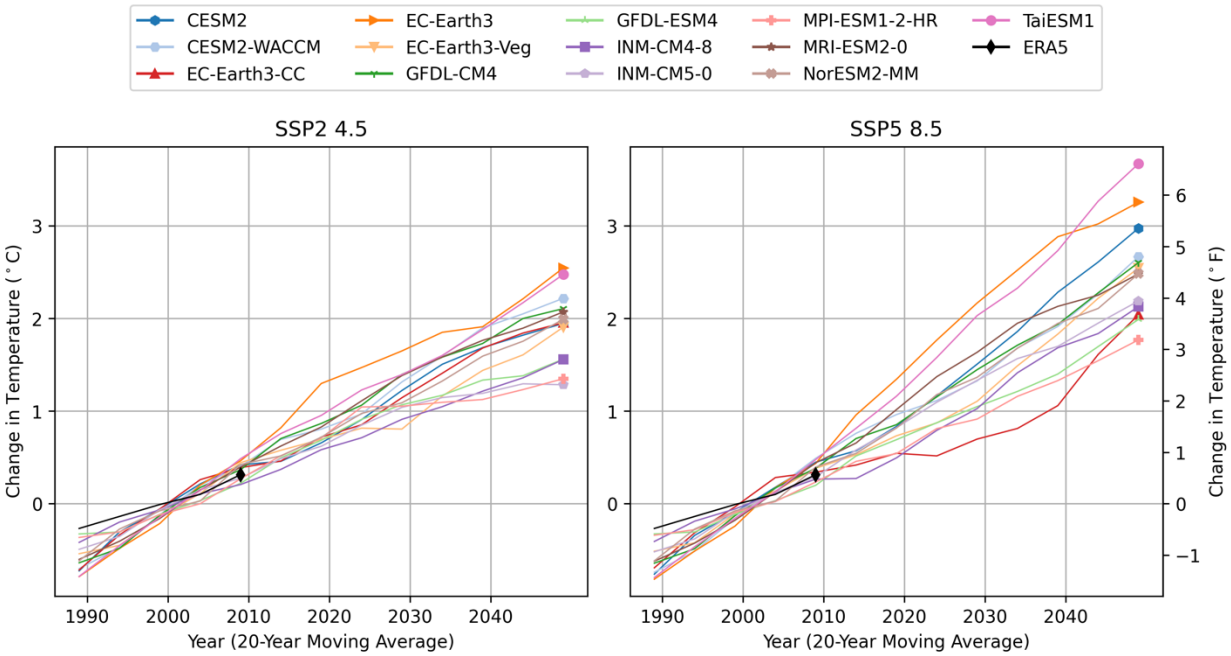

Figure 1. Comparison of GCM trends in changes to daily average near-surface air temperature for CONUS.

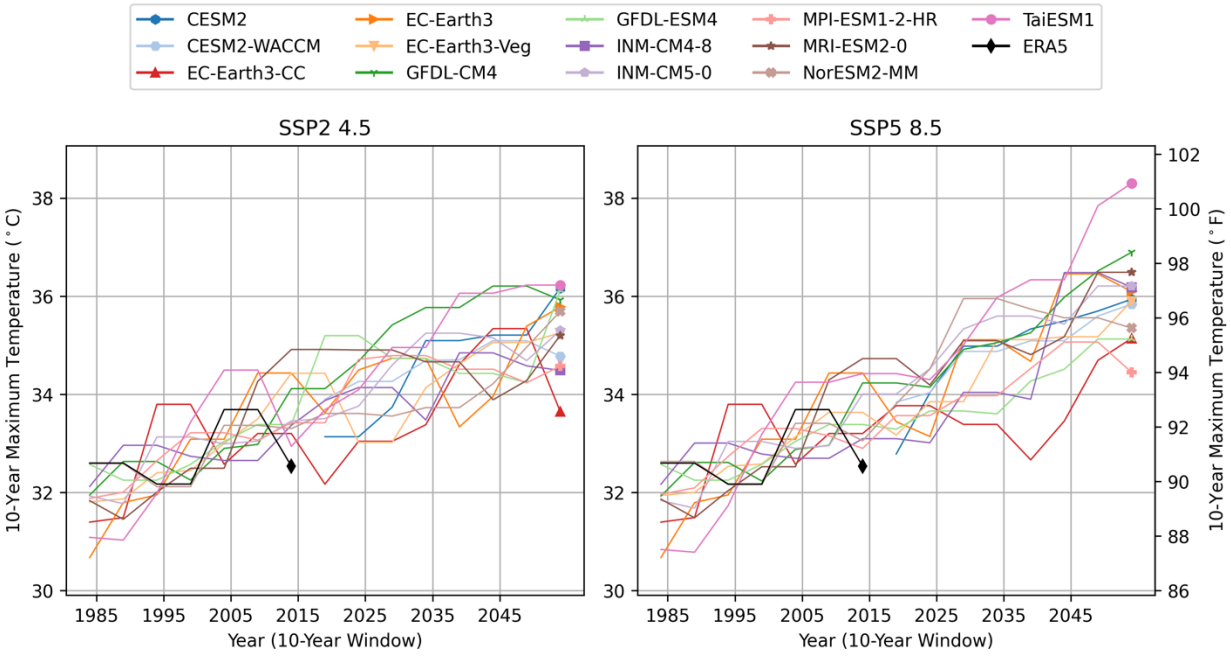

Figure 2. Comparison of GCM daily maximum air temperature events for CONUS.

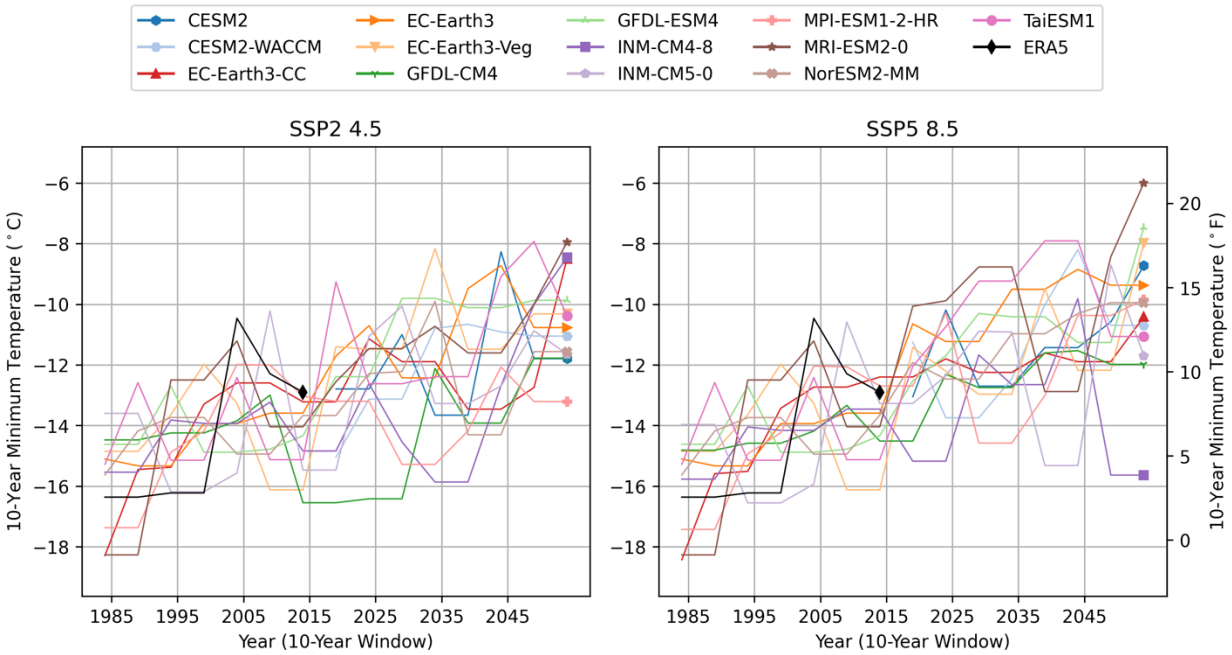

Figure 3. Comparison of GCM daily minimum air temperature events for CONUS.

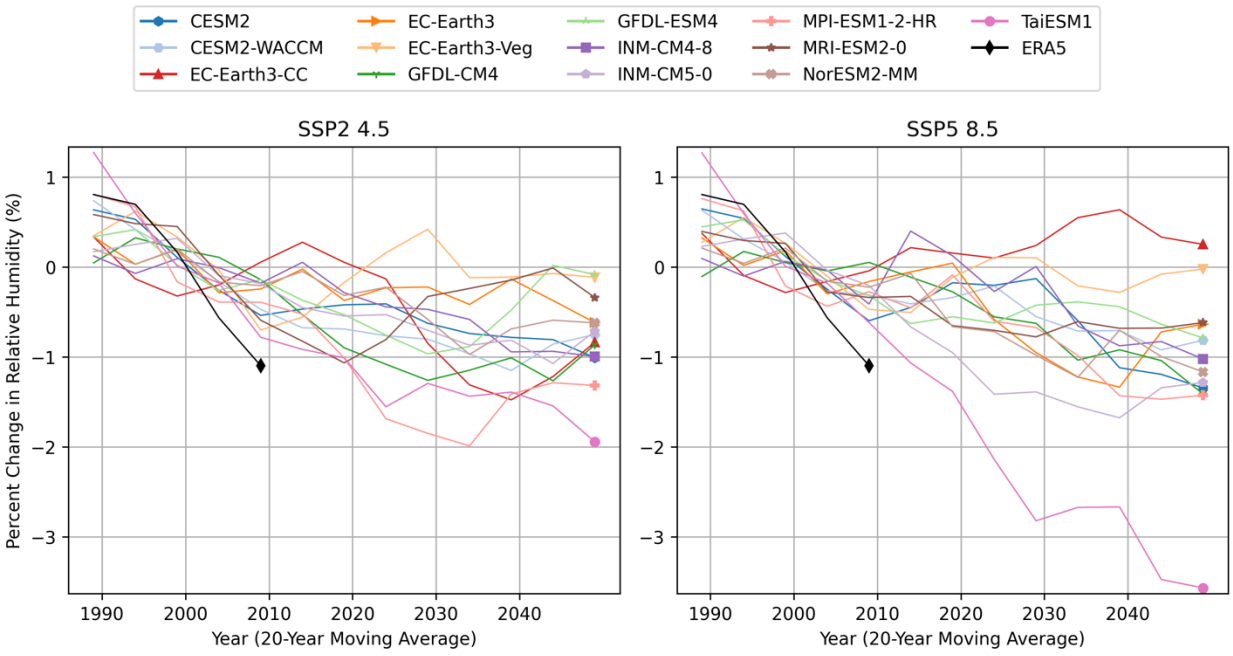

Figure 4. Comparison of GCM trends in changes to daily average near-surface relative humidity for CONUS.

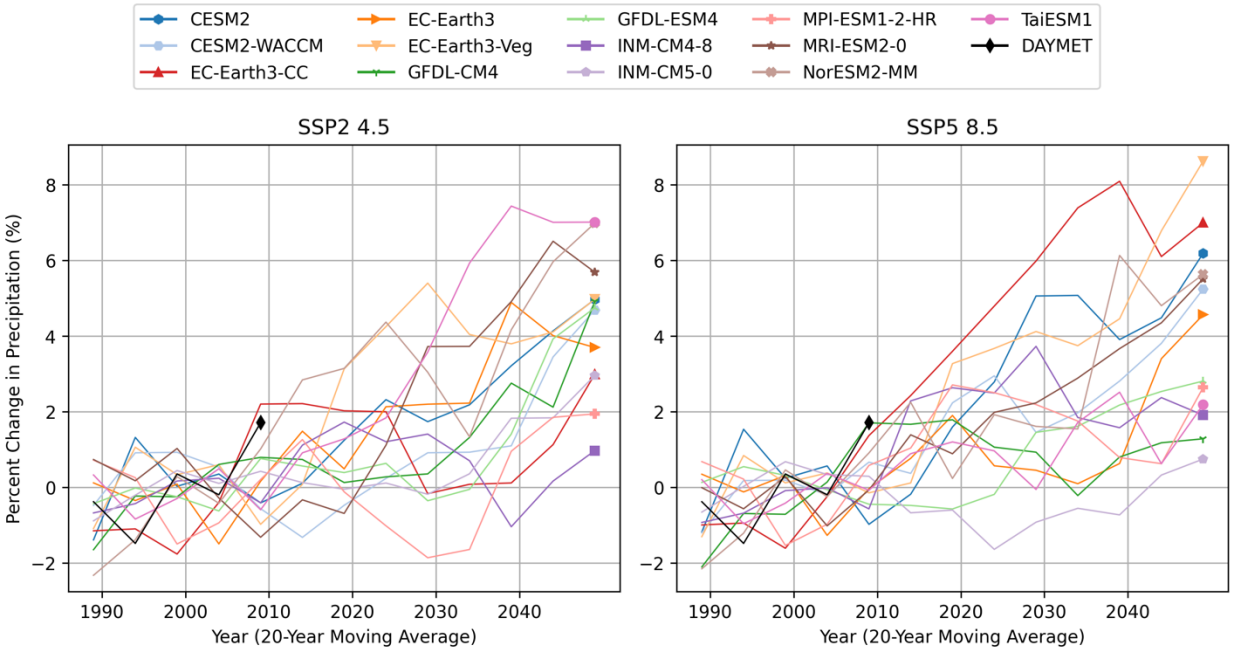

Figure 5. Comparison of GCM trends in changes to daily average precipitation for CONUS.

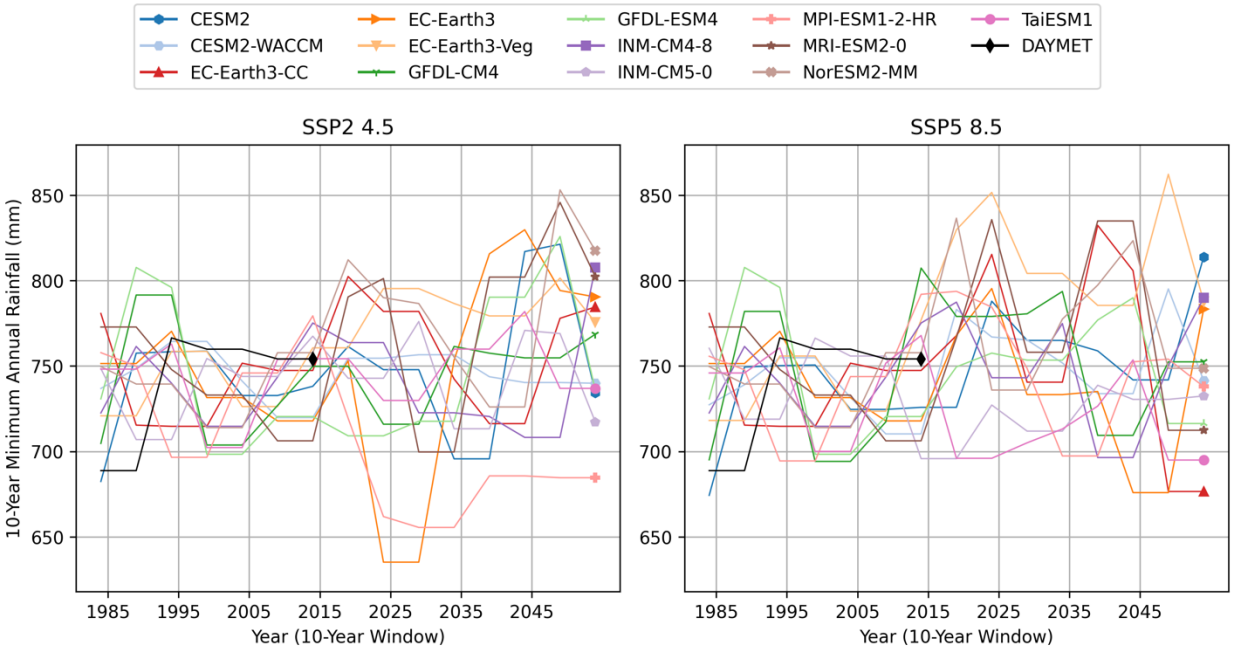

Figure 6. Comparison of GCM minimum annual rainfalls for CONUS.

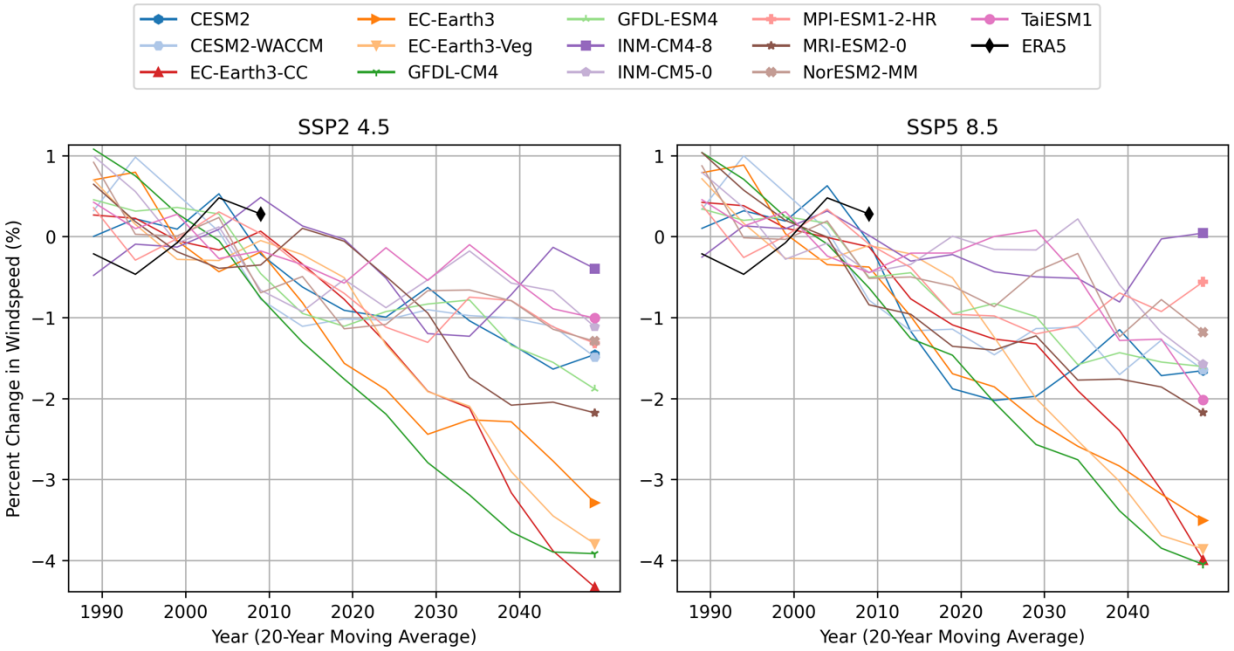

Figure 7. Comparison of GCM trends in changes to daily average 100-meter windspeed for CONUS.

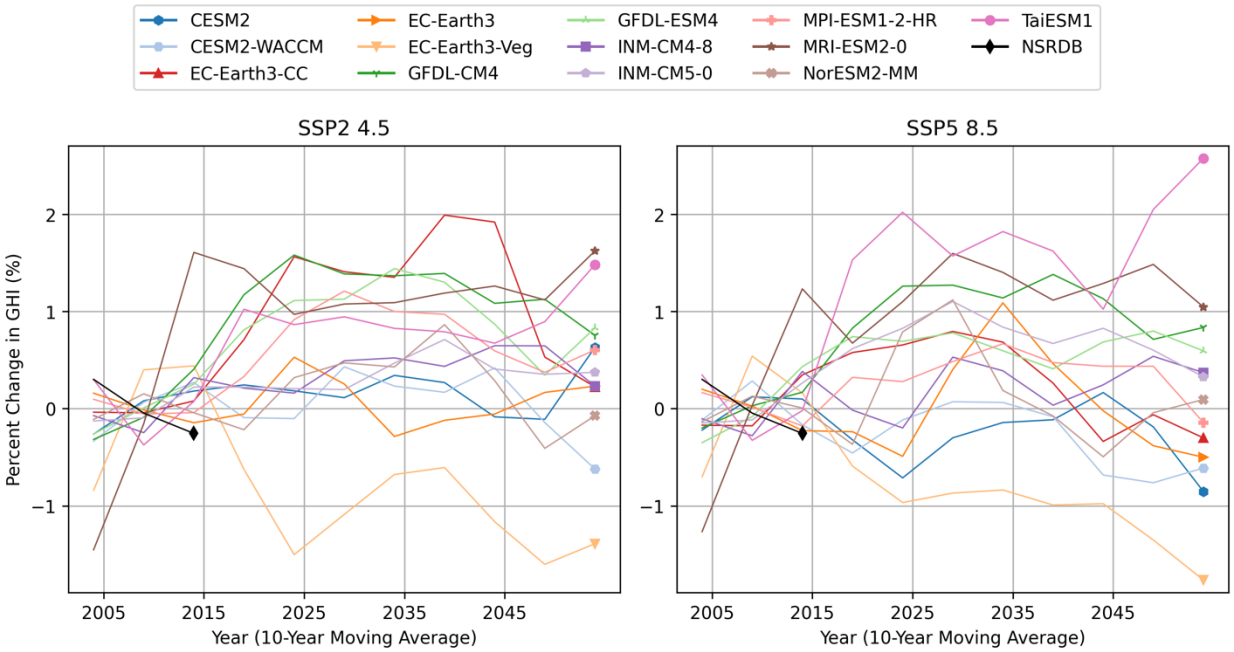

Figure 8. Comparison of GCM trends in changes to daily average GHI for CONUS.

5 Conclusion

In this report, we have presented data that can be used to evaluate the suitability of GCMs when performing research on climate impacts to energy systems. We have identified GCMs that have data records in CMIP6 suitable to support comprehensive energy system analysis, evaluated their skill against historical records, and compared their projections of future change for two climate change scenarios.

As stated previously, the goal of this report is not to recommend one or more GCMs and climate scenarios that would be best suited for all energy system analyses. Such a recommendation would be highly dependent on the focus and constraints of the desired application. However, as shown by the large range of model skill and future projections across different GCM scenario combinations, it is evident that using multiple input datasets with diverse characteristics will result in more robust research. Previous work has suggested that selecting 5 climate models could be sufficient (Pierce et al., 2009), and in practice most applied studies have used 5 to 20 different climate models (Miara et al., 2019; Craig et al., 2020; Kao et al., 2022; Szinai et al., 2023; Ralston Fonseca et al., 2021). Many applied studies to date have used only the single SSP5 8.5 scenario (Miara et al., 2019; Craig et al., 2020; Kao et al., 2022; Szinai et al., 2023), but some have considered multiple scenarios (Ralston Fonseca et al., 2021). As discussed in Section 4, the selection of climate scenarios is a contentious decision with valid arguments supporting the use of SSP5 8.5 and also criticizing SSP5 8.5 as too extreme and implausible. Ultimately, the selection of models and scenarios will depend on the unique requirements of downstream work and more pragmatic considerations such as data storage limitations and compute costs of applied energy system models.

Finally, in addition to the CONUS results presented in Section 4, we also present aggregated results for several subregions in the included appendices. We have aggregated data to the six NERC subregions and the three offshore wind regions within the CONUS exclusive economic zone. Each appendix includes the same data as Section 4 but only for the region of interest. We have also released all the figures as interactive graphs in the GitHub repository associated with this report. For details, see the section on Code and Data Availability.

List of Acronyms

CMIP6	Coupled Model Intercomparison Project 6
CONUS	Contiguous United States
ENSO	El Niño Southern Oscillation
ERA5	European Centre for Medium-Range Weather Forecasts Reanalysis v5
ESGF	Earth System Grid Federation
GCM	Global Climate Model
GHI	Global Horizontal Irradiance
KS	Kolmogorov-Smirnov
MRO	Midwest Reliability Organization
NERC	North American Electric Reliability Corporation
NPCC	Northeast Power Coordinating Council
NREL	National Renewable Energy Laboratory
NSRDB	The National Solar Radiation Database
P5	5th Percentile
P50	50th Percentile
P95	95th Percentile
PR	Precipitation
RCM	Regional Climate Model
RF	Reliability First
RH2M	Relative Humidity (2-meters)
SERC	Southeastern Electric Reliability Corporation
SSP	Shared Socioeconomic Pathway
T2M	Air Temperature (2-meters)
Texas RE	Texas Reliability Entity
WECC	Western Electricity Coordinating Council
WS	Windspeed

Code and Data Availability

All of the code and data used to support this technical report are publicly available.

This report heavily leverages the Super Resolution for Renewable Resource Data (sup3r) software (Benton et al., 2024) along with configuration files and data munging scripts that are released in the Global Climate Model Evaluation (gcm_eval) repository (Buster et al., 2024).

The climate model data used in this report is publicly available via the CMIP6 archive (see the section on "References for GCMs"). The historical reanalysis data is available via the references listed in Table 2.

The data presented in figures in this report are also released as interactive graphs in the Global Climate Model Evaluation (gcm_eval) repository (Buster et al., 2024). For example, go to https://nrel.github.io/gcm_eval/regions/conus.html to see interactive graphs on the CONUS results presented in Section 4.

Acknowledgements

We thank Deeksha Rastogi, Andrew Kumler, Meghan Mooney, and Dan Bilello for their thoughtful reviews of this report.

This work was authored by the National Renewable Energy Laboratory, operated by Alliance for Sustainable Energy, LLC, for the U.S. Department of Energy (DOE) under Contract No. DE-AC36-08GO28308. Funding provided by the DOE Office of Energy Efficiency and Renewable Energy (EERE), the DOE Office of Electricity (OE), the DOE Office of Fossil Energy and Carbon Management (FECM), and the DOE Office of Cybersecurity, Energy Security, and Emergency Response (CESER). The research was performed using computational resources sponsored by the DOE Office of Energy Efficiency and Renewable Energy and located at the National Renewable Energy Laboratory. The views expressed in the article do not necessarily represent the views of the DOE or the U.S. Government. The U.S. Government retains and the publisher, by accepting the article for publication, acknowledges that the U.S. Government retains a nonexclusive, paid-up, irrevocable, worldwide license to publish or reproduce the published form of this work, or allow others to do so, for U.S. Government purposes.

References

Ashfaq, M., Rastogi, D., Abid, M. A. & Kao, S.-C. Evaluation of CMIP6 GCMs over the CONUS for downscaling studies. Preprint at https://doi.org/10.1002/essoar.10510589.1 (2022).

Bloomfield, H. C., Brayshaw, D. J., Shaffrey, L. C., Coker, P. J. & Thornton, H. E. Quantifying the increasing sensitivity of power systems to climate variability. *Environ. Res. Lett.* **11**, 124025 (2016).

Brinkman, G. et al. The North American Renewable Integration Study: A U.S. Perspective. (2021).

Buster, G, Podgorny, S, Benton, B. NREL Global Climate Model Evaluation Repository (gcm_eval). https://github.com/NREL/gcm_eval (version v0.0.0), 2024.

California Governor's Office of Planning and Research (OPR). Planning and Investing for a Resilient California: A Guidebook for State Agencies. ResilientCA. https://opr.ca.gov/docs/20180313-Building_a_Resilient_CA.pdf (2017).

Cannon, A. J., Sobie, S. R. & Murdock, T. Q. Bias Correction of GCM Precipitation by Quantile Mapping: How Well Do Methods Preserve Changes in Quantiles and Extremes? Journal of Climate 28, 6938–6959 (2015).

Capellán-Pérez, I., Arto, I., M. Polanco-Martínez, J., González-Eguino, M. & B. Neumann, M. Likelihood of climate change pathways under uncertainty on fossil fuel resource availability. Energy & Environmental Science 9, 2482–2496 (2016).

Carvallo, J. et al. A Guide for Improved Resource Adequacy Assessments in Evolving Power Systems: Institutional and Technical Dimensions. https://eta-publications.lbl.gov/sites/default/files/ra_project_-_final.pdf (2023).

Chhin, R. & Yoden, S. Ranking CMIP5 GCMs for Model Ensemble Selection on Regional Scale: Case Study of the Indochina Region. Journal of Geophysical Research: Atmospheres 123, 8949–8974 (2018).

Copernicus Climate Change Service (C3S) (2017): ERA5: Fifth generation of ECMWF atmospheric reanalyses of the global climate . Copernicus Climate Change Service Climate Data Store (CDS), accessed January 2024. https://cds.climate.copernicus.eu/cdsapp#!/home

Coquard, J., Duffy, P. B., Taylor, K. E. & Iorio, J. P. Present and future surface climate in the western USA as simulated by 15 global climate models. Climate Dynamics 23, 455–472 (2004).

Craig, M. T., Jaramillo, P., Hodge, B.-M., Nijssen, B. & Brancucci, C. Compounding climate change impacts during high stress periods for a high wind and solar power system in Texas. *Environ. Res. Lett.* **15**, 024002 (2020).

Craig, M. T. et al. A review of the potential impacts of climate change on bulk power system planning and operations in the United States. Renewable and Sustainable Energy Reviews 98, 255–267 (2018).

Eyring, V., Bony, S., Meehl, G. A., Senior, C. A., Stevens, B., Stouffer, R. J., and Taylor, K. E.: Overview of the Coupled Model Intercomparison Project Phase 6 (CMIP6) experimental design and organization, Geosci. Model Dev., 9, 1937-1958, doi:10.5194/gmd-9-1937-2016, 2016.

Flato, G. et al. Evaluation of Climate Models. In: Climate Change 2013: The Physical Science Basis. Contribution of Working Group I to the Fifth Assessment Report of The Intergovernmental Panel on Climate Change. https://www.ipcc.ch/site/assets/uploads/2018/02/WG1AR5_Chapter09_FINAL.pdf (2013).

Hausfather, Z. Explainer: The high-emissions 'RCP8.5' global warming scenario. https://www.carbonbrief.org/explainer-the-high-emissions-rcp8-5-global-warming-scenario/ (2019).

Hausfather, Z. & Peters, G. P. Emissions – the 'business as usual' story is misleading. Nature 577, 618–620 (2020).

Hawkins, E. & Sutton, R. The Potential to Narrow Uncertainty in Regional Climate Predictions. Bulletin of the American Meteorological Society 90, 1095–1108 (2009).

Huard, D., Fyke, J., Capellán-Pérez, I., Matthews, H. D. & Partanen, A.-I. Estimating the Likelihood of GHG Concentration Scenarios From Probabilistic Integrated Assessment Model Simulations. Earth's Future 10, e2022EF002715 (2022).

Kao, S.-C. et al. The Third Assessment of the Effects of Climate Change on Federal Hydropower. https://www.osti.gov/biblio/1887712/ (2022) doi:10.2172/1887712.

Karnauskas, K. B., Lundquist, J. K. & Zhang, L. Southward shift of the global wind energy resource under high carbon dioxide emissions. Nature Geosci 11, 38–43 (2018).

Lybarger, N. D. et al. Improving Earth System Model Selection Methodologies for Projecting Hydroclimatic Change: Case Study in the Pacific Northwest. Journal of Geophysical Research: Atmospheres 129, e2023JD039774 (2024).

Martinez, A. & Iglesias, G. Climate change impacts on wind energy resources in North America based on the CMIP6 projections. Science of The Total Environment 806, 150580 (2022).

Martinez, A. & Iglesias, G. Global wind energy resources decline under climate change. Energy 288, 129765 (2024).

Miara, A. et al. Climate-Water Adaptation for Future US Electricity Infrastructure. Environ. Sci. Technol. 53, 14029–14040 (2019).

Parding, K. M. et al. GCMeval – An interactive tool for evaluation and selection of climate model ensembles. Climate Services 18, 100167 (2020).

Pierce, D. W., Barnett, T. P., Santer, B. D. & Gleckler, P. J. Selecting global climate models for regional climate change studies. Proceedings of the National Academy of Sciences 106, 8441–8446 (2009).

Pielke, R. & Ritchie, J. Distorting the view of our climate future: The misuse and abuse of climate pathways and scenarios. Energy Research & Social Science 72, 101890 (2021).

Polade, S. D., Pierce, D. W., Cayan, D. R., Gershunov, A. & Dettinger, M. D. The key role of dry days in changing regional climate and precipitation regimes. Sci Rep 4, 4364 (2014).

Pryor, S. C. & Barthelmie, R. J. Assessing climate change impacts on the near-term stability of the wind energy resource over the United States. Proceedings of the National Academy of Sciences 108, 8167–8171 (2011).

Ralston Fonseca, F. et al. Effects of Climate Change on Capacity Expansion Decisions of an Electricity Generation Fleet in the Southeast U.S. Environ. Sci. Technol. 55, 2522–2531 (2021).

Riahi, K. et al. The Shared Socioeconomic Pathways and their energy, land use, and greenhouse gas emissions implications: An overview. Global Environmental Change 42, 153–168 (2017).

Rastogi, D., Kao, S.-C. & Ashfaq, M. How May the Choice of Downscaling Techniques and Meteorological Reference Observations Affect Future Hydroclimate Projections? Earth's Future 10, e2022EF002734 (2022).

Schwalm, C. R., Glendon, S. & Duffy, P. B. RCP8.5 tracks cumulative CO2 emissions. Proceedings of the National Academy of Sciences 117, 19656–19657 (2020).

Sengupta, M. et al. The National Solar Radiation Data Base (NSRDB). Renewable and Sustainable Energy Reviews 89, 51–60 (2018).

Stenclik, D. *et al. Redefining Resource Adequacy for Modern Power Systems*. https://www.esig.energy/wp-content/uploads/2022/12/ESIG-Redefining-Resource-Adequacy-2021-b.pdf (2021).

Sharp, J. et al. Weather Dataset Needs for Planning and Analyzing Modern Power Systems. https://www.esig.energy/weather-data-for-power-system-planning/ (2023).

Szinai, J. et al. Climate change and its influence on water systems increases the cost of electricity system decarbonization. Preprint at https://doi.org/10.21203/rs.3.rs-3359999/v1 (2023).

Thornton, P. E., R. Shrestha, M. M. Thornton, S.-C. Kao, Y. Wei, and B. E. Wilson (2021), Gridded Daily Weather Data for North America with Comprehensive Uncertainty

Quantification: Daymet Version 4, Nature Sci. Data, 8, 190, https://doi.org/10.1038/s41597-021-00973-0.

Touma, J. S. Dependence of the Wind Profile Power Law on Stability for Various Locations. Journal of the Air Pollution Control Association 27, 863–866 (1977).

US Department of Commerce, N. LLLJP Wind Shear Formula. https://csl.noaa.gov/projects/lamar/windshearformula.html (2020).

Wootten, A., Terando, A., Reich, B. J., Boyles, R. P. & Semazzi, F. Characterizing Sources of Uncertainty from Global Climate Models and Downscaling Techniques. Journal of Applied Meteorology and Climatology 56, 3245–3262 (2017).

Yalew, S. G. et al. Impacts of climate change on energy systems in global and regional scenarios. Nat Energy 5, 794–802 (2020).

References for GCMs

Bader, David C.; Leung, Ruby; Taylor, Mark; McCoy, Renata B. (2022). E3SM-Project E3SM1.0 model output prepared for CMIP6 ScenarioMIP ssp585. Version v20220607.Earth System Grid Federation. https://doi.org/10.22033/ESGF/CMIP6.15178

Bader, David C.; Leung, Ruby; Taylor, Mark; McCoy, Renata B. (2020). E3SM-Project E3SM1.1 model output prepared for CMIP6 ScenarioMIP ssp585. Version v20201117 Earth System Grid Federation. https://doi.org/10.22033/ESGF/CMIP6.15179

Bader, David C.; Leung, Ruby; Taylor, Mark; McCoy, Renata B. (2022). E3SM-Project E3SM1.1ECA model output prepared for CMIP6 ScenarioMIP ssp585. Version v20220325.Earth System Grid Federation. https://doi.org/10.22033/ESGF/CMIP6.15180

Bentsen, Mats; Oliviè, Dirk Jan Leo; Seland, Øyvind; Toniazzo, Thomas; Gjermundsen, Ada; Graff, Lise Seland; Debernard, Jens Boldingh; Gupta, Alok Kumar; He, Yanchun; Kirkevåg, Alf; Schwinger, Jörg; Tjiputra, Jerry; Aas, Kjetil Schanke; Bethke, Ingo; Fan, Yuanchao; Griesfeller, Jan; Grini, Alf; Guo, Chuncheng; Ilicak, Mehmet; Karset, Inger Helene Hafsahl; Landgren, Oskar Andreas; Liakka, Johan; Moseid, Kine Onsum; Nummelin, Aleksi; Spensberger, Clemens; Tang, Hui; Zhang, Zhongshi; Heinze, Christoph; Iversen, Trond; Schulz, Michael (2019). NCC NorESM2-MM model output prepared for CMIP6 ScenarioMIP ssp585. Version v20191108.Earth System Grid Federation. https://doi.org/10.22033/ESGF/CMIP6.8321

Boucher, Olivier; Denvil, Sébastien; Levavasseur, Guillaume; Cozic, Anne; Caubel, Arnaud; Foujols, Marie-Alice; Meurdesoif, Yann; Cadule, Patricia; Devilliers, Marion; Dupont, Eliott; Lurton, Thibaut (2019). IPSL IPSL-CM6A-LR model output prepared for CMIP6 ScenarioMIP ssp585. Version v20190903.Earth System Grid Federation. https://doi.org/10.22033/ESGF/CMIP6.5271

Byun, Young-Hwa; Lim, Yoon-Jin; Shim, Sungbo; Sung, Hyun Min; Sun, Minah; Kim, Jisun; Kim, Byeong-Hyeon; Lee, Jae-Hee; Moon, Hyejin (2019). NIMS-KMA KACE1.0-G model output prepared for CMIP6 ScenarioMIP ssp585. Version v20200317.Earth System Grid Federation. https://doi.org/10.22033/ESGF/CMIP6.8456

Danabasoglu, Gokhan (2019). NCAR CESM2 model output prepared for CMIP6 ScenarioMIP ssp585. Version v20200528.Earth System Grid Federation. https://doi.org/10.22033/ESGF/CMIP6.7768

Danabasoglu, Gokhan (2019). NCAR CESM2-WACCM model output prepared for CMIP6 ScenarioMIP ssp585. Version v20200206.Earth System Grid Federation. https://doi.org/10.22033/ESGF/CMIP6.10115

Dix, Martin; Bi, Daohua; Dobrohotoff, Peter; Fiedler, Russell; Harman, Ian; Law, Rachel; Mackallah, Chloe; Marsland, Simon; O'Farrell, Siobhan; Rashid, Harun; Srbinovsky, Jhan; Sullivan, Arnold; Trenham, Claire; Vohralik, Peter; Watterson, Ian; Williams, Gareth; Woodhouse, Matthew; Bodman, Roger; Dias, Fabio Boeira; Domingues, Catia M.; Hannah, Nicholas; Heerdegen, Aidan; Savita, Abhishek; Wales, Scott; Allen, Chris; Druken, Kelsey; Evans, Ben; Richards, Clare; Ridzwan, Syazwan Mohamed; Roberts, Dale; Smillie, Jon; Snow, Kate; Ward, Marshall; Yang, Rui (2019). CSIRO-ARCCSS ACCESS-CM2 model output prepared for CMIP6 ScenarioMIP ssp585. Version v20210317.Earth System Grid Federation. https://doi.org/10.22033/ESGF/CMIP6.4332

E3SM Project, DOE. Energy Exascale Earth System Model v2.0.2. Computer Software. https://github.com/E3SM-Project/E3SM/releases/tag/v2.0.2. 22 Jul. 2022. Web. doi:10.11578/E3SM/dc.20221118.3.

EC-Earth Consortium (EC-Earth) (2019). EC-Earth-Consortium EC-Earth3 model output prepared for CMIP6 ScenarioMIP ssp585. Version v20200310.Earth System Grid Federation. https://doi.org/10.22033/ESGF/CMIP6.4912

EC-Earth Consortium (EC-Earth) (2021). EC-Earth-Consortium EC-Earth3-CC model output prepared for CMIP6 ScenarioMIP ssp585. Version v20210113.Earth System Grid Federation. https://doi.org/10.22033/ESGF/CMIP6.15636

EC-Earth Consortium (EC-Earth) (2019). EC-Earth-Consortium EC-Earth3-Veg model output prepared for CMIP6 ScenarioMIP ssp585. Version v20200225.Earth System Grid Federation. https://doi.org/10.22033/ESGF/CMIP6.4914

EC-Earth Consortium (EC-Earth) (2020). EC-Earth-Consortium EC-Earth3-Veg-LR model output prepared for CMIP6 ScenarioMIP ssp585. Version v20201201.Earth System Grid Federation. https://doi.org/10.22033/ESGF/CMIP6.4915

Guo, Huan; John, Jasmin G; Blanton, Chris; McHugh, Colleen; Nikonov, Serguei; Radhakrishnan, Aparna; Rand, Kristopher; Zadeh, Niki T.; Balaji, V; Durachta, Jeff; Dupuis, Christopher; Menzel, Raymond; Robinson, Thomas; Underwood, Seth; Vahlenkamp, Hans;

Dunne, Krista A.; Gauthier, Paul PG; Ginoux, Paul; Griffies, Stephen M.; Hallberg, Robert; Harrison, Matthew; Hurlin, William; Lin, Pu; Malyshev, Sergey; Naik, Vaishali; Paulot, Fabien; Paynter, David J; Ploshay, Jeffrey; Schwarzkopf, Daniel M; Seman, Charles J; Shao, Andrew; Silvers, Levi; Wyman, Bruce; Yan, Xiaoqin; Zeng, Yujin; Adcroft, Alistair; Dunne, John P.; Held, Isaac M; Krasting, John P.; Horowitz, Larry W.; Milly, Chris; Shevliakova, Elena; Winton, Michael; Zhao, Ming; Zhang, Rong (2018). NOAA-GFDL GFDL-CM4 model output prepared for CMIP6 ScenarioMIP ssp585. Version v20180701.Earth System Grid Federation. https://doi.org/10.22033/ESGF/CMIP6.9268

Jackson, Laura (2020). MOHC HadGEM3-GC31-MM model output prepared for CMIP6 ScenarioMIP ssp585. Version v20200515.Earth System Grid Federation. https://doi.org/10.22033/ESGF/CMIP6.10902

John, Jasmin G; Blanton, Chris; McHugh, Colleen; Radhakrishnan, Aparna; Rand, Kristopher; Vahlenkamp, Hans; Wilson, Chandin; Zadeh, Niki T.; Dunne, John P.; Dussin, Raphael; Horowitz, Larry W.; Krasting, John P.; Lin, Pu; Malyshev, Sergey; Naik, Vaishali; Ploshay, Jeffrey; Shevliakova, Elena; Silvers, Levi; Stock, Charles; Winton, Michael; Zeng, Yujin (2018). NOAA-GFDL GFDL-ESM4 model output prepared for CMIP6 ScenarioMIP ssp585. Version v20190726.Earth System Grid Federation. https://doi.org/10.22033/ESGF/CMIP6.8706

Lee, Wei-Liang; Liang, Hsin-Chien (2020). AS-RCEC TaiESM1.0 model output prepared for CMIP6 ScenarioMIP ssp585. Version v20200902.Earth System Grid Federation. https://doi.org/10.22033/ESGF/CMIP6.9823

Lovato, Tomas; Peano, Daniele (2020). CMCC CMCC-CM2-SR5 model output prepared for CMIP6 ScenarioMIP ssp585. Version v20200622.Earth System Grid Federation. https://doi.org/10.22033/ESGF/CMIP6.3896

Lovato, Tomas; Peano, Daniele; Butenschön, Momme (2021). CMCC CMCC-ESM2 model output prepared for CMIP6 ScenarioMIP ssp585. Version v20210126.Earth System Grid Federation. https://doi.org/10.22033/ESGF/CMIP6.13259

Rong, Xinyao (2019). CAMS CAMS-CSM1.0 model output prepared for CMIP6 ScenarioMIP ssp585. Version v20191106.Earth System Grid Federation. https://doi.org/10.22033/ESGF/CMIP6.11052

Semmler, Tido; Danilov, Sergey; Rackow, Thomas; Sidorenko, Dmitry; Barbi, Dirk; Hegewald, Jan; Pradhan, Himansu Kesari; Sein, Dmitri; Wang, Qiang; Jung, Thomas (2019). AWI AWI-CM1.1MR model output prepared for CMIP6 ScenarioMIP ssp585. Version v20190529.Earth System Grid Federation. https://doi.org/10.22033/ESGF/CMIP6.2817

Shiogama, Hideo; Abe, Manabu; Tatebe, Hiroaki (2019). MIROC MIROC6 model output prepared for CMIP6 ScenarioMIP ssp585. Version v20191016.Earth System Grid Federation. https://doi.org/10.22033/ESGF/CMIP6.5771

Schupfner, Martin; Wieners, Karl-Hermann; Wachsmann, Fabian; Steger, Christian; Bittner, Matthias; Jungclaus, Johann; Früh, Barbara; Pankatz, Klaus; Giorgetta, Marco; Reick, Christian; Legutke, Stephanie; Esch, Monika; Gayler, Veronika; Haak, Helmuth; de Vrese, Philipp; Raddatz, Thomas; Mauritsen, Thorsten; von Storch, Jin-Song; Behrens, Jörg; Brovkin, Victor; Claussen, Martin; Crueger, Traute; Fast, Irina; Fiedler, Stephanie; Hagemann, Stefan; Hohenegger, Cathy; Jahns, Thomas; Kloster, Silvia; Kinne, Stefan; Lasslop, Gitta; Kornblueh, Luis; Marotzke, Jochem; Matei, Daniela; Meraner, Katharina; Mikolajewicz, Uwe; Modali, Kameswarrao; Müller, Wolfgang; Nabel, Julia; Notz, Dirk; Peters-von Gehlen, Karsten; Pincus, Robert; Pohlmann, Holger; Pongratz, Julia; Rast, Sebastian; Schmidt, Hauke; Schnur, Reiner; Schulzweida, Uwe; Six, Katharina; Stevens, Bjorn; Voigt, Aiko; Roeckner, Erich (2019). DKRZ MPI-ESM1.2-HR model output prepared for CMIP6 ScenarioMIP ssp585. Version v20190710.Earth System Grid Federation. https://doi.org/10.22033/ESGF/CMIP6.4403

Swart, Neil Cameron; Cole, Jason N.S.; Kharin, Viatcheslav V.; Lazare, Mike; Scinocca, John F.; Gillett, Nathan P.; Anstey, James; Arora, Vivek; Christian, James R.; Jiao, Yanjun; Lee, Warren G.; Majaess, Fouad; Saenko, Oleg A.; Seiler, Christian; Seinen, Clint; Shao, Andrew; Solheim, Larry; von Salzen, Knut; Yang, Duo; Winter, Barbara; Sigmond, Michael (2019). CCCma CanESM5 model output prepared for CMIP6 ScenarioMIP ssp585. Version v20190429.Earth System Grid Federation. https://doi.org/10.22033/ESGF/CMIP6.3696

Tang, Qi, Jean-Christophe Golaz, Luke P. Van Roekel, Mark A. Taylor, Wuyin Lin, Benjamin R. Hillman, Paul A. Ullrich, et al. "The Fully Coupled Regionally Refined Model of E3SM Version 2: Overview of the Atmosphere, Land, and River Results." Geoscientific Model Development 16, no. 13 (July 13, 2023): 3953–95. https://doi.org/10.5194/gmd-16-3953-2023.

Voldoire, Aurore (2019). CNRM-CERFACS CNRM-ESM2-1 model output prepared for CMIP6 ScenarioMIP ssp585. Version v20191021.Earth System Grid Federation. https://doi.org/10.22033/ESGF/CMIP6.4226

Volodin, Evgeny; Mortikov, Evgeny; Gritsun, Andrey; Lykossov, Vasily; Galin, Vener; Diansky, Nikolay; Gusev, Anatoly; Kostrykin, Sergey; Iakovlev, Nikolay; Shestakova, Anna; Emelina, Svetlana (2019). INM INM-CM4-8 model output prepared for CMIP6 ScenarioMIP ssp585. Version v20190603.Earth System Grid Federation. https://doi.org/10.22033/ESGF/CMIP6.12337

Volodin, Evgeny; Mortikov, Evgeny; Gritsun, Andrey; Lykossov, Vasily; Galin, Vener; Diansky, Nikolay; Gusev, Anatoly; Kostrykin, Sergey; Iakovlev, Nikolay; Shestakova, Anna; Emelina, Svetlana (2019). INM INM-CM5-0 model output prepared for CMIP6 ScenarioMIP ssp585. Version v20190724.Earth System Grid Federation. https://doi.org/10.22033/ESGF/CMIP6.12338

Wieners, Karl-Hermann; Giorgetta, Marco; Jungclaus, Johann; Reick, Christian; Esch, Monika; Bittner, Matthias; Gayler, Veronika; Haak, Helmuth; de Vrese, Philipp; Raddatz, Thomas; Mauritsen, Thorsten; von Storch, Jin-Song; Behrens, Jörg; Brovkin, Victor; Claussen, Martin; Crueger, Traute; Fast, Irina; Fiedler, Stephanie; Hagemann, Stefan; Hohenegger, Cathy; Jahns, Thomas; Kloster, Silvia; Kinne, Stefan; Lasslop, Gitta; Kornblueh, Luis; Marotzke, Jochem;

Matei, Daniela; Meraner, Katharina; Mikolajewicz, Uwe; Modali, Kameswarrao; Müller, Wolfgang; Nabel, Julia; Notz, Dirk; Peters-von Gehlen, Karsten; Pincus, Robert; Pohlmann, Holger; Pongratz, Julia; Rast, Sebastian; Schmidt, Hauke; Schnur, Reiner; Schulzweida, Uwe; Six, Katharina; Stevens, Bjorn; Voigt, Aiko; Roeckner, Erich (2019). MPI-M MPI-ESM1.2-LR model output prepared for CMIP6 ScenarioMIP ssp585. Version v20190710.Earth System Grid Federation. https://doi.org/10.22033/ESGF/CMIP6.6705

Yu, Yongqiang (2019). CAS FGOALS-f3-L model output prepared for CMIP6 ScenarioMIP ssp585. Version v20191013.Earth System Grid Federation. https://doi.org/10.22033/ESGF/CMIP6.3502

Yukimoto, Seiji; Koshiro, Tsuyoshi; Kawai, Hideaki; Oshima, Naga; Yoshida, Kohei; Urakawa, Shogo; Tsujino, Hiroyuki; Deushi, Makoto; Tanaka, Taichu; Hosaka, Masahiro; Yoshimura, Hiromasa; Shindo, Eiki; Mizuta, Ryo; Ishii, Masayoshi; Obata, Atsushi; Adachi, Yukimasa (2019). MRI MRI-ESM2.0 model output prepared for CMIP6 ScenarioMIP ssp585. Version v20191108.Earth System Grid Federation. https://doi.org/10.22033/ESGF/CMIP6.6929

Xin, Xiaoge; Wu, Tongwen; Shi, Xueli; Zhang, Fang; Li, Jianglong; Chu, Min; Liu, Qianxia; Yan, Jinghui; Ma, Qiang; Wei, Min (2019). BCC BCC-CSM2MR model output prepared for CMIP6 ScenarioMIP ssp585. Version v20190318.Earth System Grid Federation. https://doi.org/10.22033/ESGF/CMIP6.3050

Appendix A. NERC Region: Midwest Reliability Organization (MRO)

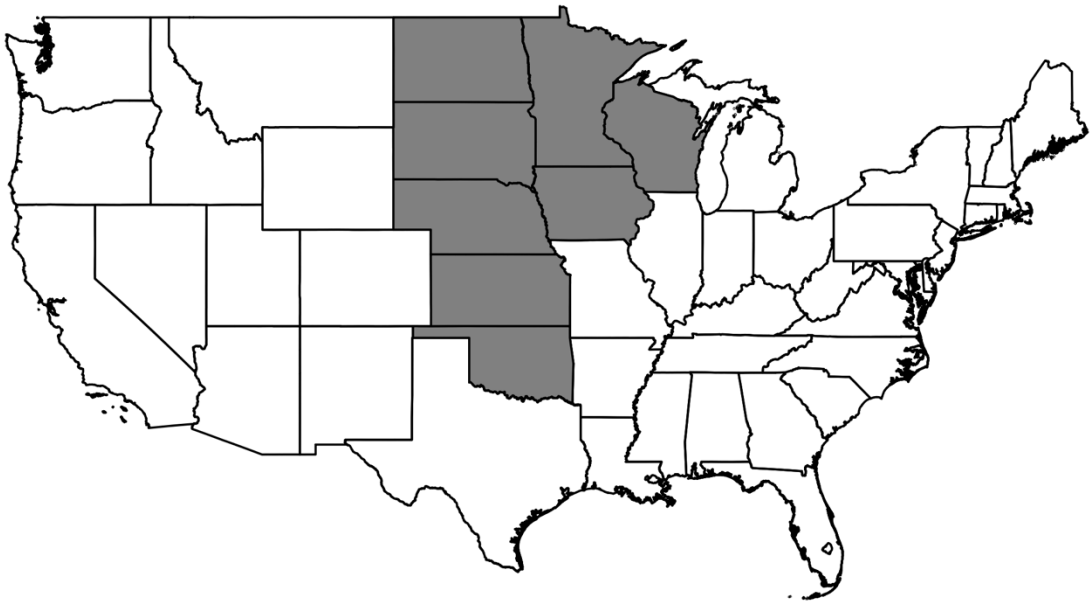

Figure 9. NERC Region: MRO (included states shaded in grey).

Note that we used a simple state mask, and the region may not perfectly match the spatial boundary of the true NERC region.

Table 4. Summary of historical GCM skill using KS statistic and bias metrics for MRO. Values for a given metric in each row are ranked from best to worst historical skill (dark blue to dark red).

	MPI-ESM1-2-HR	TaiESM1	EC-Earth3-Veg	EC-Earth3-CC	GFDL-CM4	EC-Earth3	MRI-ESM2-0	GFDL-ESM4	NorESM2-MM	CESM2-WACCM	CESM2	INM-CM5-0	INM-CM4-8
T2M KS	0.04	0.03	0.04	0.03	0.04	0.05	0.05	0.04	0.08	0.07	0.06	0.04	0.05
T2M Bias P50 (°C)	0.22	1.34	-0.94	-0.71	-1.59	-1.66	-0.11	-2.04	2.07	2.39	2.41	0.68	1.71
T2M Max KS	0.04	0.05	0.04	0.04	0.05	0.04	0.05	0.05	0.10	0.07	0.09	0.07	0.08
T2M Max Bias P95 (°C)	0.73	1.74	-0.18	-0.10	-1.35	-0.59	-0.72	-0.13	6.24	-1.06	6.01	4.05	6.51
T2M Min KS	0.05	0.03	0.04	0.04	0.03	0.05	0.05	0.04	0.07	0.09	0.08	0.05	0.05
T2M Min Bias P5 (°C)	0.74	-0.75	-1.91	-2.04	1.34	-3.70	4.73	2.28	0.59	9.21	4.62	2.80	5.17
RH2M KS	0.14	0.08	0.07	0.07	0.06	0.07	0.08	0.12	0.13	0.11	0.11	0.14	0.16
RH2M Bias P50 (%)	5.7	4.6	9.3	10.1	10.3	10.2	0.9	18.0	-19.8	-16.1	-16.1	-2.3	-7.5
RH2M Max KS	0.23		0.07	0.06	0.09	0.06	0.19					0.24	0.27
RH2M Max Bias P95 (%)	9.74		0.14	0.19	5.33	0.19	1.43					3.44	3.39
RH2M Min KS	0.10		0.08	0.08	0.07	0.08	0.06					0.09	0.10
RH2M Min Bias P5 (%)	-0.3		7.0	8.4	1.4	10.3	9.4					-13.3	-19.6
PR KS	0.08	0.09	0.09	0.09	0.11	0.09	0.12	0.12	0.08	0.09	0.09	0.15	0.13
PR Bias P50 (%)	0.82	0.73	0.22	0.24	2.48	0.22	2.55	3.43	0.71	0.91	0.82	5.05	4.11
GHI KS	0.03	0.04	0.07	0.08	0.03	0.07	0.04	0.05	0.04	0.04	0.04	0.03	0.03
GHI Bias P50 (%)	-0.1	1.4	2.8	-1.2	-1.8	1.4	9.9	-8.0	18.1	11.8	12.8	6.7	8.8
WS 100m KS	0.13	0.04	0.11	0.11	0.04	0.08	0.13	0.04	0.13	0.25	0.25	0.21	0.20
WS 100m Bias P50 (%)	-8.9	-27.6	-3.6	-3.8	-21.6	-20.0	-49.3	-30.2	0.8	44.8	44.2	-65.7	-64.7
Process Skill	0.09	0.29	0.06	0.05	0.06	0.06	0.34	0.14	0.04	0.16	0.20	0.82	0.85

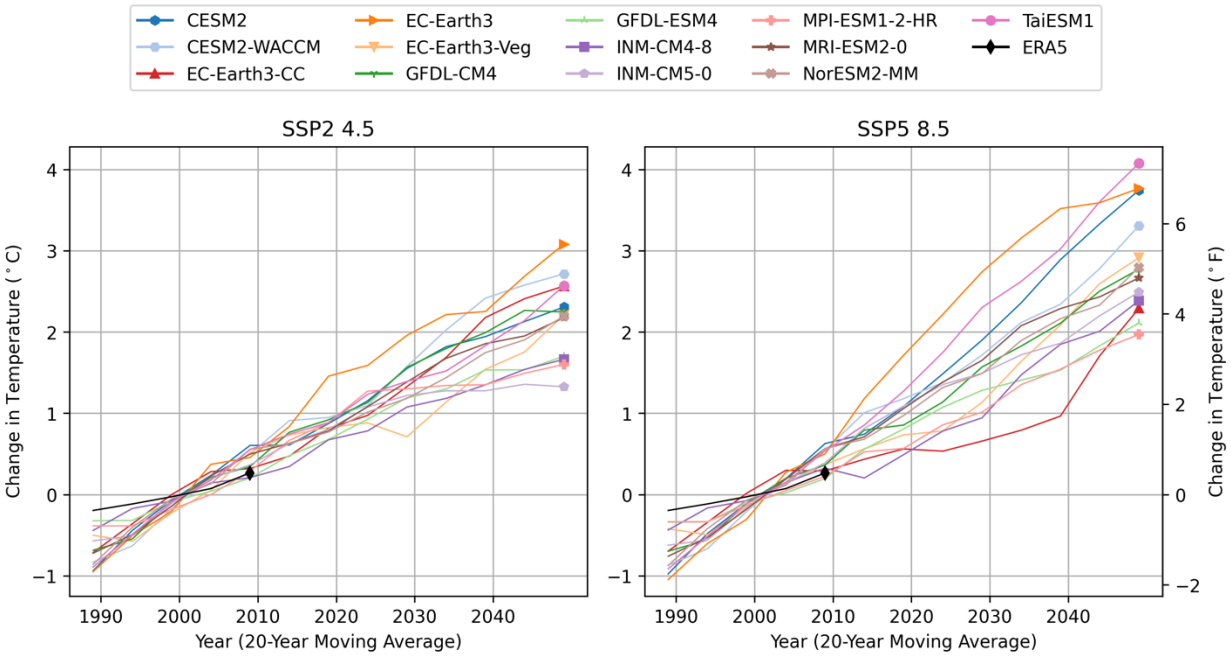

Figure 10. Comparison of GCM trends in changes to daily average near-surface air temperature for MRO.

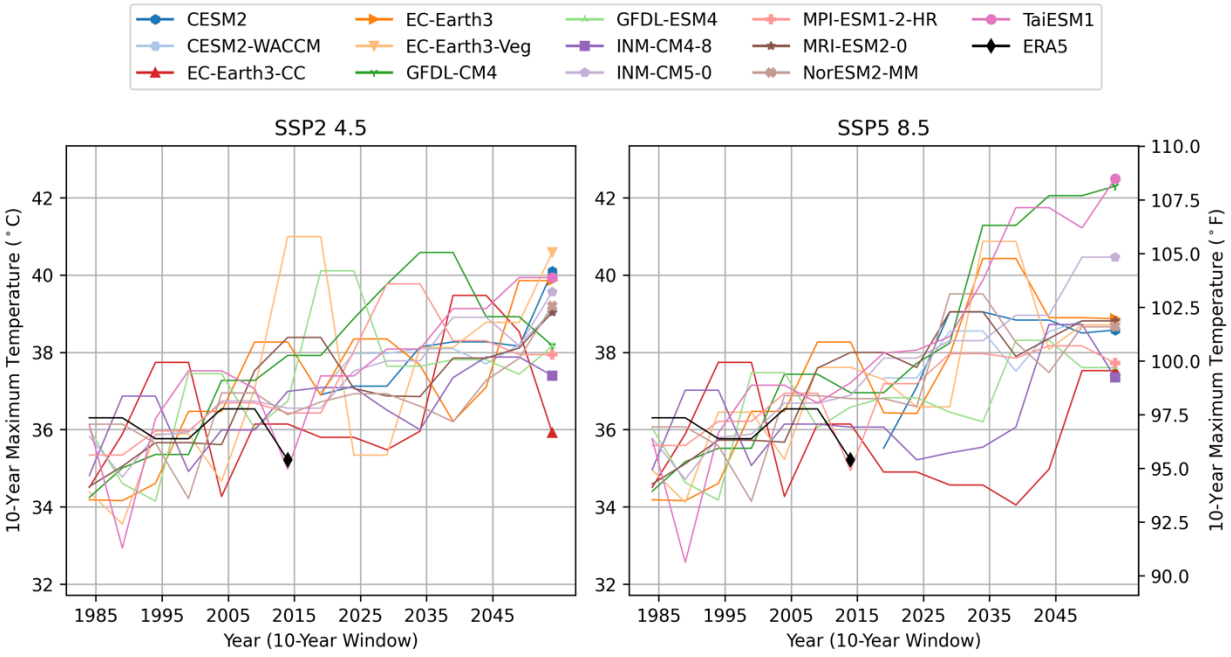

Figure 11. Comparison of GCM daily maximum air temperature events for MRO.

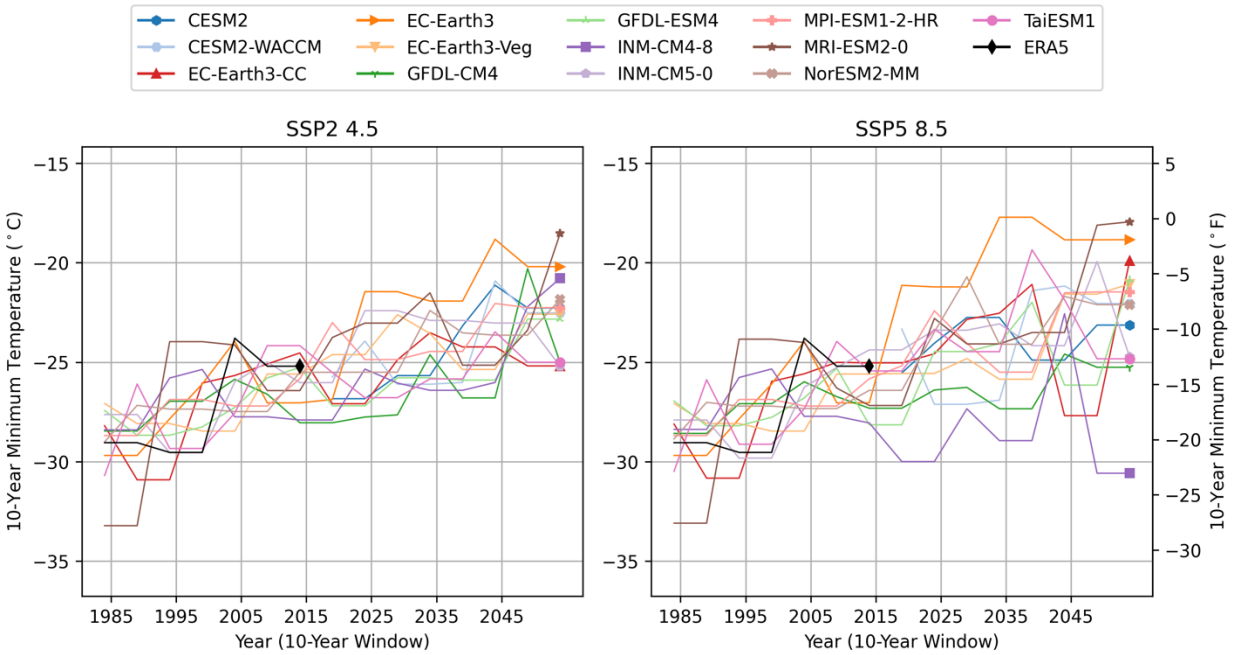

Figure 12. Comparison of GCM daily minimum air temperature events for MRO.

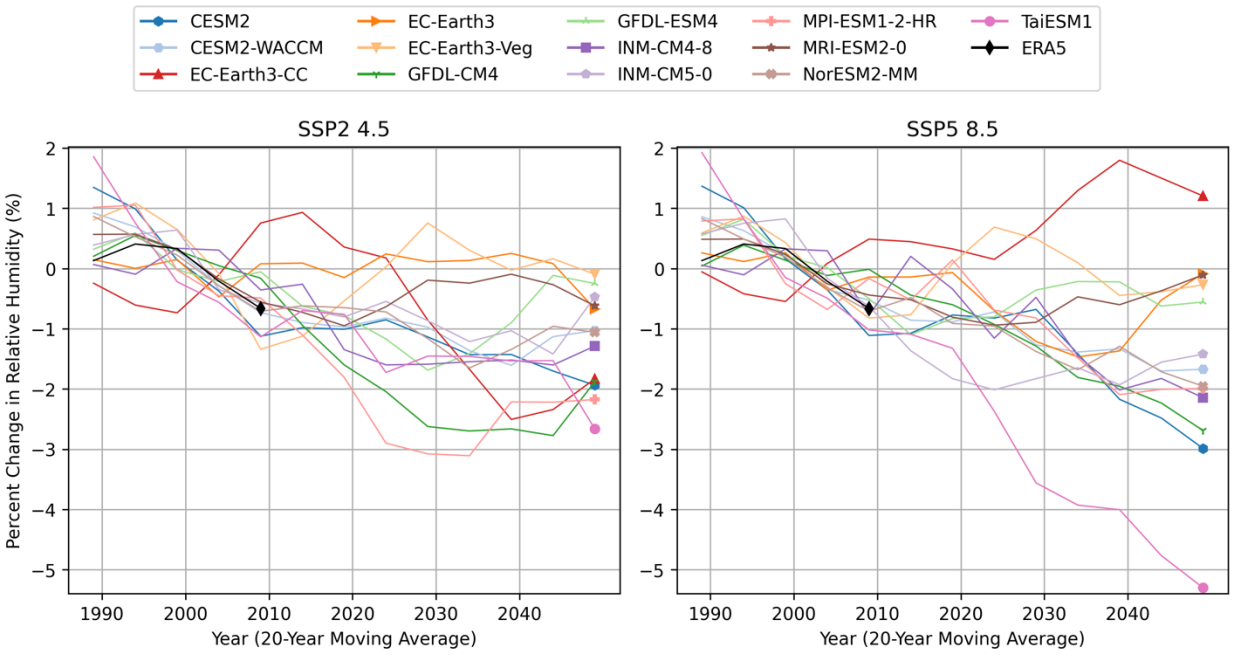

Figure 13. Comparison of GCM trends in changes to daily average near-surface relative humidity for MRO.

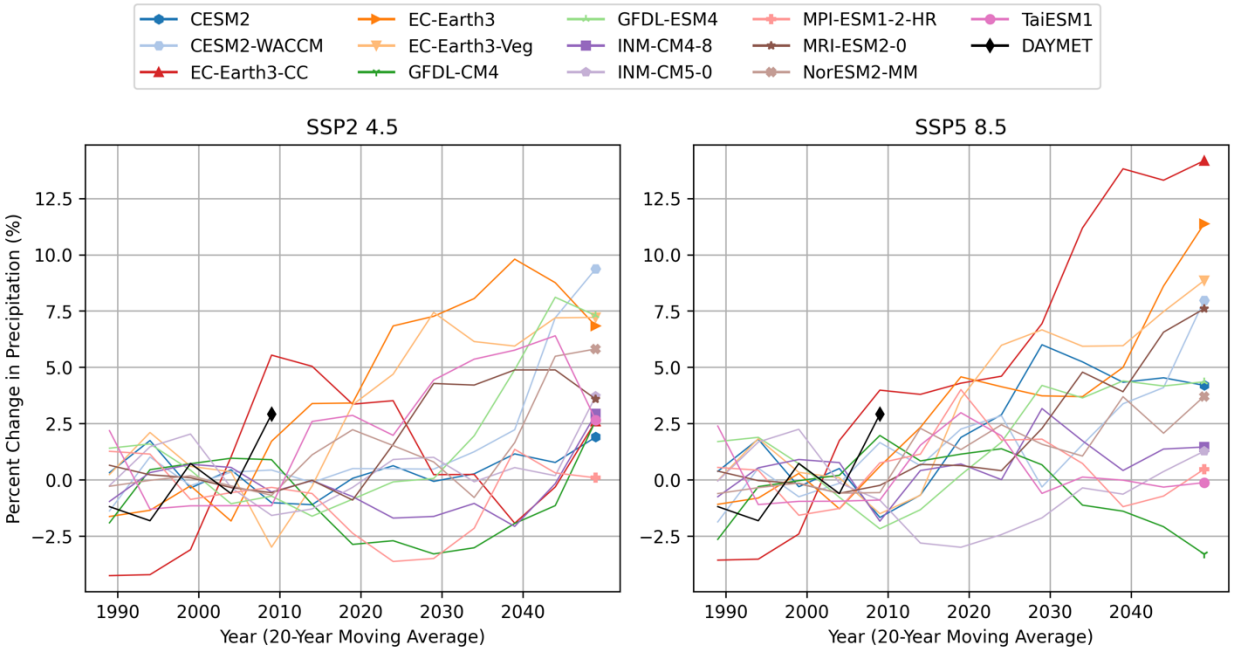

Figure 14. Comparison of GCM trends in changes to daily average precipitation for MRO.

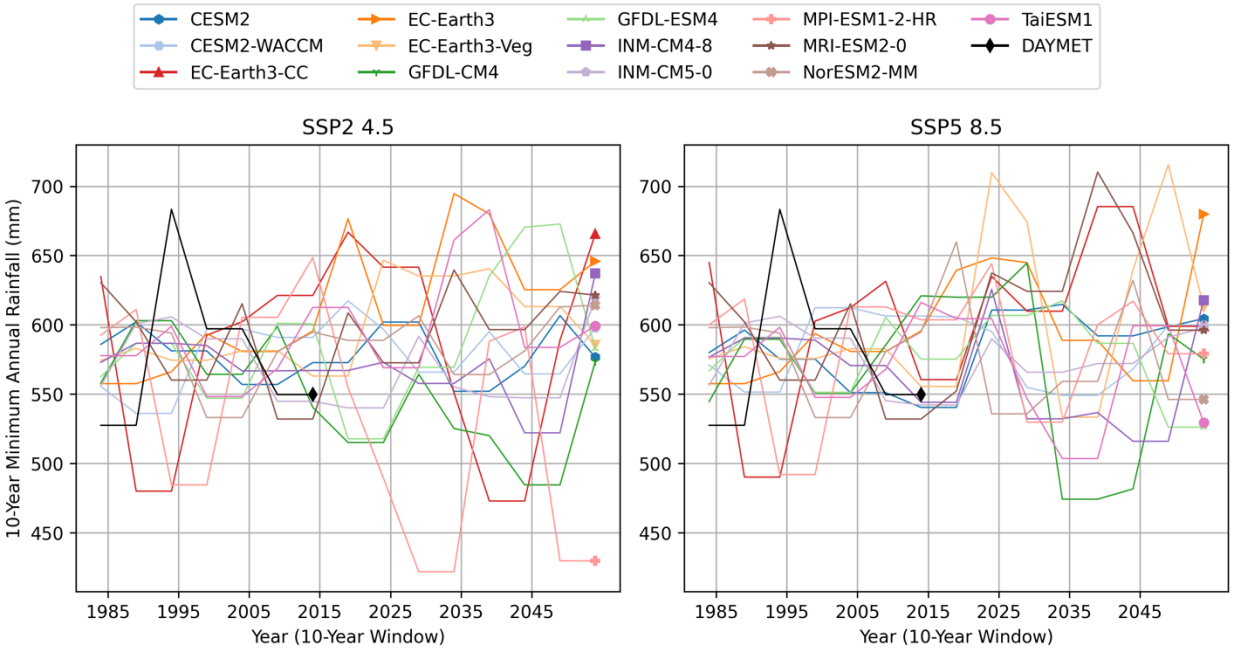

Figure 15. Comparison of GCM minimum annual rainfalls for MRO.

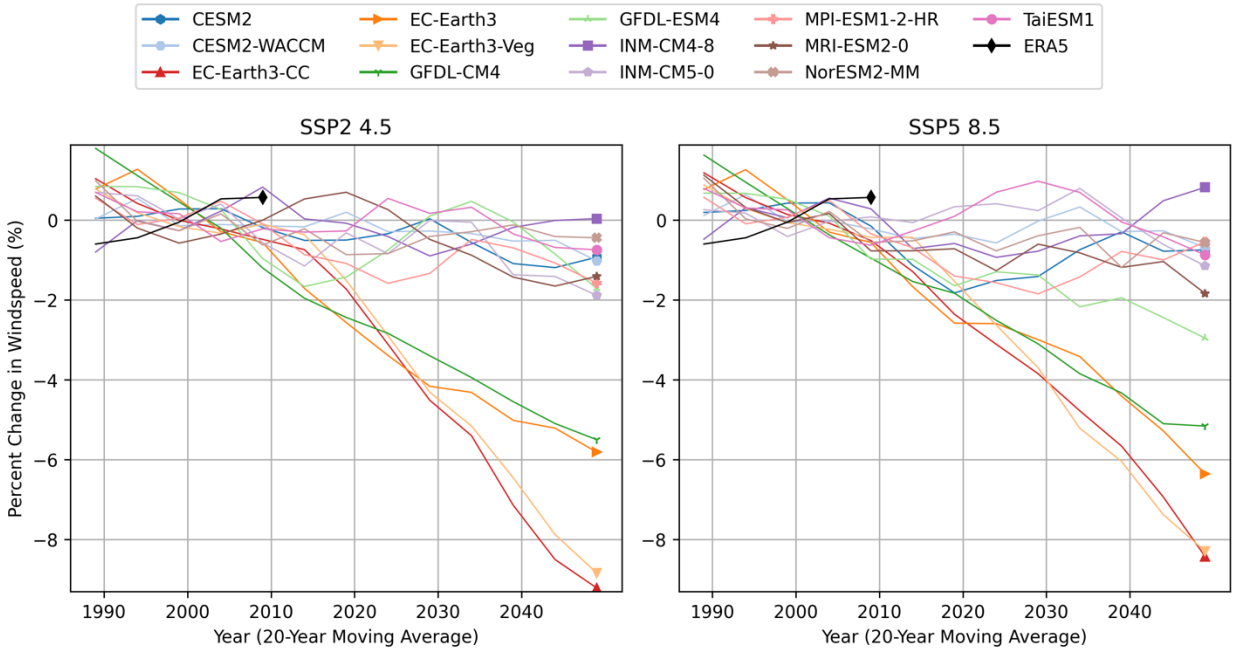

Figure 16. Comparison of GCM trends in changes to daily average 100-meter windspeed for MRO.

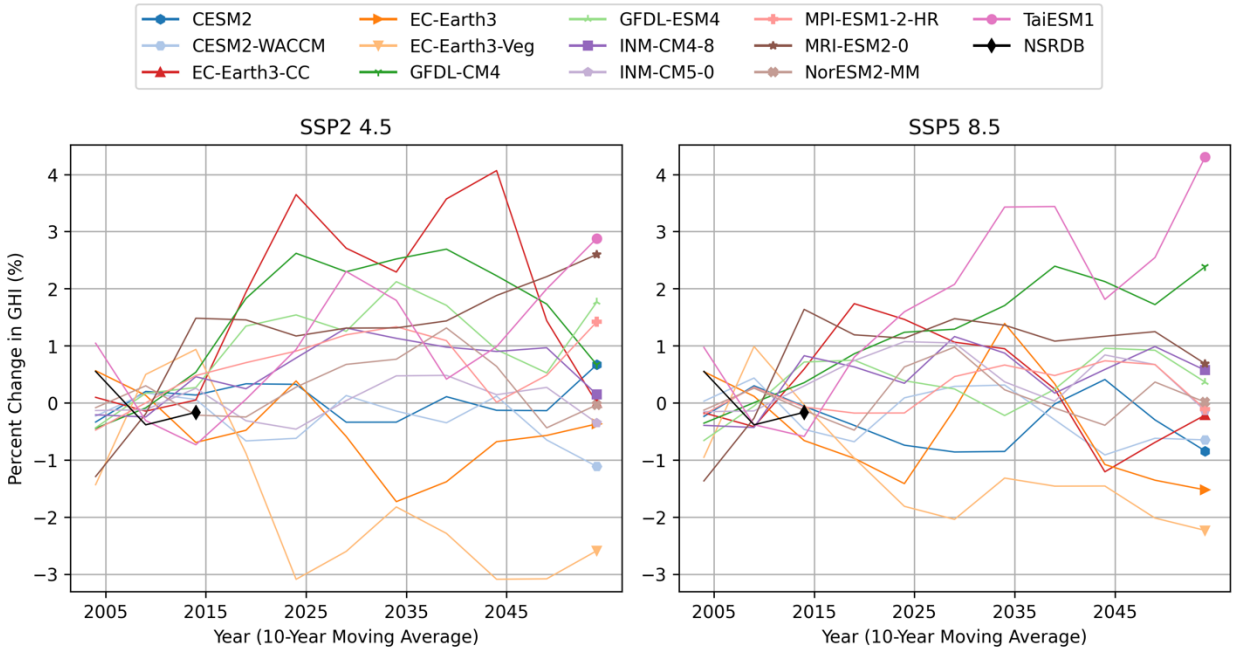

Figure 17. Comparison of GCM trends in changes to daily average GHI for MRO.

Appendix B. NERC Region: Northeast Power Coordinating Council (NPCC)

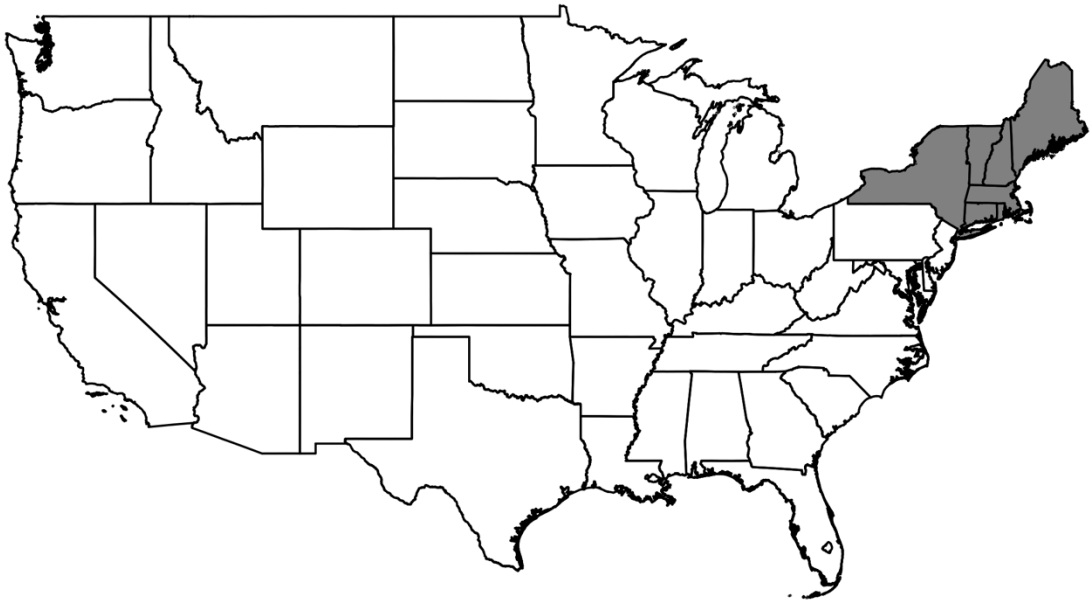

Figure 18. NERC Region: NPCC (included states shaded in grey).

Note that we used a simple state mask, and the region may not perfectly match the spatial boundary of the true NERC region.

Table 5. Summary of historical GCM skill using KS statistic and bias metrics for NPCC. Values for a given metric in each row are ranked from best to worst historical skill (dark blue to dark red).

	EC-Earth3-Veg	GFDL-CM4	EC-Earth3-CC	EC-Earth3	TaiESM1	NorESM2-MM	MPI-ESM1-2-HR	CESM2-WACCM	CESM2	MRI-ESM2-0	GFDL-ESM4	INM-CM5-0	INM-CM4-8
T2M KS	0.02	0.02	0.02	0.02	0.04	0.05	0.05	0.04	0.04	0.04	0.02	0.03	0.05
T2M Bias P50 (°C)	-0.65	-1.43	-0.45	-1.22	1.15	-0.42	-0.64	0.68	0.50	-0.75	-2.27	0.97	2.29
T2M Max KS	0.02	0.02	0.02	0.03	0.04	0.07	0.04	0.04	0.06	0.03	0.03	0.05	0.07
T2M Max Bias P95 (°C)	-1.01	-2.57	-0.80	-1.46	1.64	3.24	-1.85	-2.75	2.52	-0.28	-2.86	-1.44	-0.82
T2M Min KS	0.02	0.03	0.02	0.03	0.04	0.04	0.05	0.07	0.06	0.04	0.02	0.04	0.05
T2M Min Bias P5 (°C)	-2.04	-1.62	-2.13	-3.34	-4.38	-1.05	-1.93	6.43	2.42	-2.68	-0.15	-0.37	2.47
RH2M KS	0.04	0.05	0.04	0.04	0.08	0.05	0.08	0.05	0.05	0.06	0.14	0.12	0.12
RH2M Bias P50 (%)	5.3	8.2	5.6	4.9	3.1	-2.2	17.0	-0.5	-0.8	10.4	19.4	4.6	3.9
RH2M Max KS	0.10	0.17	0.10	0.09			0.11			0.21		0.22	0.23
RH2M Max Bias P95 (%)	0.51	7.24	0.53	0.50			9.76			3.64		2.66	2.73
RH2M Min KS	0.04	0.05	0.04	0.04			0.08			0.07		0.08	0.08
RH2M Min Bias P5 (%)	16.0	2.0	16.2	15.5			20.5			14.1		-10.0	-11.1
PR KS	0.08	0.09	0.09	0.08	0.07	0.08	0.09	0.08	0.08	0.09	0.12	0.11	0.10
PR Bias P50 (%)	7.44	5.35	8.41	7.68	-2.87	-1.17	6.38	0.73	0.48	6.95	10.82	4.79	4.32
GHI KS	0.05	0.03	0.05	0.05	0.05	0.06	0.04	0.05	0.05	0.06	0.02	0.02	0.02
GHI Bias P50 (%)	3.01	1.18	3.49	3.36	4.16	11.20	-7.66	5.45	5.83	7.48	-6.40	12.59	13.46
WS 100m KS	0.07	0.05	0.06	0.06	0.04	0.10	0.12	0.27	0.27	0.10	0.07	0.22	0.22
WS 100m Bias P50 (%)	0.5	-19.7	0.1	-21.4	-19.9	-5.2	-7.2	53.6	54.2	-43.4	-20.9	-64.1	-63.9
Process Skill	0.06	0.06	0.05	0.06	0.29	0.04	0.09	0.16	0.20	0.34	0.14	0.82	0.85

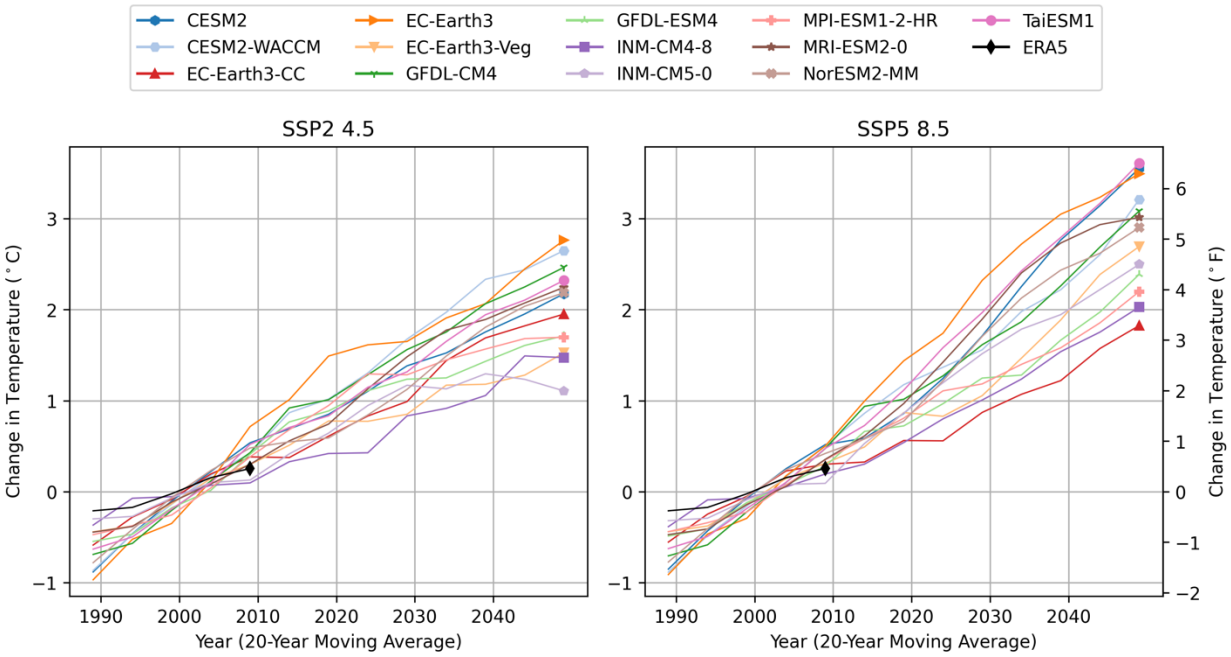

Figure 19. Comparison of GCM trends in changes to daily average near-surface air temperature for NPCC.

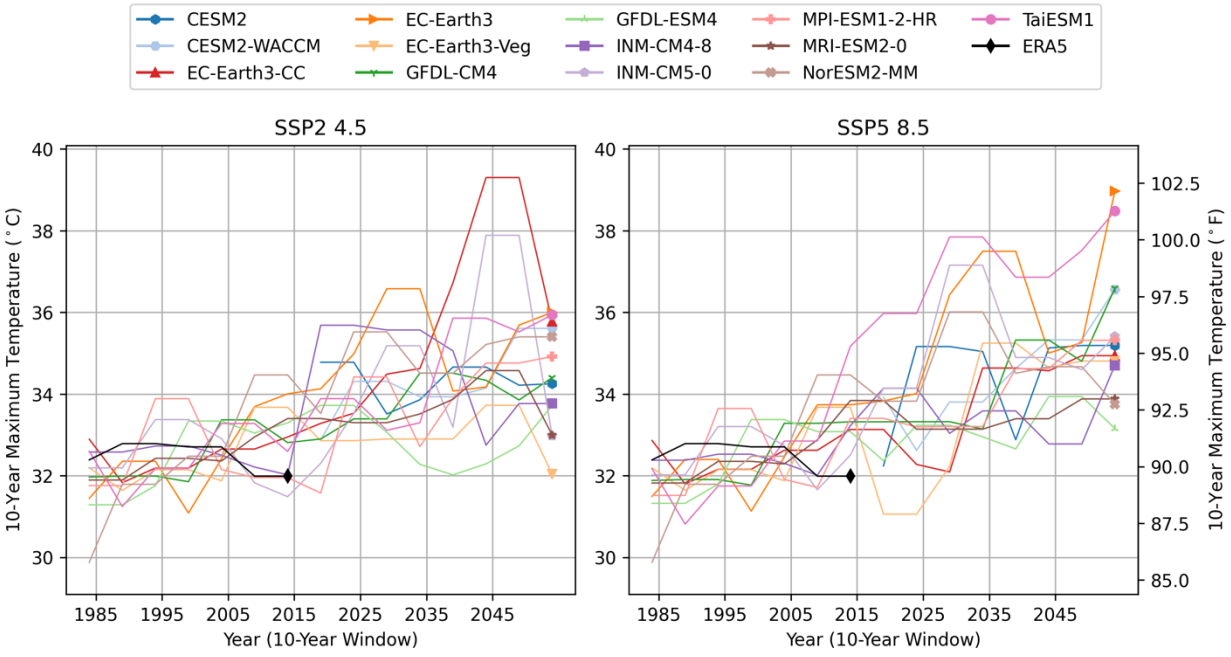

Figure 20. Comparison of GCM daily maximum air temperature events for NPCC.

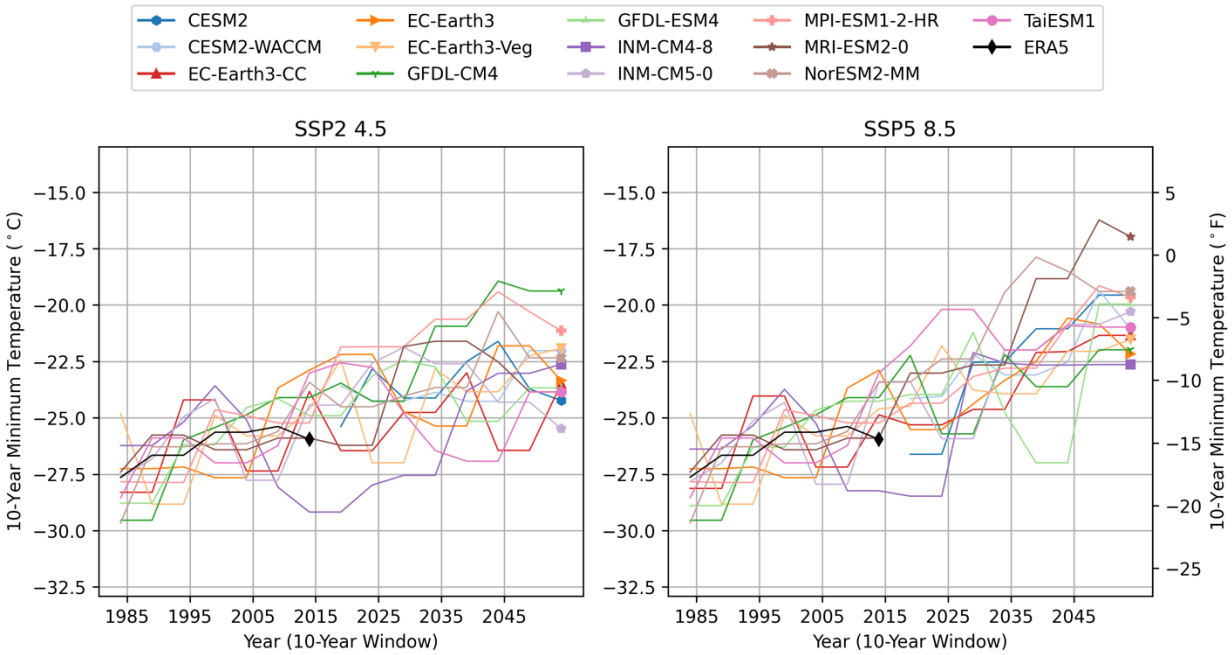

Figure 21. Comparison of GCM daily minimum air temperature events for NPCC.

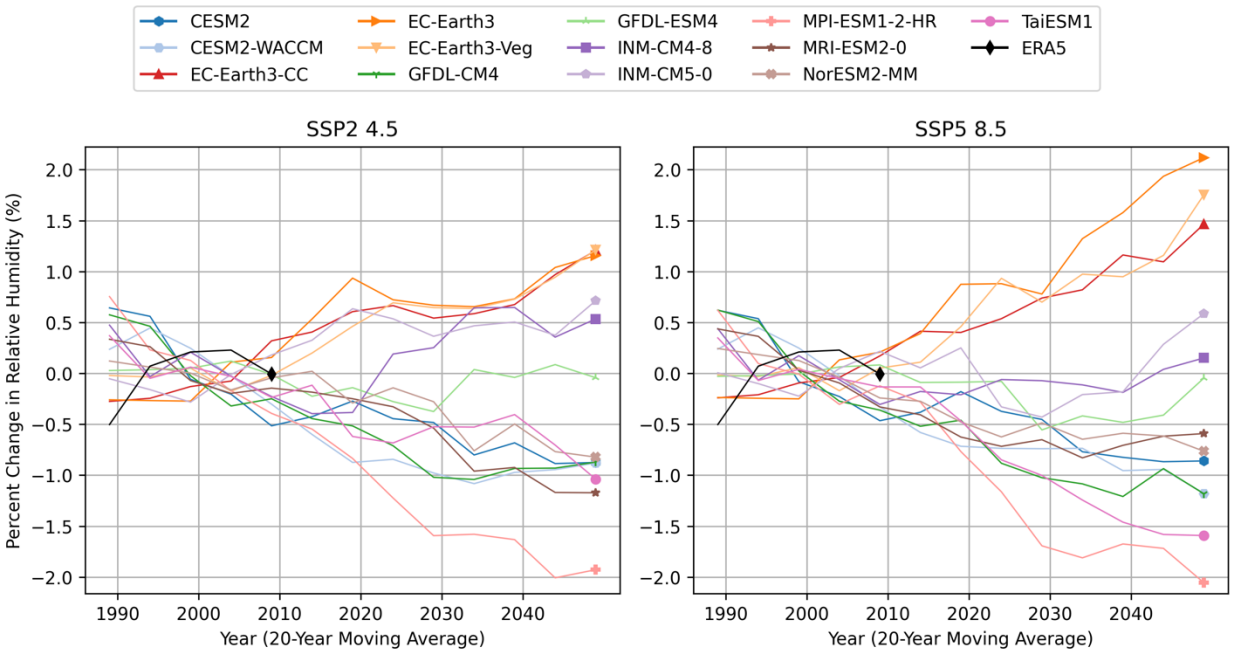

Figure 22. Comparison of GCM trends in changes to daily average near-surface relative humidity for NPCC.

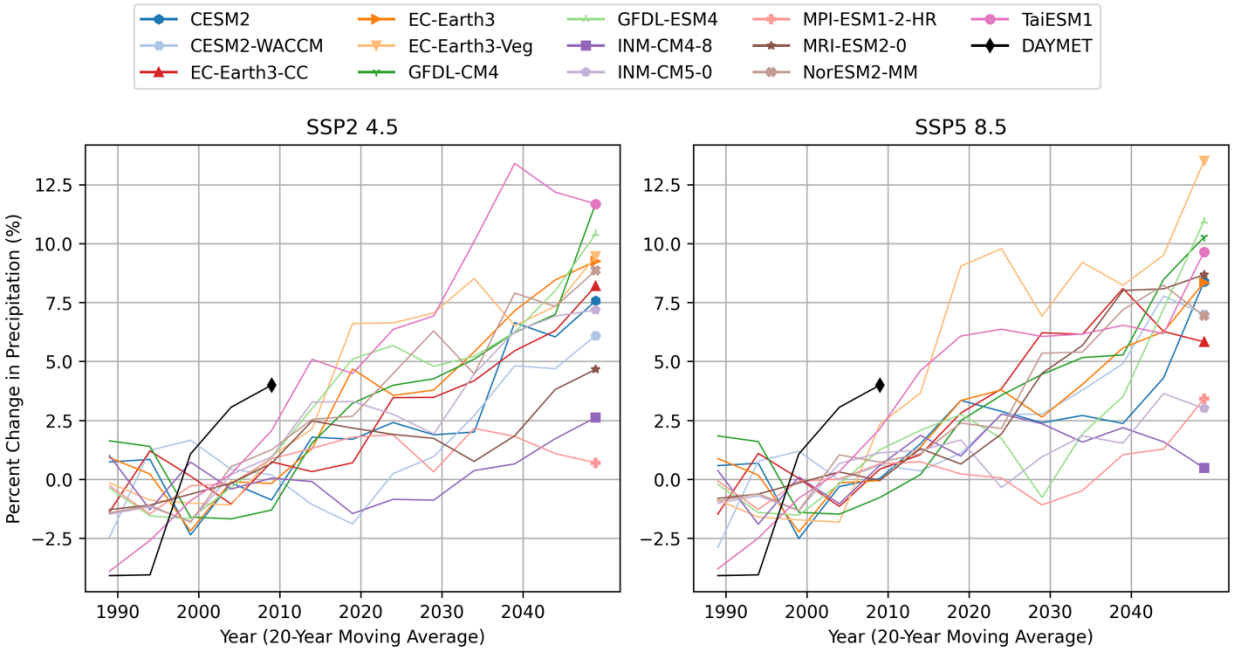

Figure 23. Comparison of GCM trends in changes to daily average precipitation for NPCC.

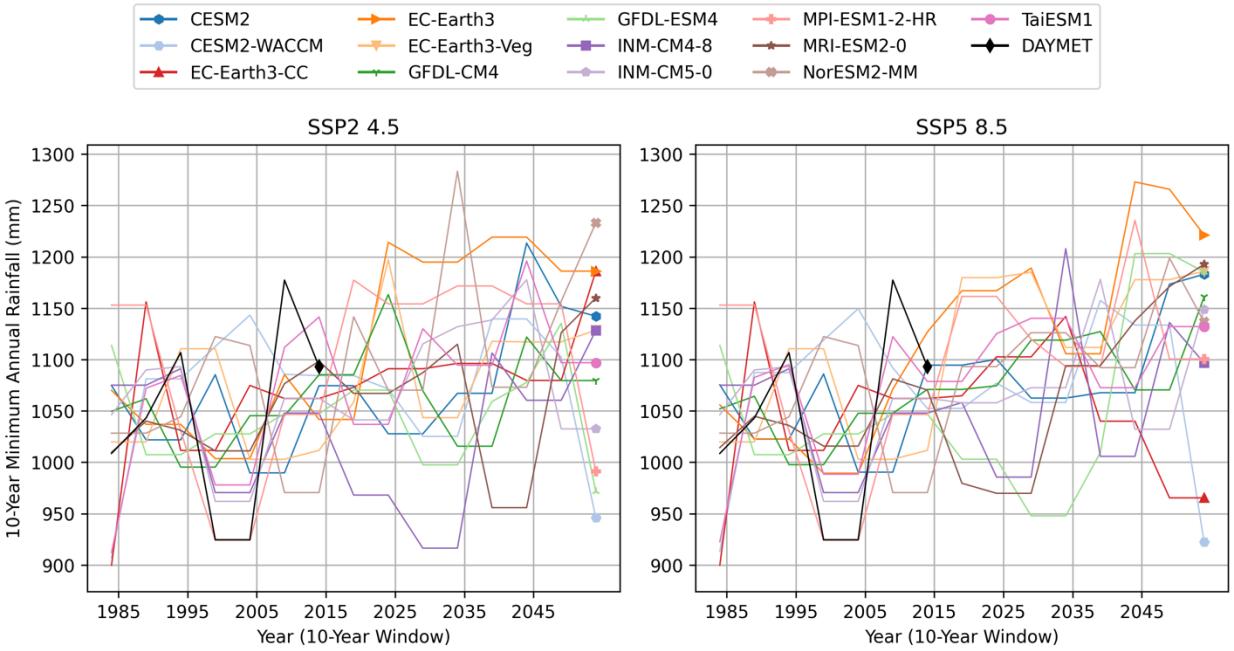

Figure 24. Comparison of GCM minimum annual rainfalls for NPCC.

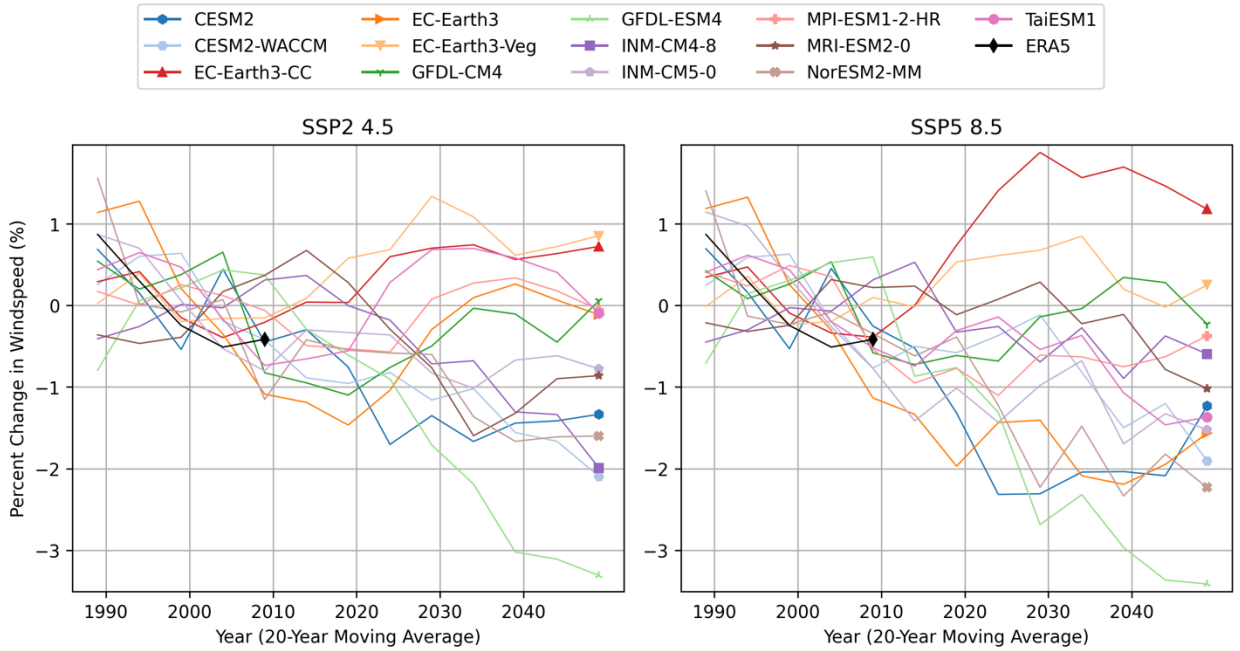

Figure 25. Comparison of GCM trends in changes to daily average 100-meter windspeed for NPCC.

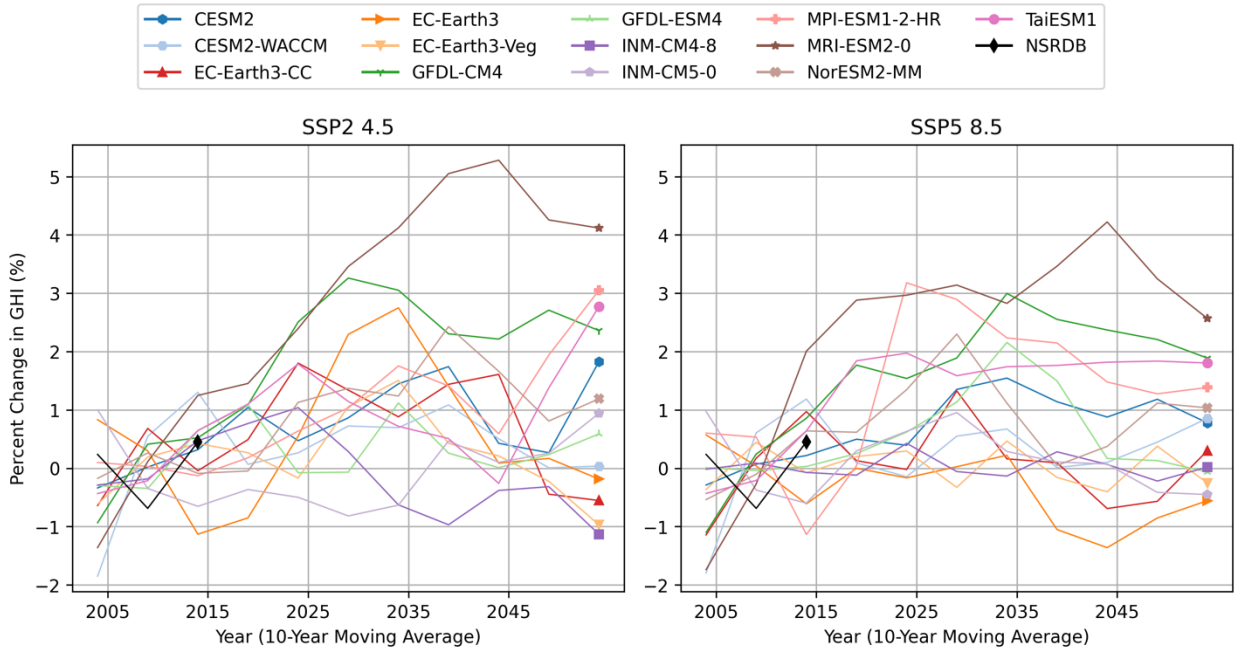

Figure 26. Comparison of GCM trends in changes to daily average GHI for NPCC.

Appendix C. NERC Region: Reliability First (RF)

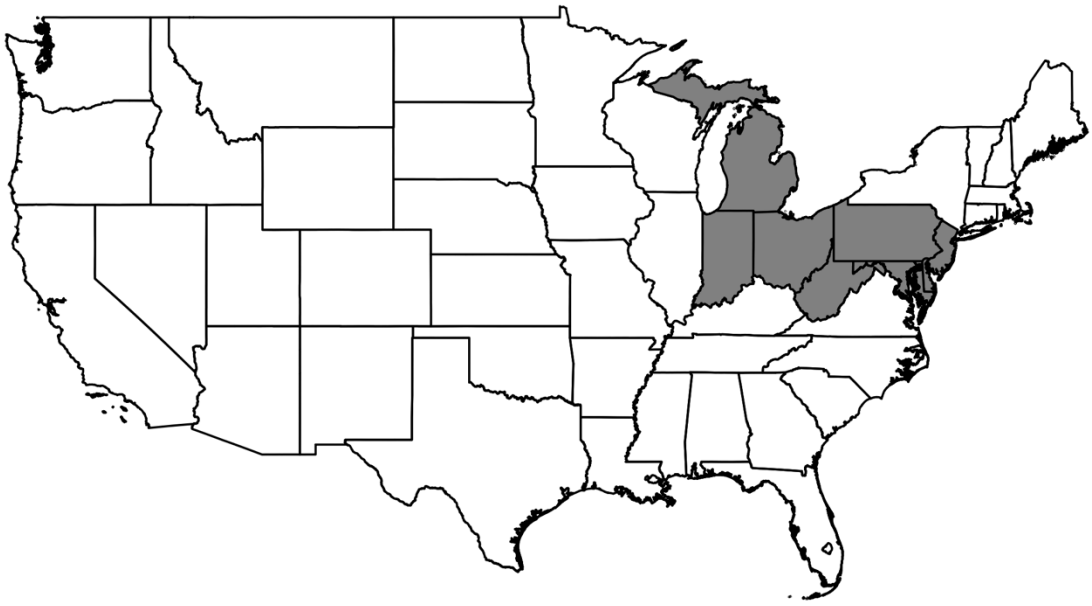

Figure 27. NERC Region: RF (included states shaded in grey).

Note that we used a simple state mask, and the region may not perfectly match the spatial boundary of the true NERC region.

Table 6. Summary of historical GCM skill using KS statistic and bias metrics for RF. Values for a given metric in each row are ranked from best to worst historical skill (dark blue to dark red).

	GFDL-CM4	TaiESM1	EC-Earth3-Veg	EC-Earth3-CC	EC-Earth3	MPI-ESM1-2-HR	NorESM2-MM	CESM2-WACCM	MRI-ESM2-0	CESM2	GFDL-ESM4	INM-CM5-0	INM-CM4-8
T2M KS	0.03	0.03	0.03	0.03	0.03	0.06	0.07	0.06	0.05	0.05	0.03	0.04	0.04
T2M Bias P50 (°C)	-1.95	0.10	-1.46	-1.21	-1.82	-1.11	0.86	1.19	-0.95	0.98	-2.66	-0.02	0.99
T2M Max KS	0.03	0.05	0.03	0.03	0.03	0.05	0.08	0.05	0.05	0.07	0.04	0.05	0.06
T2M Max Bias P95 (°C)	-2.76	-0.12	-1.66	-1.58	-2.19	-1.50	4.04	-2.17	0.33	3.48	-2.53	1.12	2.45
T2M Min KS	0.03	0.04	0.03	0.03	0.04	0.06	0.05	0.07	0.04	0.06	0.03	0.05	0.05
T2M Min Bias P5 (°C)	-0.99	-4.48	-2.95	-3.25	-4.84	-3.78	-1.04	5.97	-1.21	1.97	-0.02	2.26	3.54
RH2M KS	0.06	0.07	0.06	0.06	0.05	0.09	0.10	0.09	0.08	0.09	0.15	0.12	0.13
RH2M Bias P50 (%)	10.4	7.6	9.3	9.7	9.1	16.5	-6.6	-3.2	5.3	-4.0	20.7	2.9	1.2
RH2M Max KS	0.16		0.12	0.12	0.11	0.14			0.19			0.21	0.23
RH2M Max Bias P95 (%)	5.21		0.81	0.84	0.87	9.35			1.92			3.26	3.28
RH2M Min KS	0.07		0.05	0.05	0.05	0.07			0.07			0.09	0.09
RH2M Min Bias P5 (%)	8.2		21.1	23.3	22.3	22.8			9.7			-11.1	-13.8
PR KS	0.10	0.07	0.09	0.10	0.09	0.09	0.07	0.08	0.09	0.08	0.13	0.11	0.09
PR Bias P50 (%)	8.9	1.0	9.9	11.4	10.5	8.5	0.5	3.1	8.5	2.7	15.8	8.7	5.8
GHI KS	0.02	0.03	0.06	0.07	0.06	0.04	0.06	0.04	0.06	0.05	0.04	0.02	0.03
GHI Bias P50 (%)	0.0	1.6	1.6	-1.1	1.2	-3.9	16.7	7.9	10.4	8.9	-11.1	13.4	15.3
WS 100m KS	0.04	0.05	0.10	0.10	0.07	0.11	0.11	0.28	0.11	0.27	0.06	0.29	0.29
WS 100m Bias P50 (%)	-17.4	-25.6	1.9	1.9	-21.3	-9.3	-0.4	53.9	-44.9	53.8	-23.2	-74.3	-74.8
Process Skill	0.06	0.29	0.06	0.05	0.06	0.09	0.04	0.16	0.34	0.20	0.14	0.82	0.85

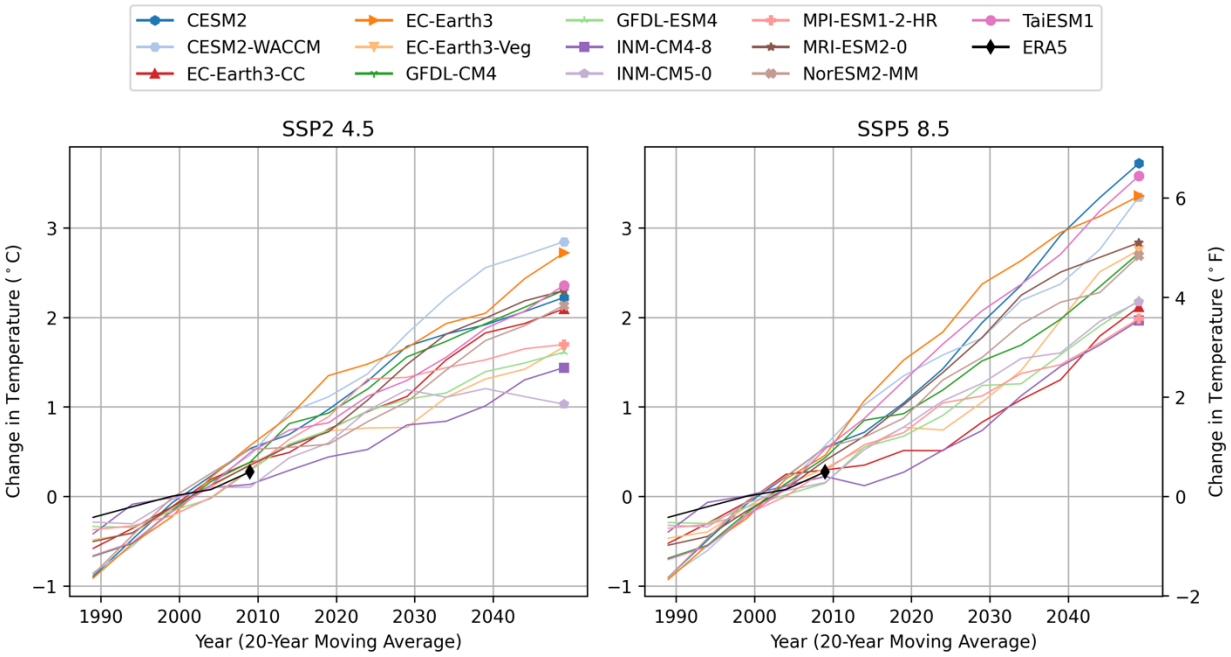

Figure 28. Comparison of GCM trends in changes to daily average near-surface air temperature for RF.

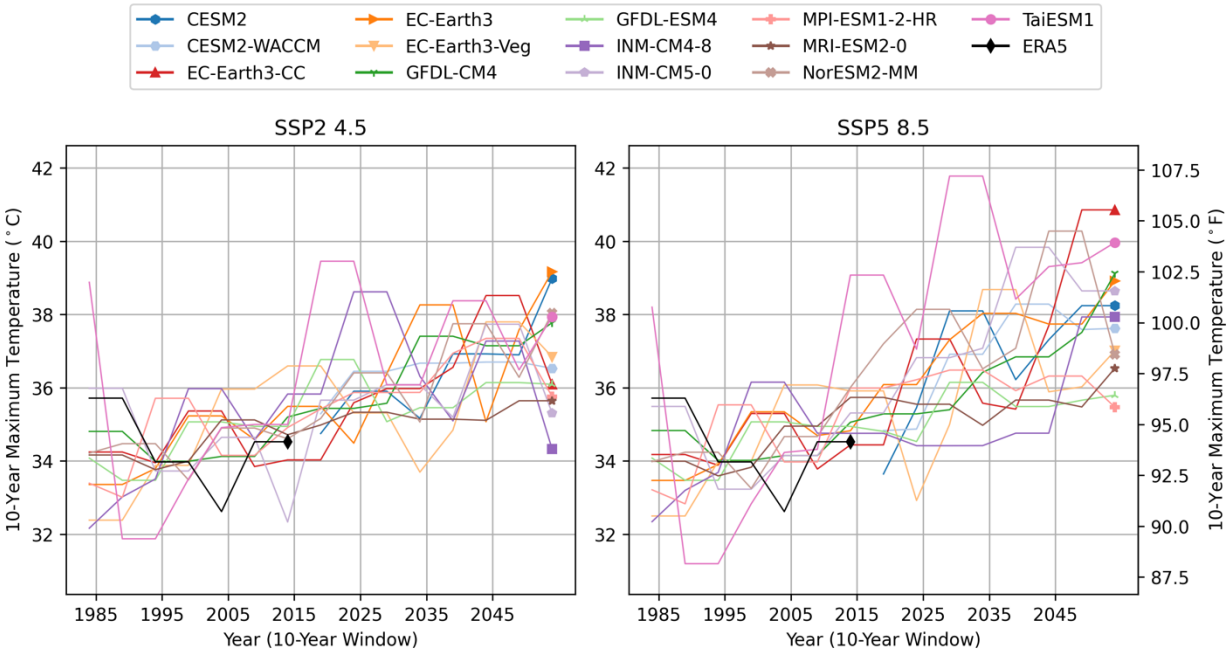

Figure 29. Comparison of GCM daily maximum air temperature events for RF.

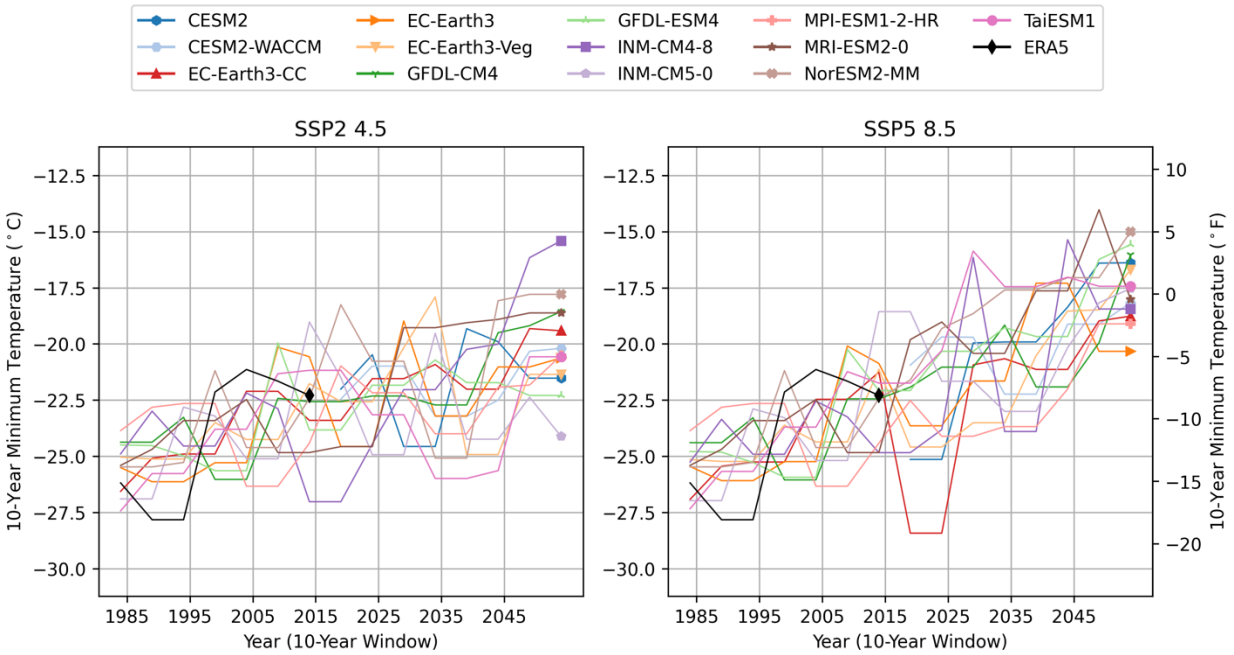

Figure 30. Comparison of GCM daily minimum air temperature events for RF.

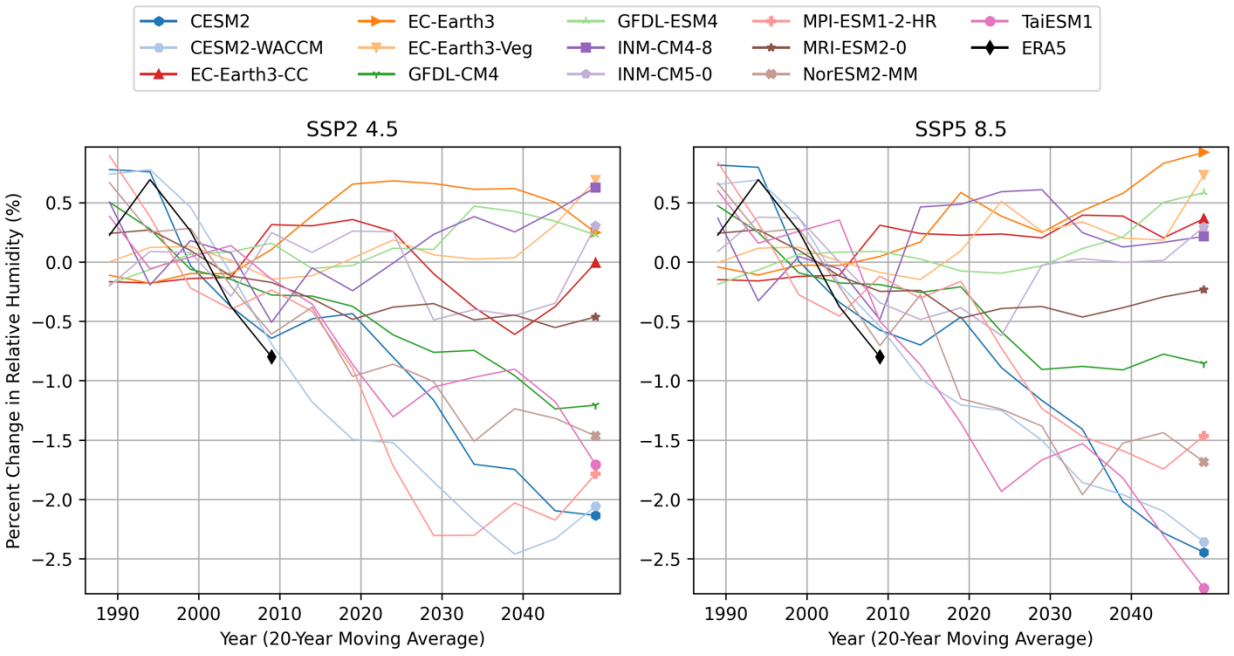

Figure 31. Comparison of GCM trends in changes to daily average near-surface relative humidity for RF.

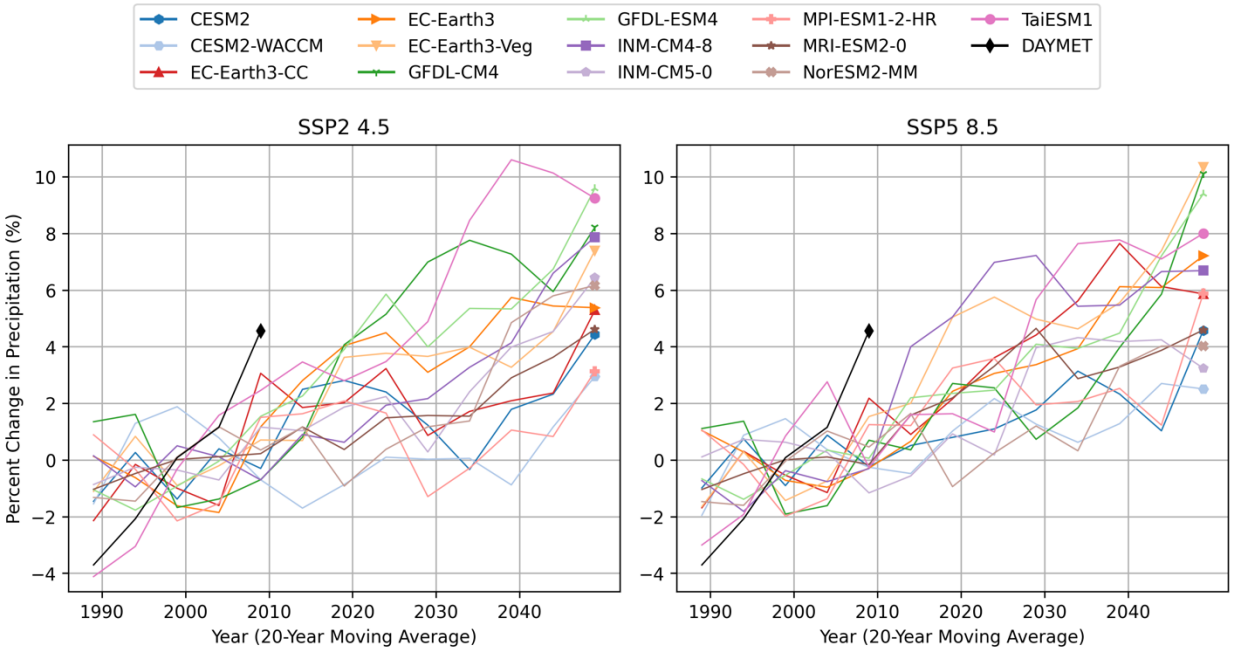

Figure 32. Comparison of GCM trends in changes to daily average precipitation for RF.

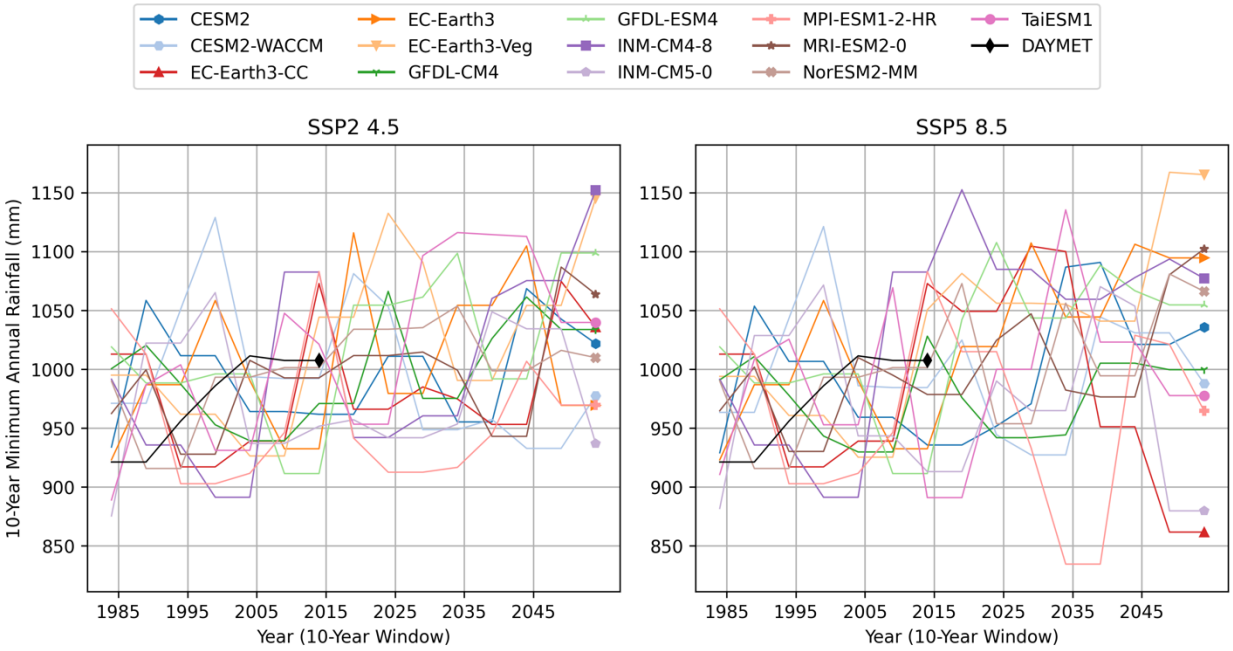

Figure 33. Comparison of GCM minimum annual rainfalls for RF.

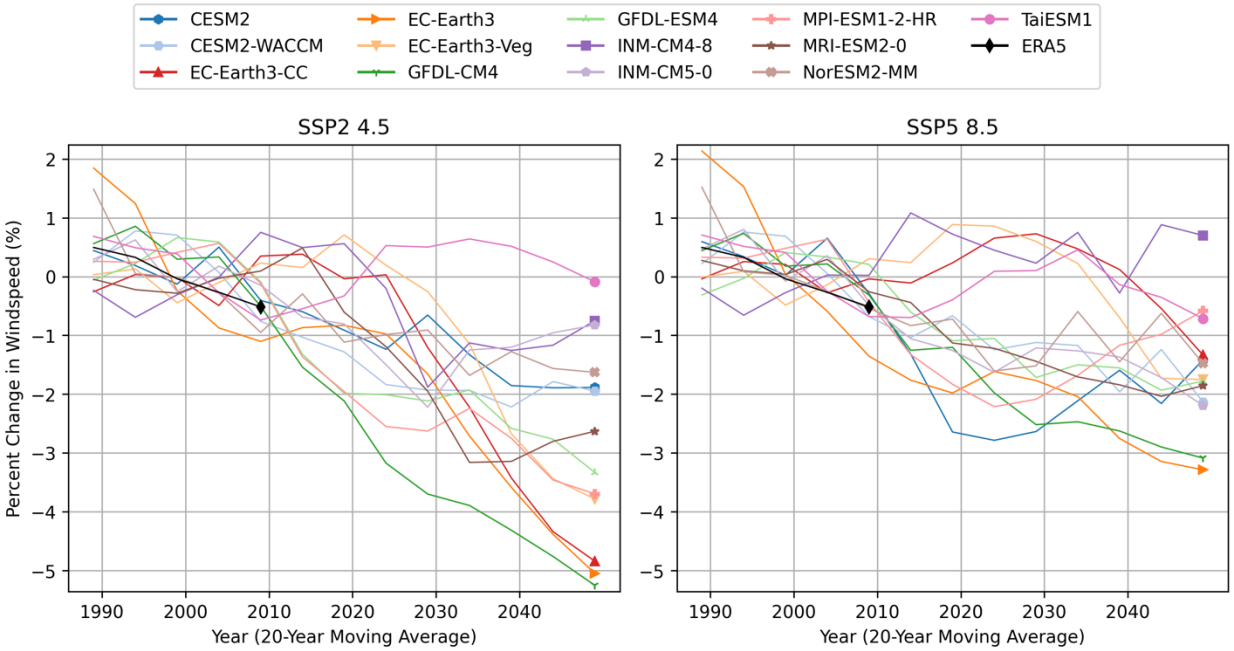

Figure 34. Comparison of GCM trends in changes to daily average 100-meter windspeed for RF.

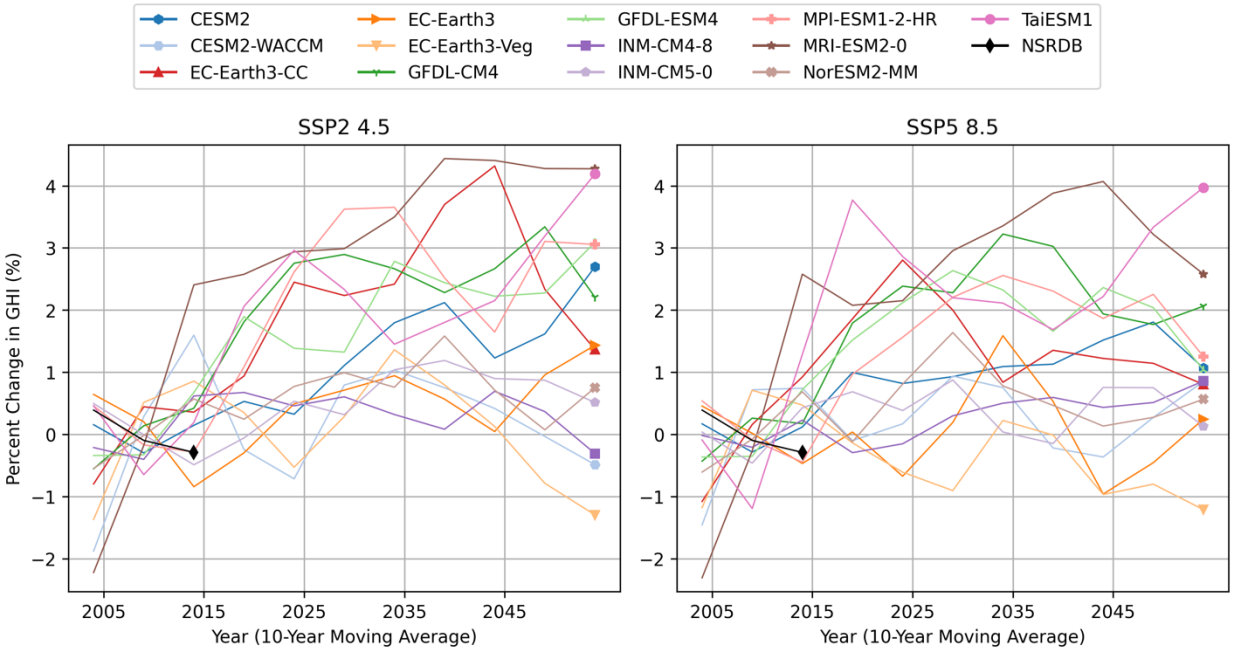

Figure 35. Comparison of GCM trends in changes to daily average GHI for RF.

Appendix D. NERC Region: Southeastern Electric Reliability Corporation (SERC)

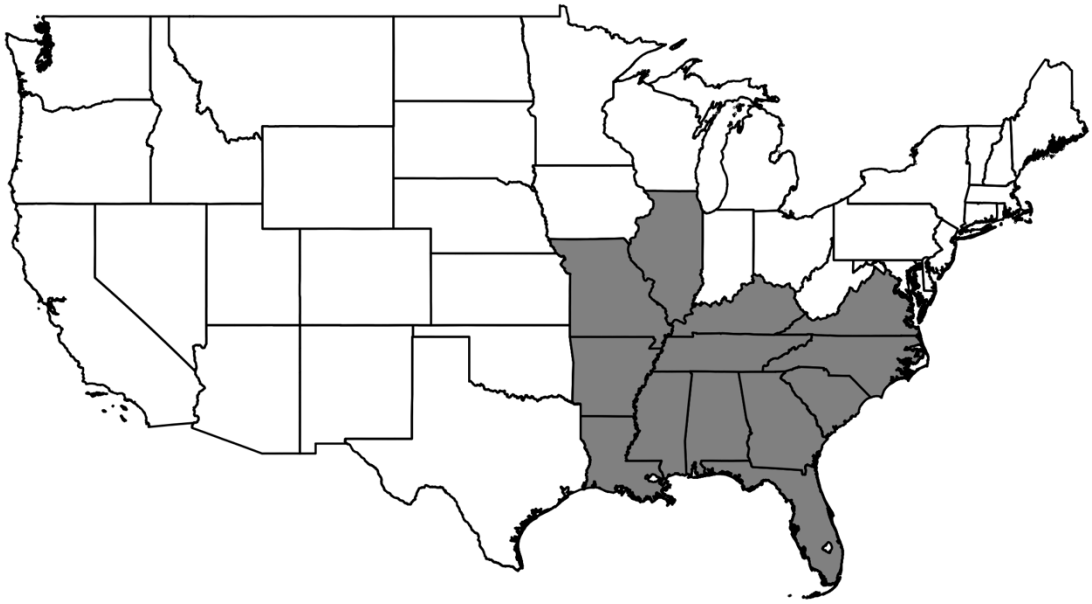

Figure 36. NERC Region: SERC (included states shaded in grey).

Note that we used a simple state mask, and the region may not perfectly match the spatial boundary of the true NERC region.

Table 7. Summary of historical GCM skill using KS statistic and bias metrics for SERC. Values for a given metric in each row are ranked from best to worst historical skill (dark blue to dark red).

	GFDL-CM4	EC-Earth3-Veg	EC-Earth3-CC	EC-Earth3	TaiESM1	MPI-ESM1-2-HR	NorESM2-MM	MRI-ESM2-0	CESM2-WACCM	CESM2	GFDL-ESM4	INM-CM5-0	INM-CM4-8
T2M KS	0.05	0.04	0.05	0.05	0.03	0.06	0.05	0.05	0.04	0.04	0.06	0.08	0.08
T2M Bias P50 (°C)	-2.05	-1.24	-1.02	-1.51	-0.14	-0.86	1.75	-0.75	2.12	2.09	-2.58	-0.59	0.11
T2M Max KS	0.04	0.06	0.06	0.06	0.05	0.05	0.05	0.05	0.05	0.06	0.06	0.09	0.10
T2M Max Bias P95 (°C)	-1.52	0.34	0.71	0.01	0.86	-1.40	2.95	-0.09	-2.91	3.35	-1.72	1.75	3.13
T2M Min KS	0.05	0.04	0.04	0.05	0.03	0.05	0.05	0.05	0.07	0.07	0.06	0.09	0.08
T2M Min Bias P5 (°C)	-1.92	-1.53	-1.70	-2.72	-1.76	-1.72	0.78	0.85	6.50	2.13	-0.98	3.18	3.03
RH2M KS	0.05	0.07	0.06	0.06	0.06	0.08	0.09	0.07	0.08	0.09	0.13	0.13	0.14
RH2M Bias P50 (%)	7.4	7.6	7.7	7.9	6.0	8.4	-11.7	0.6	-8.5	-9.2	17.6	-0.4	-3.1
RH2M Max KS	0.15	0.10	0.10	0.09		0.17		0.23				0.28	0.29
RH2M Max Bias P95 (%)	2.61	0.34	0.33	0.42		3.74		0.51				2.66	2.62
RH2M Min KS	0.07	0.07	0.07	0.06		0.07		0.05				0.11	0.12
RH2M Min Bias P5 (%)	6.7	11.6	12.0	14.3		18.1		14.0				-15.1	-18.1
PR KS	0.09	0.09	0.09	0.10	0.09	0.08	0.08	0.07	0.09	0.09	0.11	0.14	0.12
PR Bias P50 (%)	3.2	1.5	1.6	1.6	4.0	1.8	2.6	3.2	4.2	3.9	6.1	21.1	18.0
GHI KS	0.02	0.03	0.04	0.03	0.04	0.05	0.04	0.04	0.03	0.03	0.02	0.03	0.03
GHI Bias P50 (%)	-1.33	-3.04	-5.06	-3.57	-3.34	-0.50	8.69	8.77	1.16	2.34	-7.10	6.02	8.39
WS 100m KS	0.05	0.08	0.08	0.06	0.05	0.09	0.11	0.15	0.26	0.26	0.08	0.21	0.21
WS 100m Bias P50 (%)	-20.2	-0.6	-0.2	-17.5	-20.4	-13.3	3.1	-50.2	44.4	45.0	-13.3	-56.0	-56.5
Process Skill	0.06	0.06	0.05	0.06	0.29	0.09	0.04	0.34	0.16	0.20	0.14	0.82	0.85

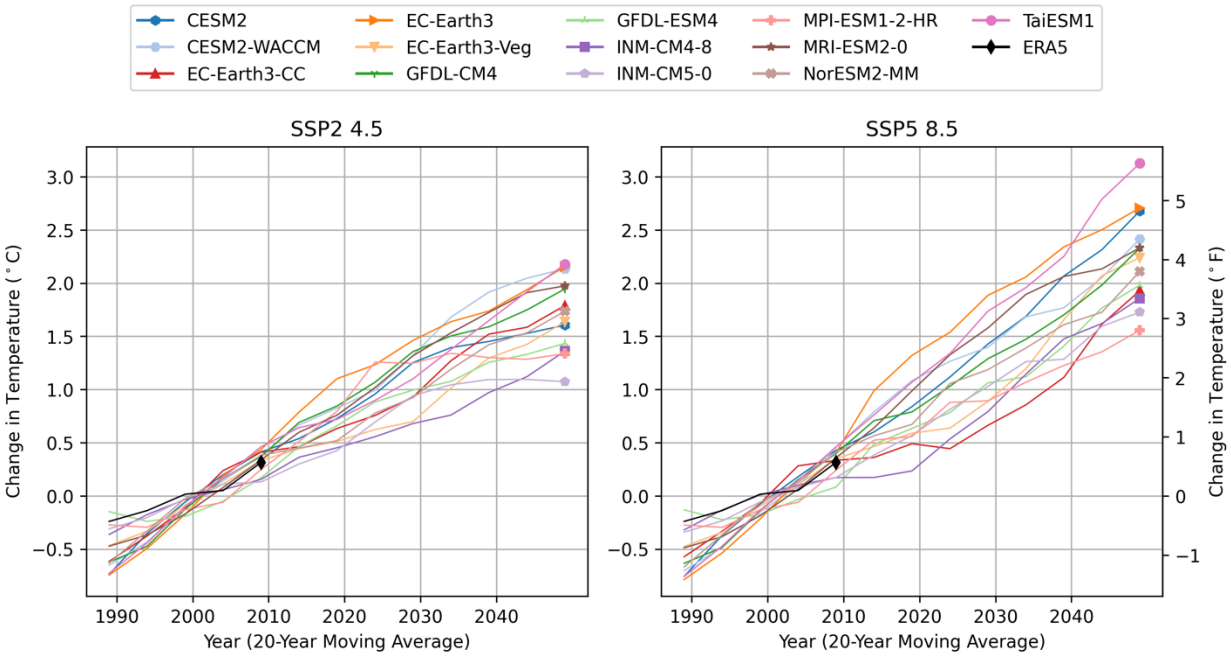

Figure 37. Comparison of GCM trends in changes to daily average near-surface air temperature for SERC.

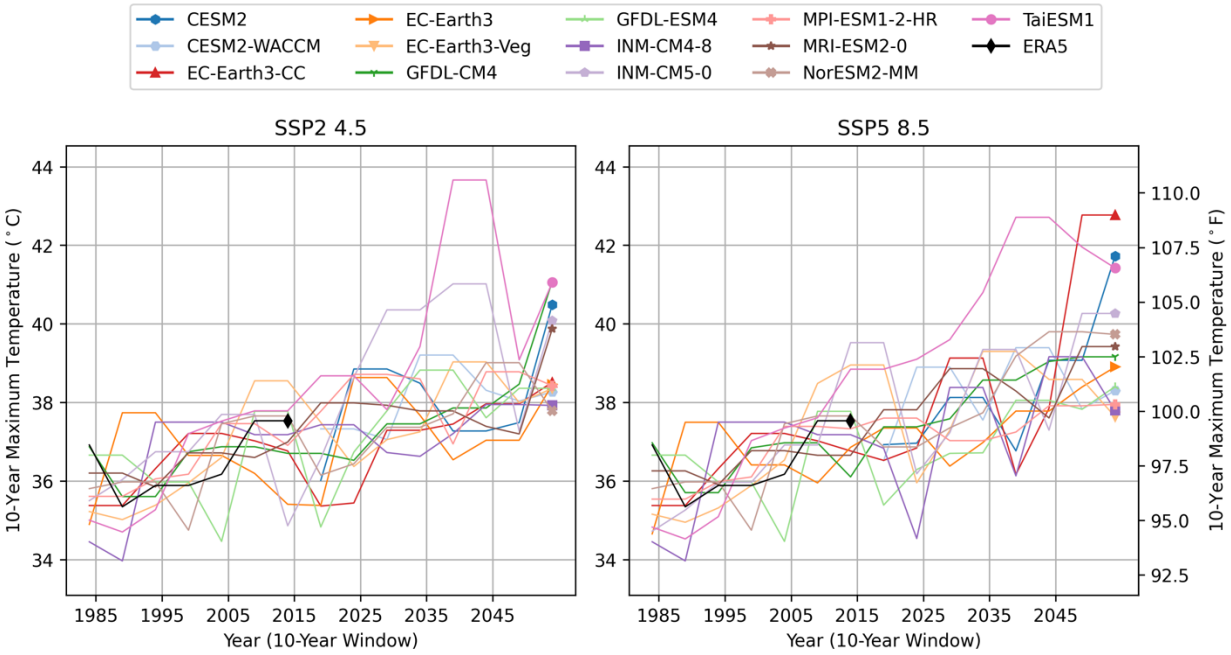

Figure 38. Comparison of GCM daily maximum air temperature events for SERC.

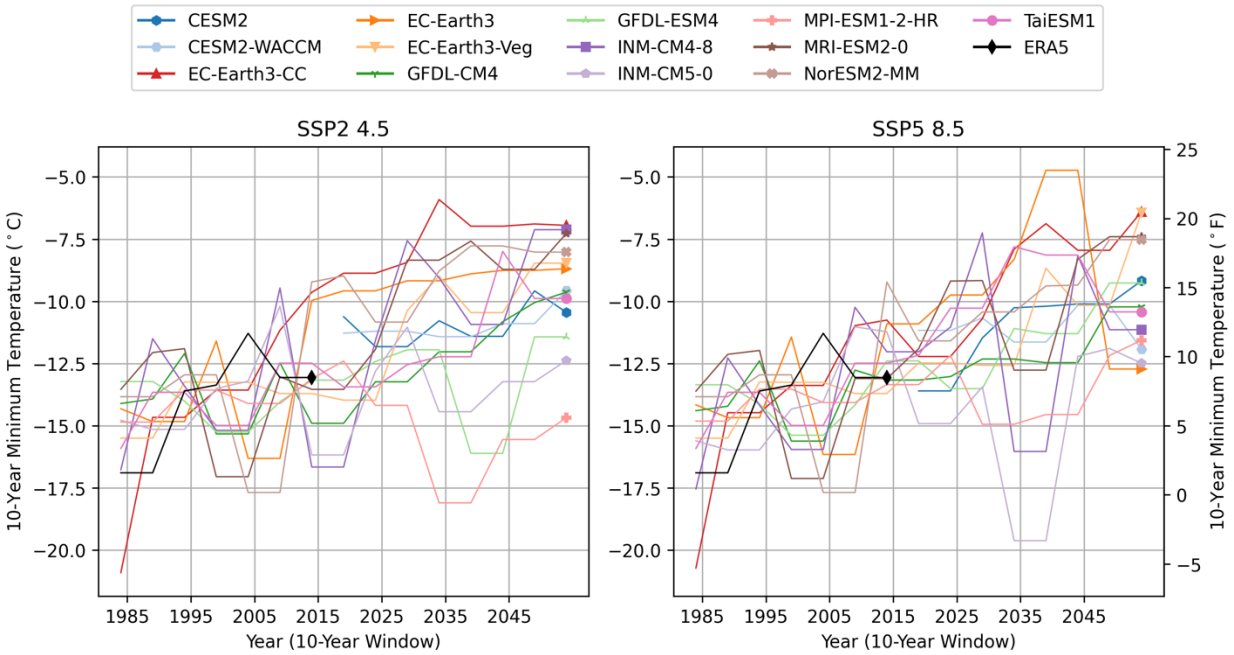

Figure 39. Comparison of GCM daily minimum air temperature events for SERC.

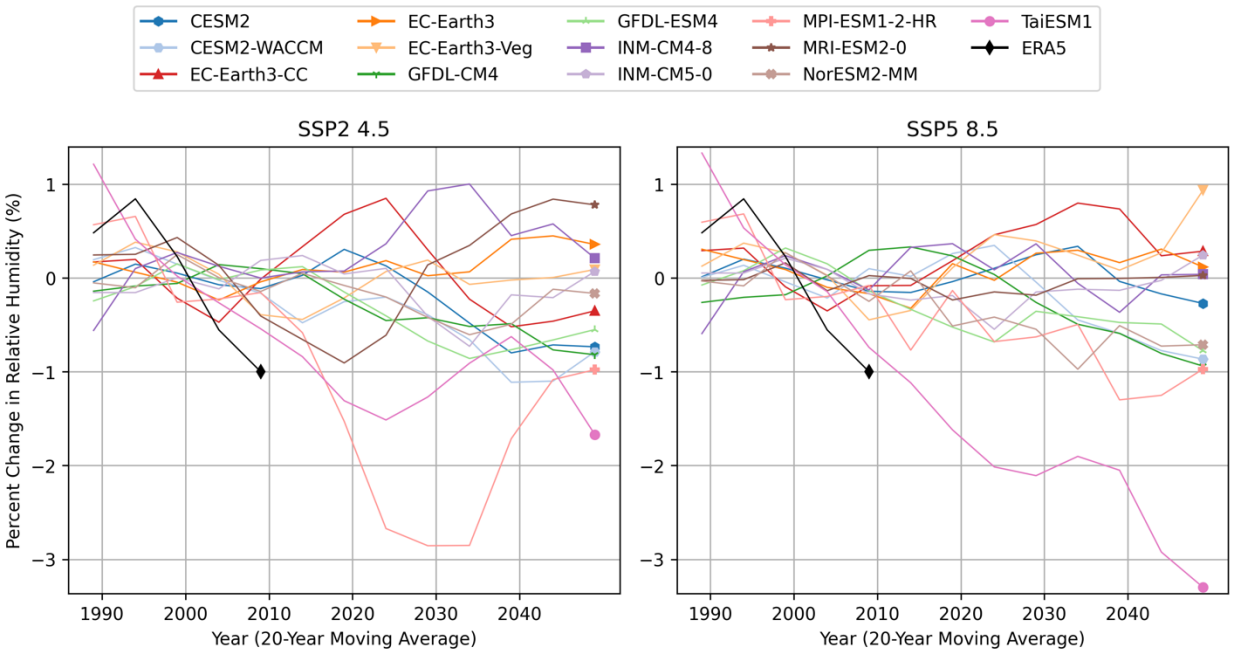

Figure 40. Comparison of GCM trends in changes to daily average near-surface relative humidity for SERC.

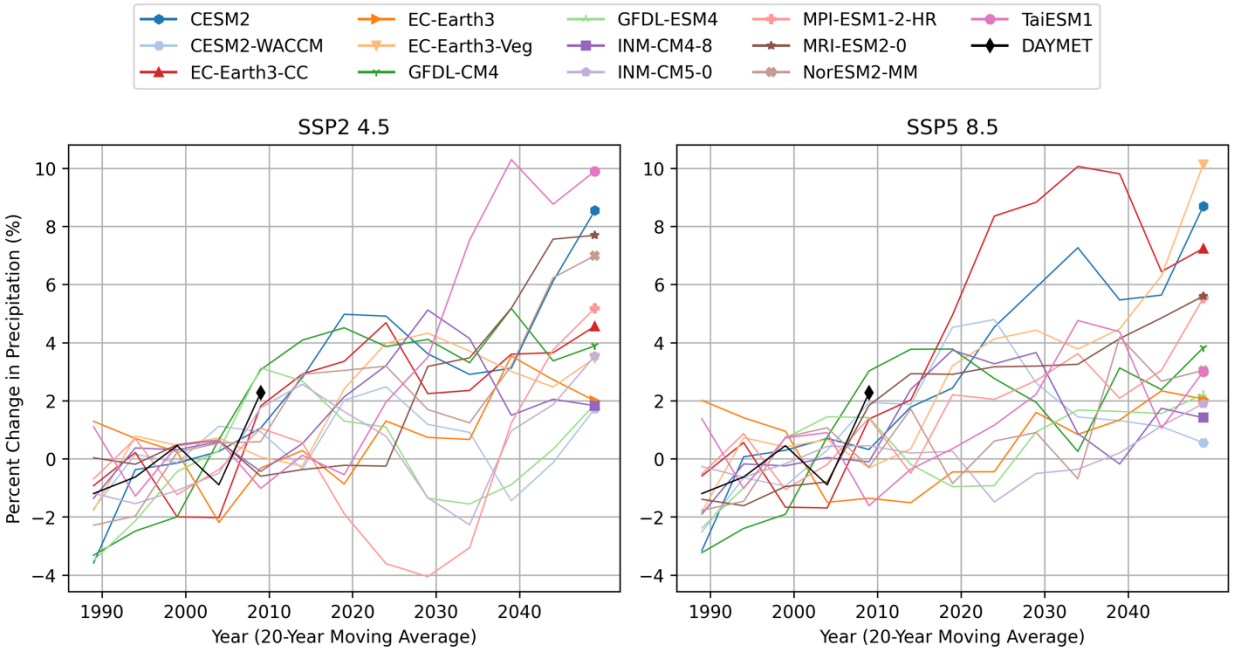

Figure 41. Comparison of GCM trends in changes to daily average precipitation for SERC.

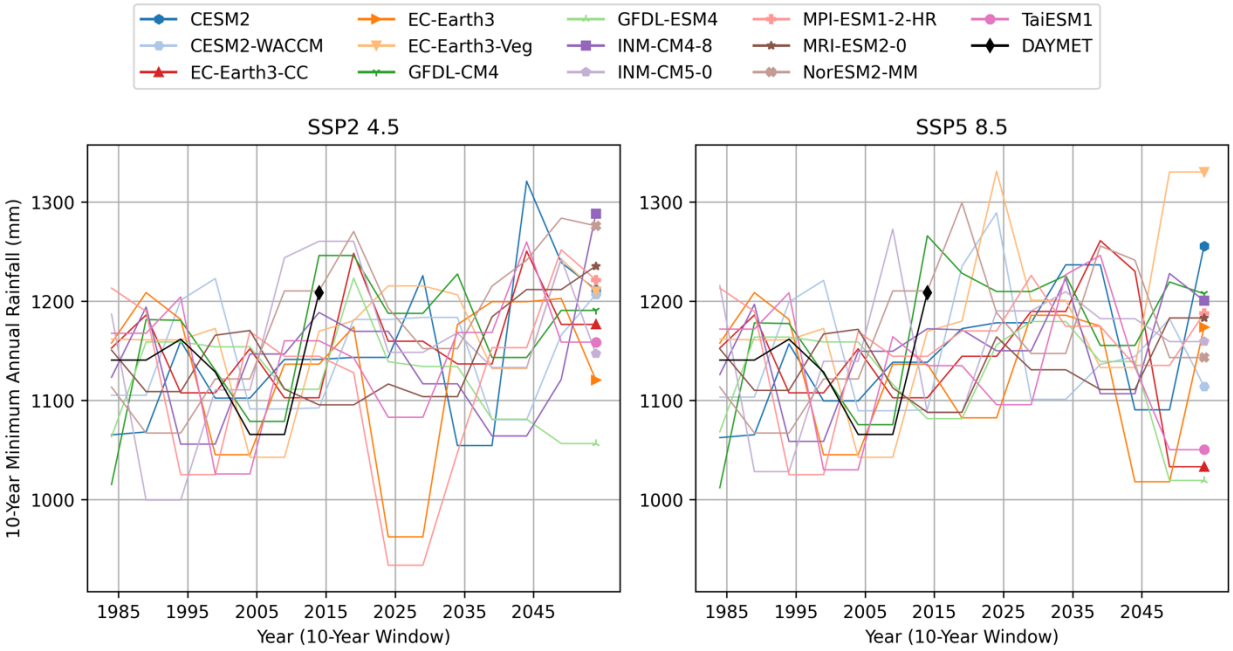

Figure 42. Comparison of GCM minimum annual rainfalls for SERC.

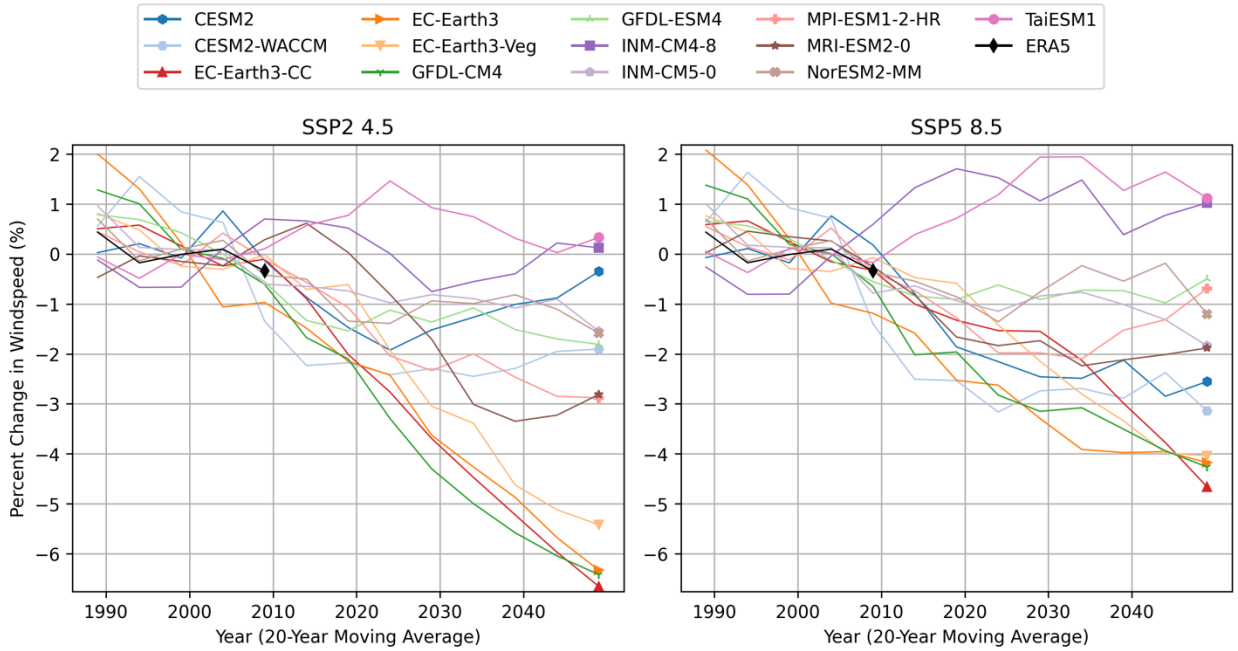

Figure 43. Comparison of GCM trends in changes to daily average 100-meter windspeed for SERC.

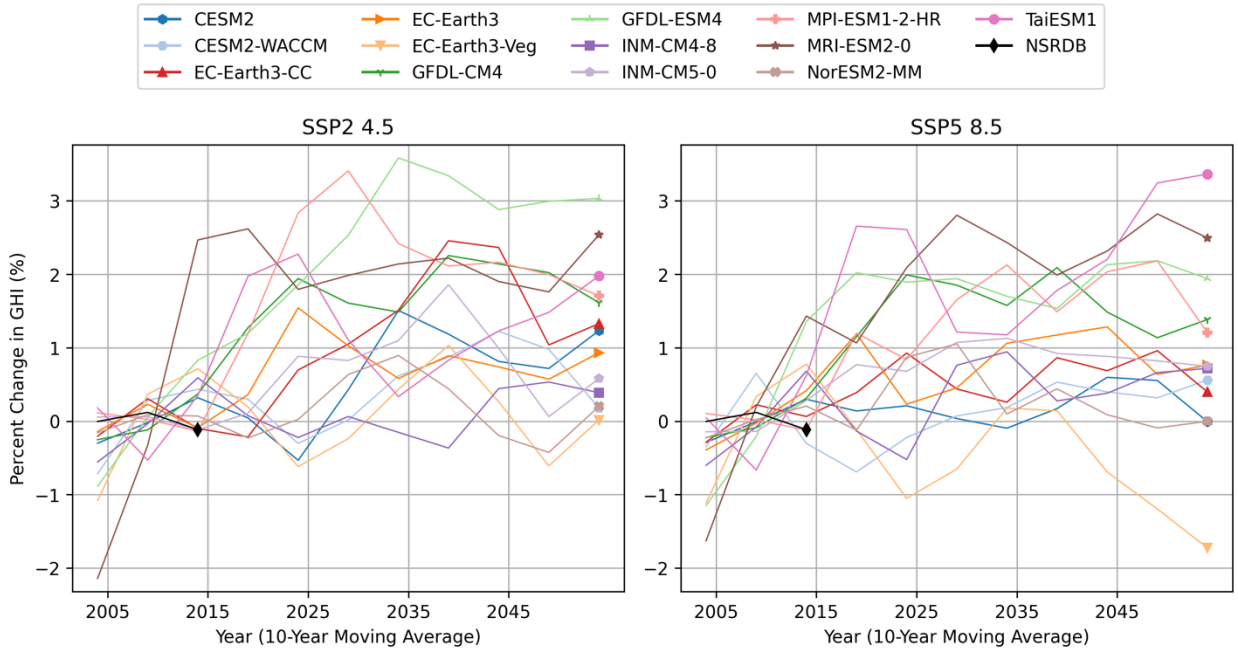

Figure 44. Comparison of GCM trends in changes to daily average GHI for SERC.

Appendix E. NERC Region: Texas Reliability Entity (Texas RE)

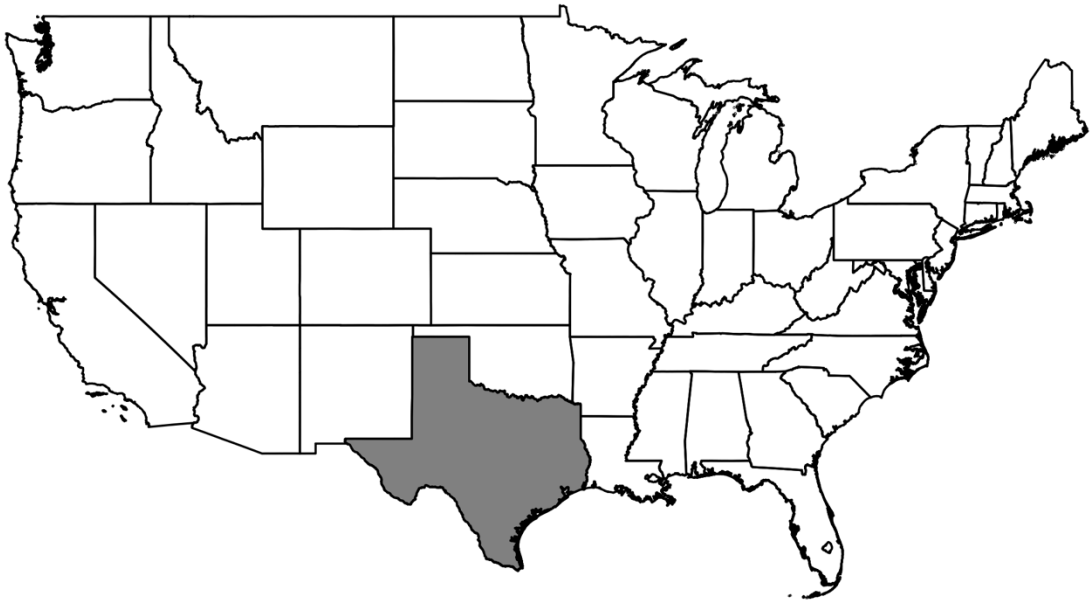

Figure 45. NERC Region: Texas RE (included states shaded in grey).

Note that we used a simple state mask, and the region may not perfectly match the spatial boundary of the true NERC region.

Table 8. Summary of historical GCM skill using KS statistic and bias metrics for Texas RE. Values for a given metric in each row are ranked from best to worst historical skill (dark blue to dark red).

	EC-Earth3-Veg	EC-Earth3-CC	EC-Earth3	TaiESM1	NorESM2-MM	GFDL-CM4	GFDL-ESM4	MPI-ESM1-2-HR	CESM2	CESM2-WACCM	MRI-ESM2-0	INM-CM5-0	INM-CM4-8
T2M KS	0.10	0.10	0.10	0.05	0.05	0.09	0.10	0.11	0.04	0.04	0.07	0.05	0.06
T2M Bias P50 (°C)	-1.27	-1.22	-1.91	-0.28	1.44	-2.88	-2.10	0.30	1.86	1.81	-1.01	-0.73	-0.07
T2M Max KS	0.11	0.12	0.12	0.06	0.05	0.10	0.10	0.10	0.08	0.06	0.09	0.07	0.07
T2M Max Bias P95 (°C)	2.08	2.19	1.66	1.58	1.15	0.82	0.60	2.13	1.94	-3.77	2.67	2.29	2.99
T2M Min KS	0.09	0.09	0.10	0.04	0.04	0.10	0.10	0.12	0.06	0.06	0.06	0.06	0.05
T2M Min Bias P5 (°C)	-1.26	-1.18	-2.16	0.45	1.64	-2.27	-0.85	0.10	2.74	7.59	2.00	-0.12	-0.84
RH2M KS	0.09	0.09	0.09	0.08	0.07	0.08	0.10	0.12	0.07	0.07	0.10	0.12	0.13
RH2M Bias P50 (%)	4.9	6.3	8.4	5.1	-16.5	12.6	10.9	-12.2	-15.0	-14.6	-4.2	-6.7	-8.4
RH2M Max KS	0.13	0.12	0.11			0.10		0.24			0.21	0.26	0.27
RH2M Max Bias P95 (%)	1.01	1.04	1.21			3.37		4.31			1.27	4.28	4.30
RH2M Min KS	0.11	0.11	0.12			0.09		0.09			0.09	0.09	0.09
RH2M Min Bias P5 (%)	-2.4	-1.4	1.2			4.0		-7.3			0.2	-12.9	-16.4
PR KS	0.08	0.08	0.09	0.10	0.08	0.10	0.10	0.05	0.08	0.08	0.08	0.14	0.14
PR Bias P50 (%)	0.00	0.00	0.00	0.00	0.00	0.33	0.31	0.00	0.00	0.00	0.08	4.16	4.46
GHI KS	0.03	0.03	0.03	0.04	0.03	0.03	0.03	0.04	0.03	0.03	0.04	0.04	0.05
GHI Bias P50 (%)	-1.36	-3.08	-2.89	-3.02	7.23	-2.11	-3.19	5.06	3.07	2.59	6.40	1.97	3.21
WS 100m KS	0.06	0.07	0.06	0.05	0.10	0.03	0.07	0.08	0.22	0.22	0.12	0.21	0.22
WS 100m Bias P50 (%)	-6.2	-6.4	-14.6	-22.7	0.5	-27.0	-20.7	-8.4	39.8	39.0	-37.7	-65.0	-65.5
Process Skill	0.06	0.05	0.06	0.29	0.04	0.06	0.14	0.09	0.20	0.16	0.34	0.82	0.85

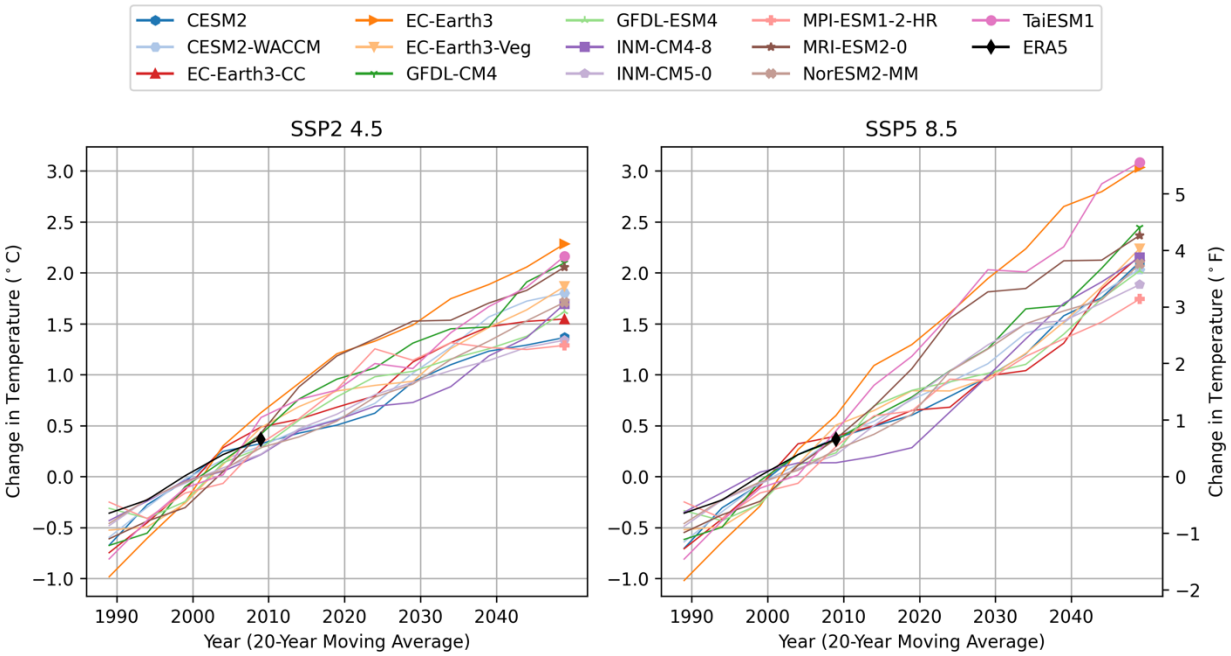

Figure 46. Comparison of GCM trends in changes to daily average near-surface air temperature for Texas RE.

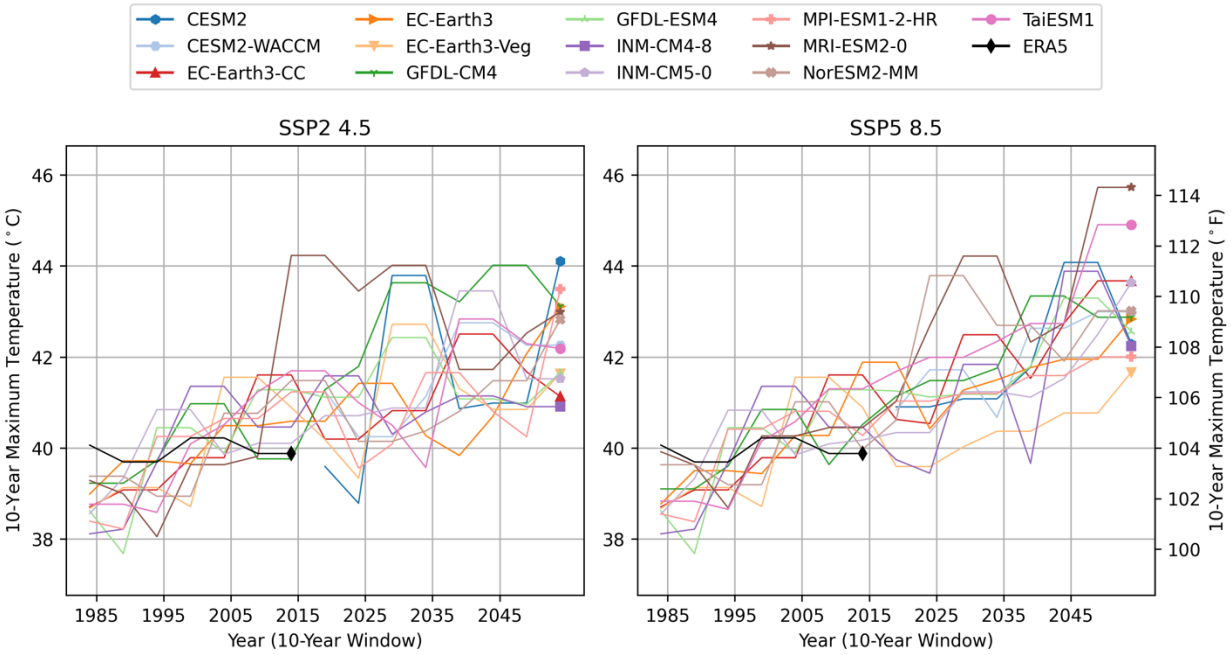

Figure 47. Comparison of GCM daily maximum air temperature events for Texas RE.

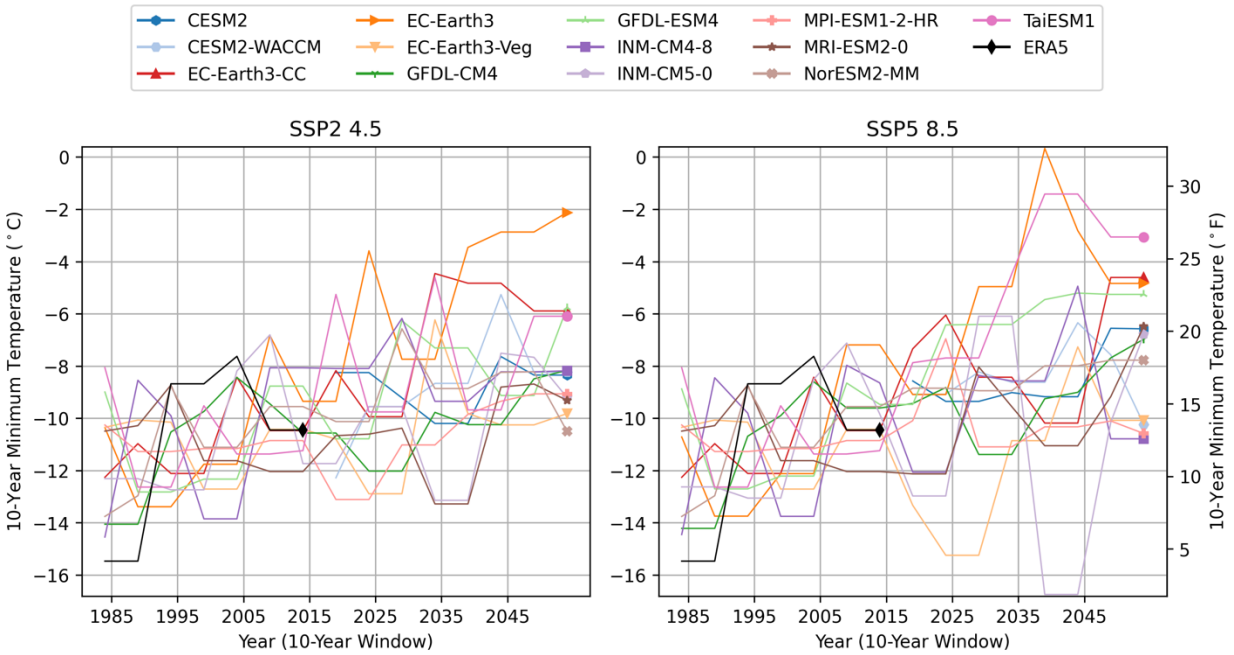

Figure 48. Comparison of GCM daily minimum air temperature events for Texas RE.

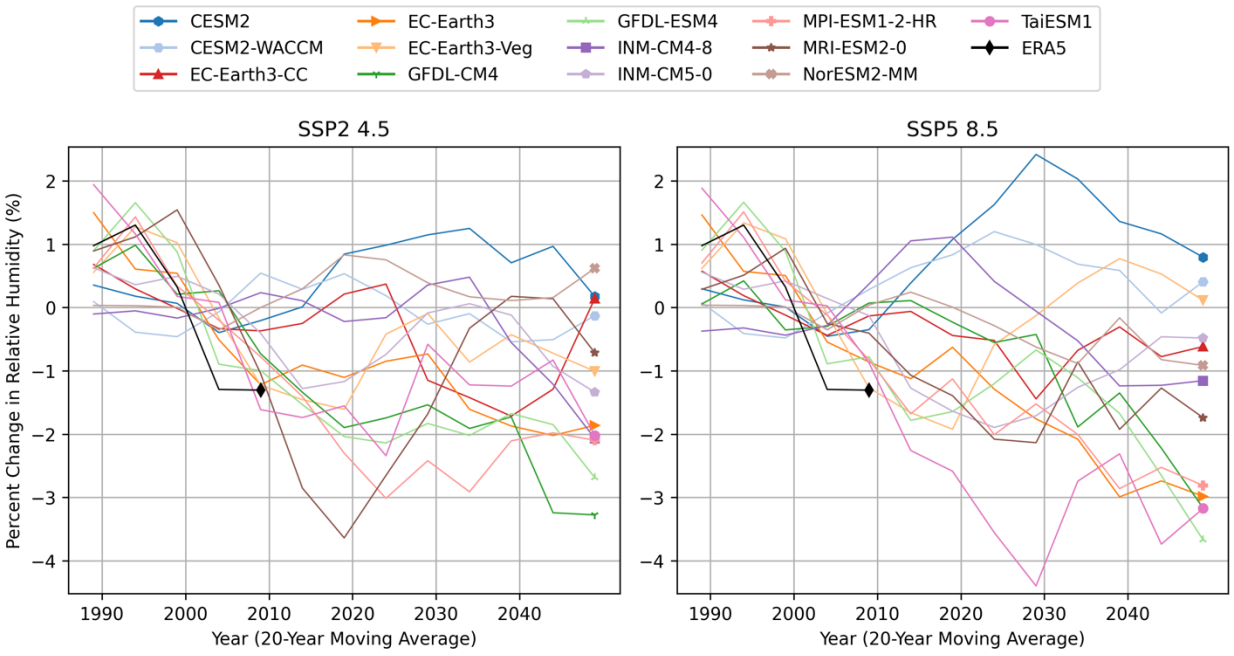

Figure 49. Comparison of GCM trends in changes to daily average near-surface relative humidity for Texas RE.

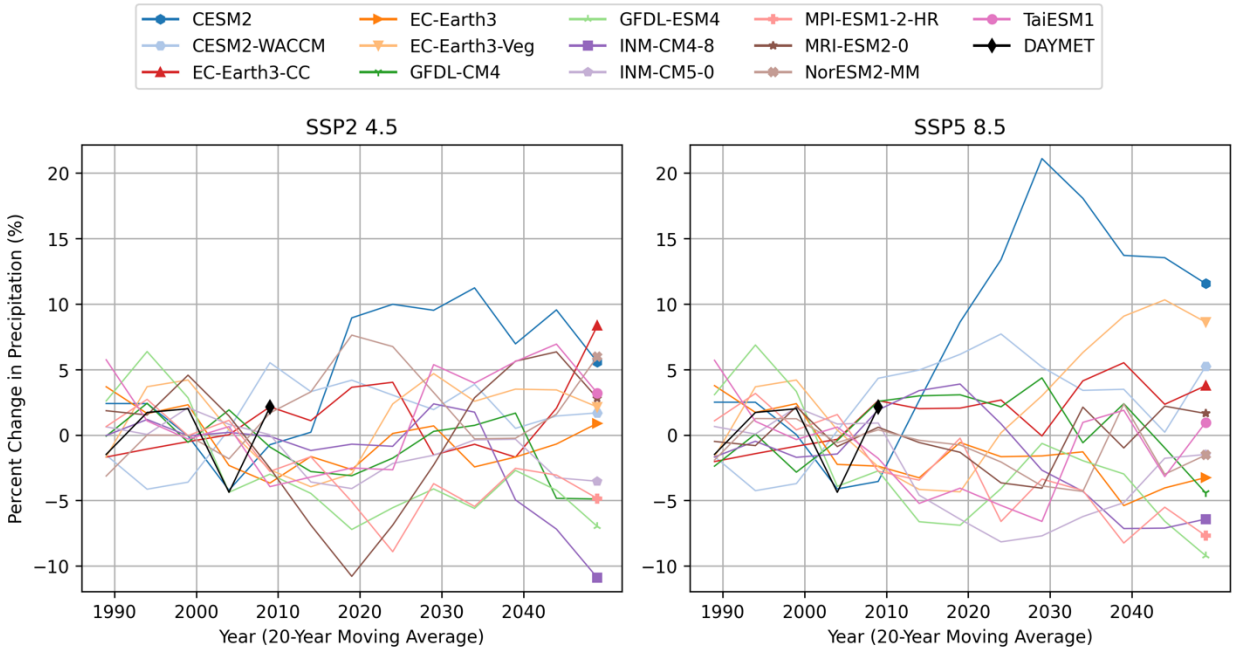

Figure 50. Comparison of GCM trends in changes to daily average precipitation for Texas RE.

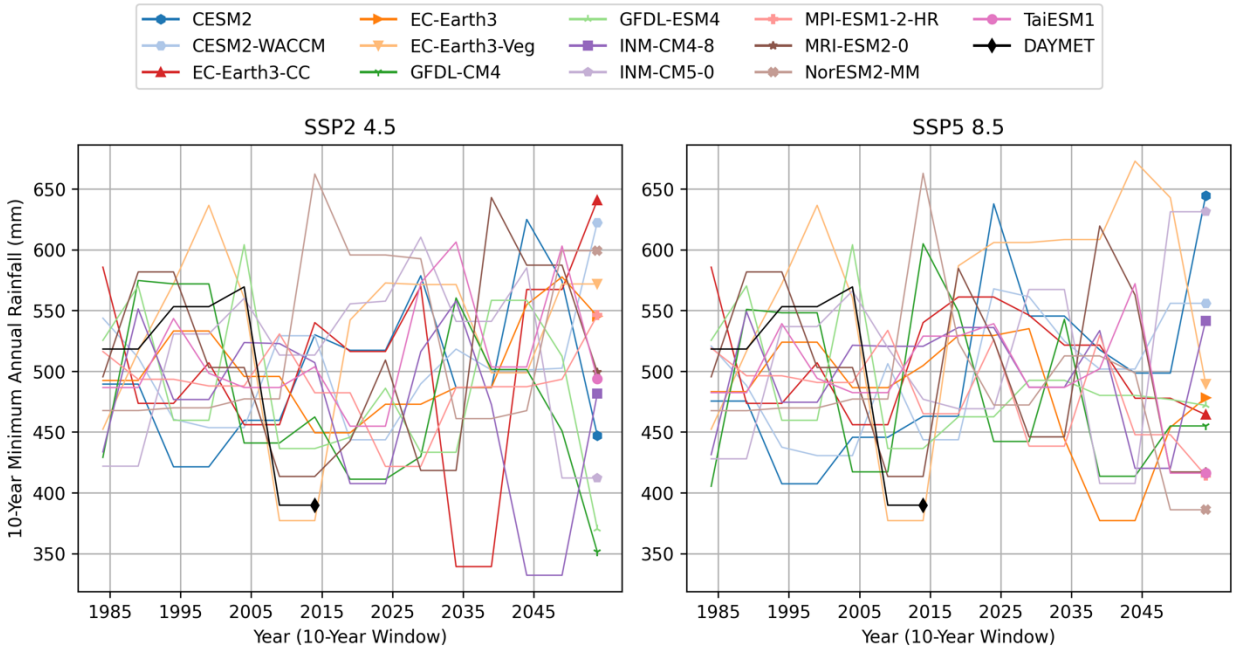

Figure 51. Comparison of GCM minimum annual rainfalls for Texas RE.

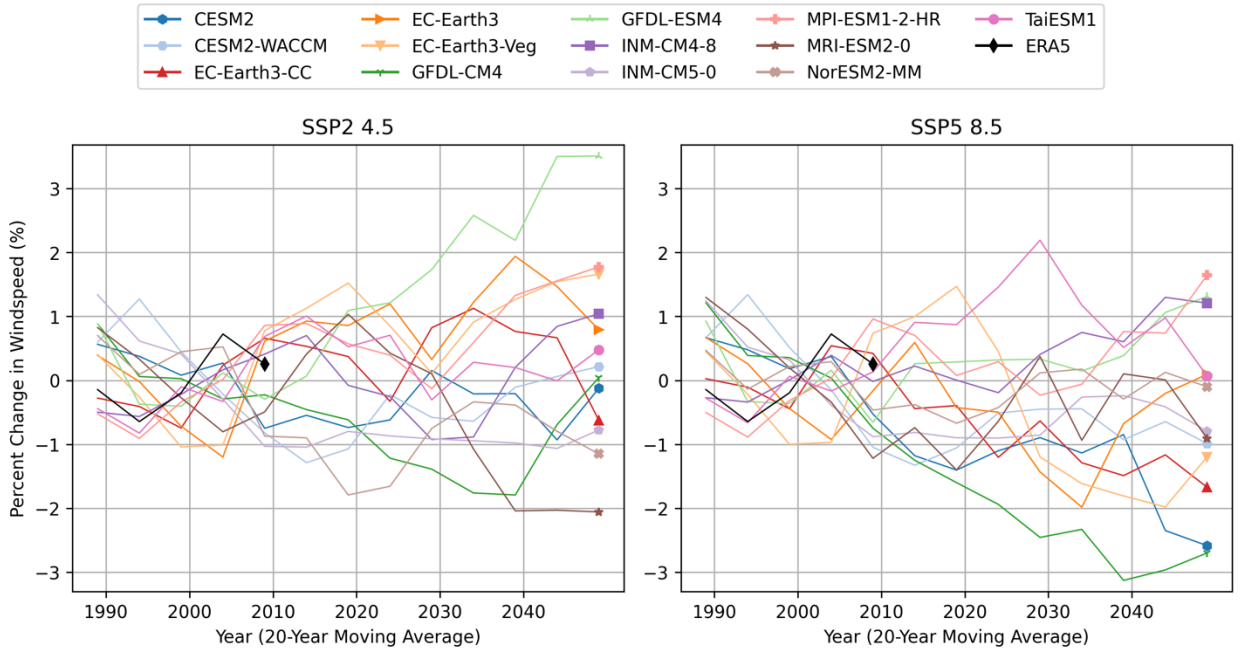

Figure 52. Comparison of GCM trends in changes to daily average 100-meter windspeed for Texas RE.

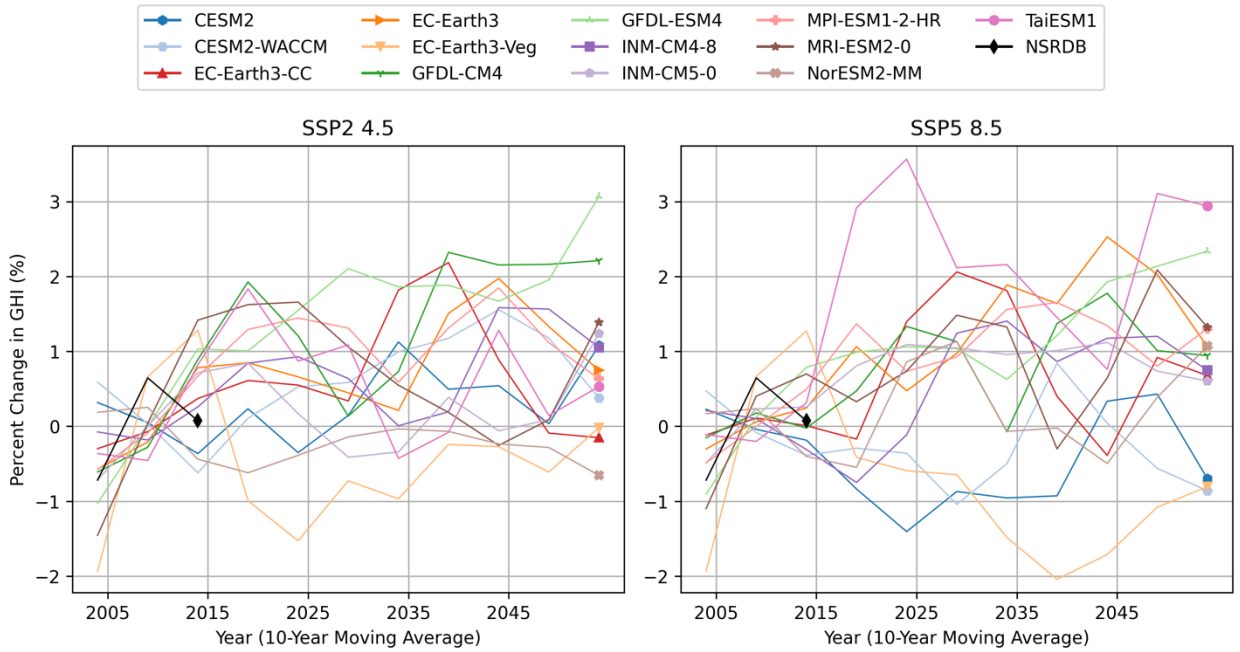

Figure 53. Comparison of GCM trends in changes to daily average GHI for Texas RE.

Appendix F. NERC Region: Western Electricity Coordinating Council (WECC)

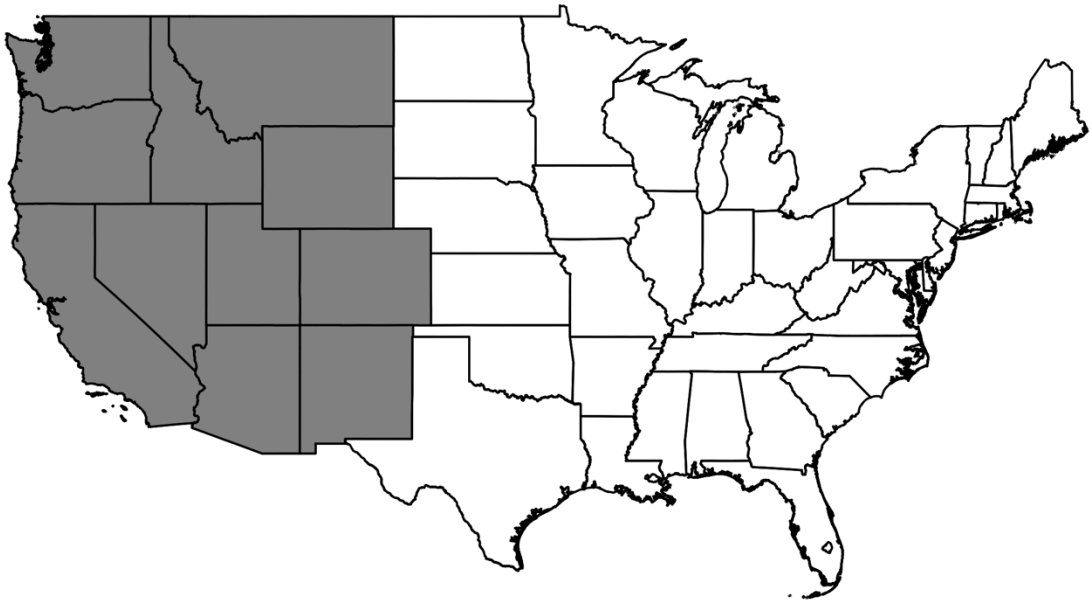

Figure 54. NERC Region: WECC (included states shaded in grey).

Note that we used a simple state mask, and the region may not perfectly match the spatial boundary of the true NERC region.

Table 9. Summary of historical GCM skill using KS statistic and bias metrics for WECC. Values for a given metric in each row are ranked from best to worst historical skill (dark blue to dark red).

	TaiESM1	EC-Earth3-CC	GFDL-CM4	EC-Earth3-Veg	MPI-ESM1-2-HR	NorESM2-MM	EC-Earth3	CESM2	CESM2-WACCM	GFDL-ESM4	MRI-ESM2-0	INM-CM5-0	INM-CM4-8
T2M KS	0.04	0.05	0.05	0.06	0.06	0.06	0.06	0.05	0.05	0.06	0.07	0.05	0.07
T2M Bias P50 (°C)	0.02	-1.20	-2.76	-1.56	-1.27	1.12	-2.26	1.93	1.80	-2.52	-1.94	0.24	0.69
T2M Max KS	0.05	0.05	0.07	0.06	0.06	0.08	0.06	0.06	0.07	0.07	0.09	0.08	0.10
T2M Max Bias P95 (°C)	0.81	0.19	-1.54	0.13	0.53	1.86	-0.59	1.40	-5.25	-0.96	-2.34	2.83	4.08
T2M Min KS	0.05	0.05	0.05	0.06	0.06	0.06	0.06	0.06	0.11	0.05	0.07	0.07	0.06
T2M Min Bias P5 (°C)	-1.86	-3.12	-2.31	-3.66	-0.70	1.53	-4.64	2.93	7.57	-1.61	2.96	1.02	0.91
RH2M KS	0.10	0.08	0.09	0.08	0.17	0.10	0.09	0.08	0.08	0.14	0.11	0.14	0.15
RH2M Bias P50 (%)	11.3	10.5	18.8	10.0	10.0	-10.8	12.7	-5.3	-5.6	19.6	25.5	8.7	0.0
RH2M Max KS		0.09	0.15	0.09	0.24		0.09				0.16	0.20	0.23
RH2M Max Bias P95 (%)		4.0	12.9	3.9	17.9		4.1				7.9	9.9	9.1
RH2M Min KS		0.12	0.12	0.12	0.17		0.13				0.15	0.13	0.12
RH2M Min Bias P5 (%)		0.6	5.1	-0.5	-2.5		3.0				20.5	-6.4	-11.4
PR KS	0.11	0.09	0.12	0.09	0.07	0.09	0.09	0.10	0.10	0.12	0.15	0.18	0.16
PR Bias P50 (%)	1.4	2.0	7.0	1.8	-1.7	-1.9	2.5	0.2	0.5	9.8	14.6	15.6	10.2
GHI KS	0.04	0.05	0.04	0.05	0.04	0.04	0.05	0.04	0.04	0.04	0.04	0.04	0.05
GHI Bias P50 (%)	0.25	4.96	-3.24	7.20	1.36	8.19	5.61	4.38	4.01	-5.32	3.00	2.03	6.42
WS 100m KS	0.13	0.10	0.11	0.10	0.18	0.19	0.11	0.28	0.28	0.11	0.15	0.16	0.17
WS 100m Bias P50 (%)	-3.8	0.8	-5.8	1.8	11.3	20.6	-11.6	44.2	44.6	-14.2	9.5	-41.2	-40.4
Process Skill	0.29	0.05	0.06	0.06	0.09	0.04	0.06	0.20	0.16	0.14	0.34	0.82	0.85

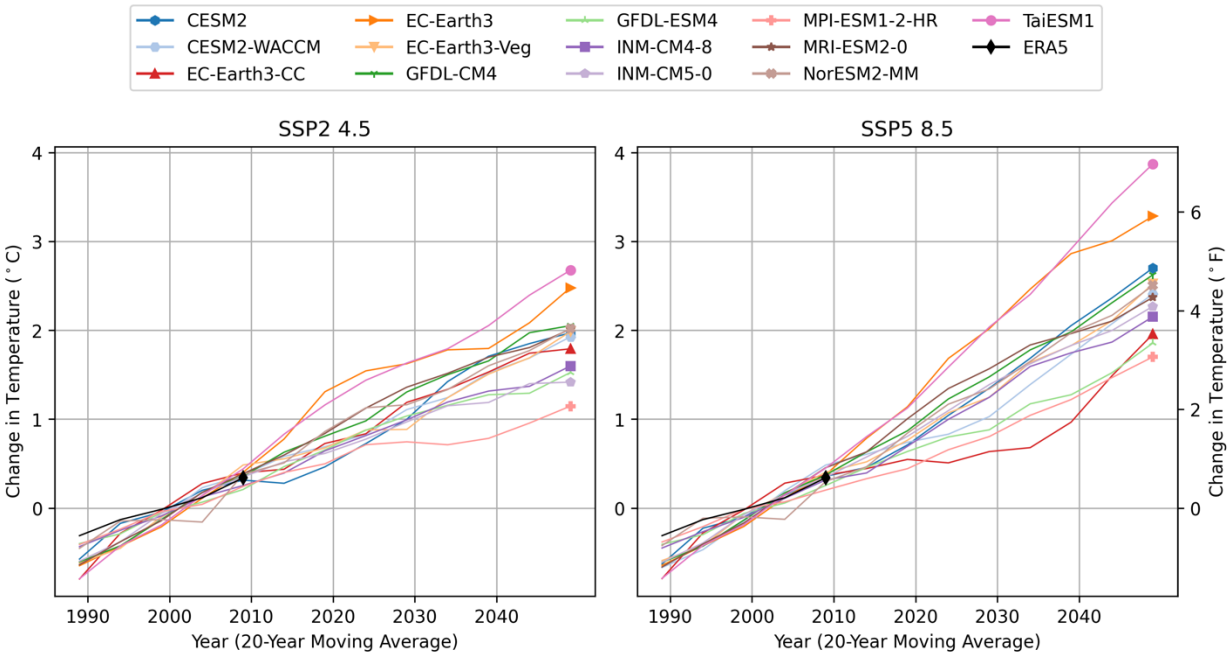

Figure 55. Comparison of GCM trends in changes to daily average near-surface air temperature for WECC.

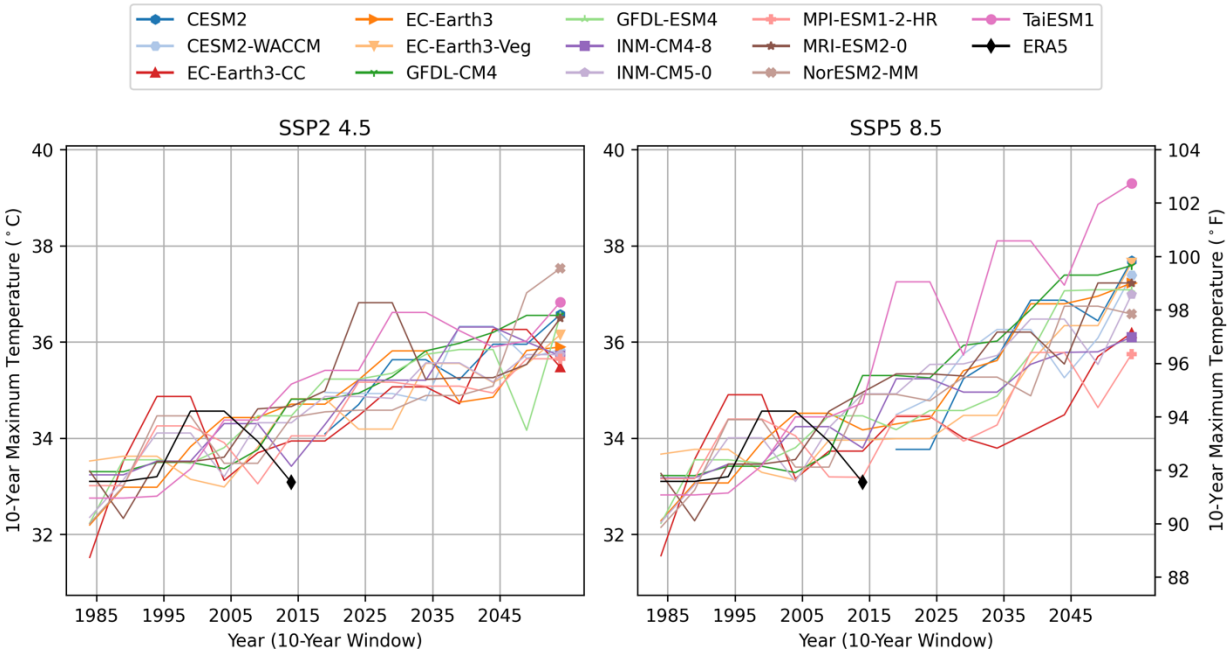

Figure 56. Comparison of GCM daily maximum air temperature events for WECC.

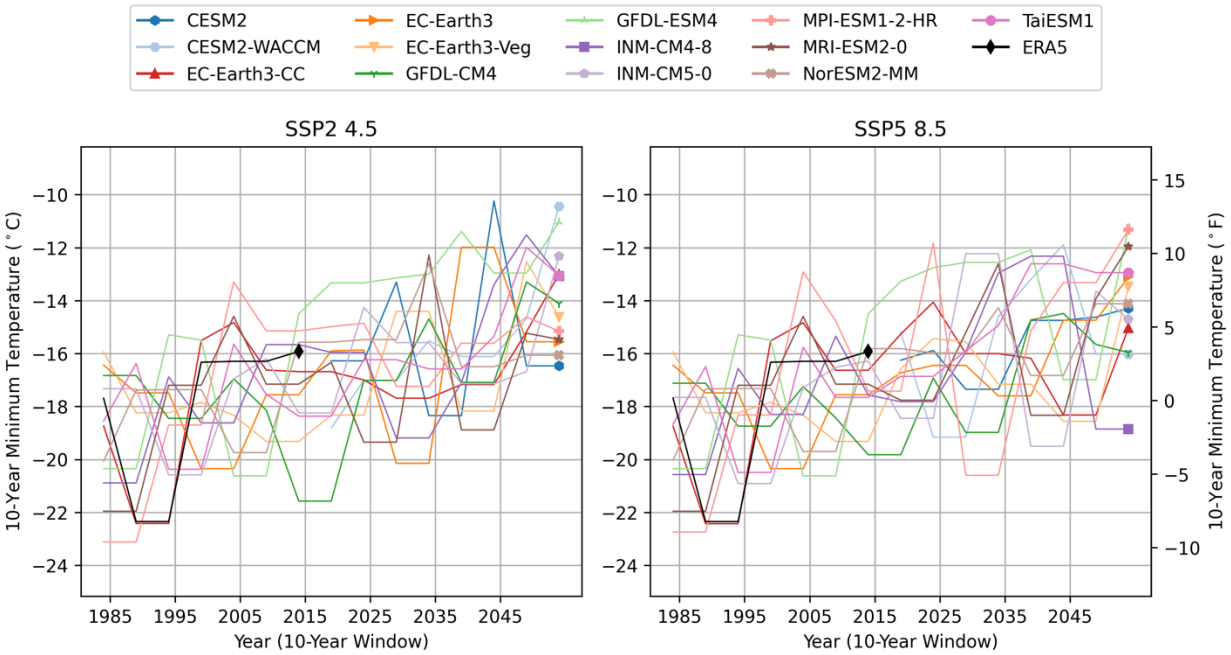

Figure 57. Comparison of GCM daily minimum air temperature events for WECC.

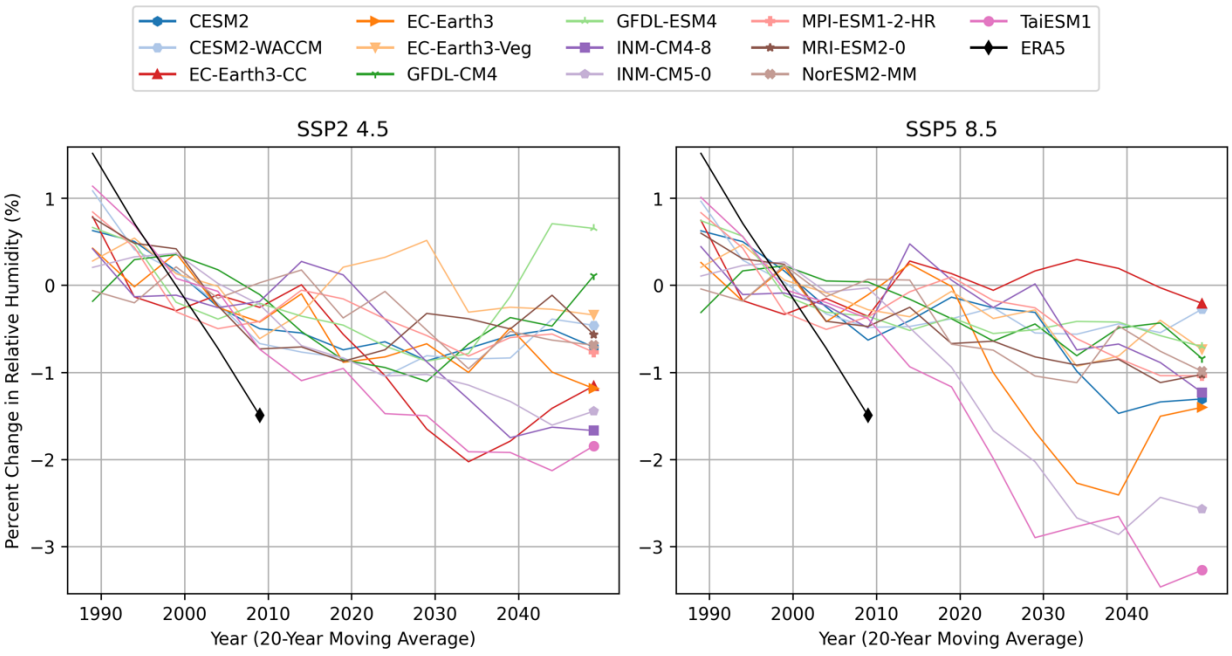

Figure 58. Comparison of GCM trends in changes to daily average near-surface relative humidity for WECC.

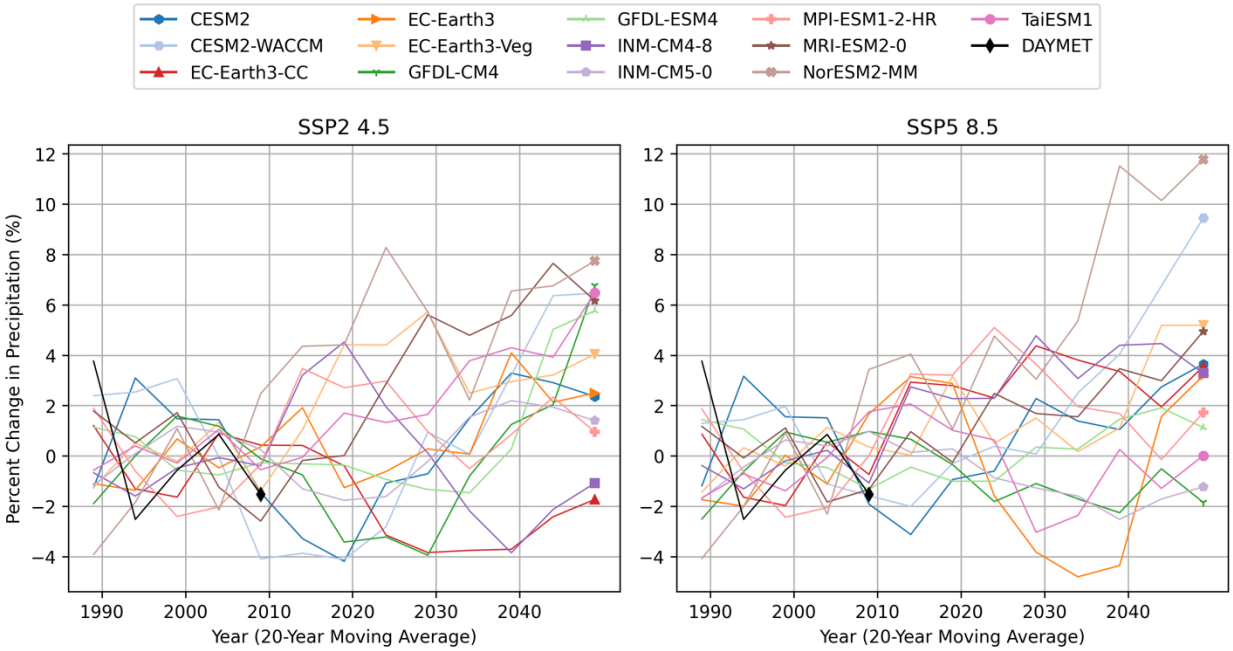

Figure 59. Comparison of GCM trends in changes to daily average precipitation for WECC.

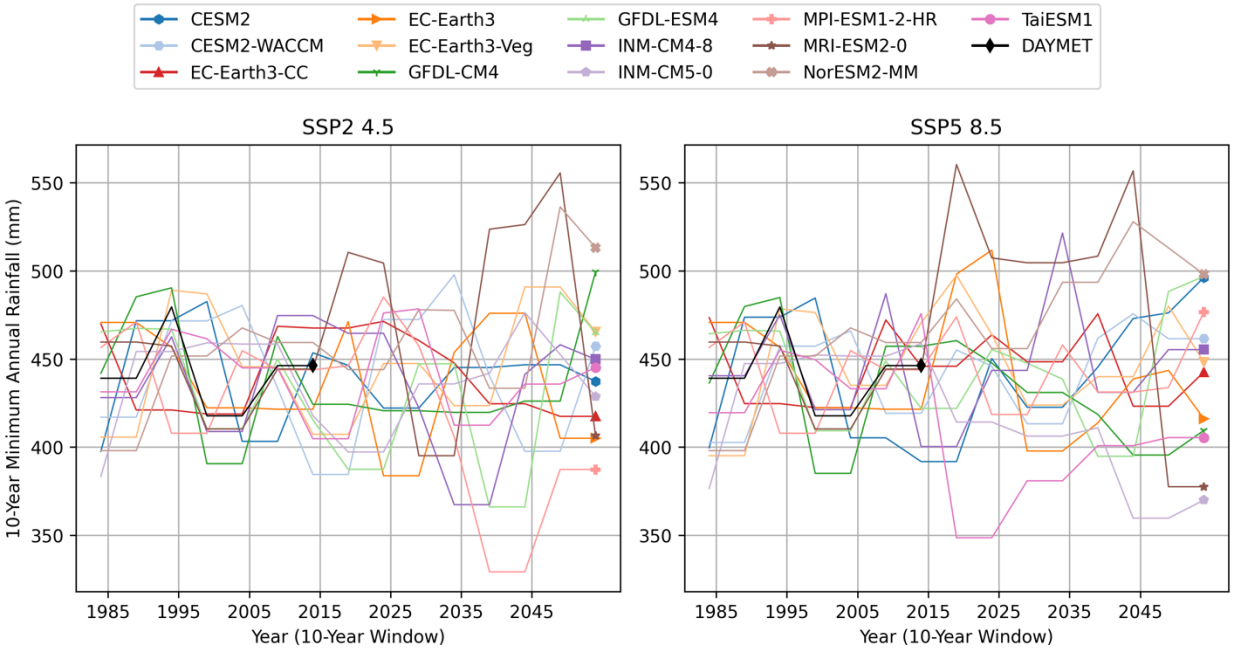

Figure 60. Comparison of GCM minimum annual rainfalls for WECC.

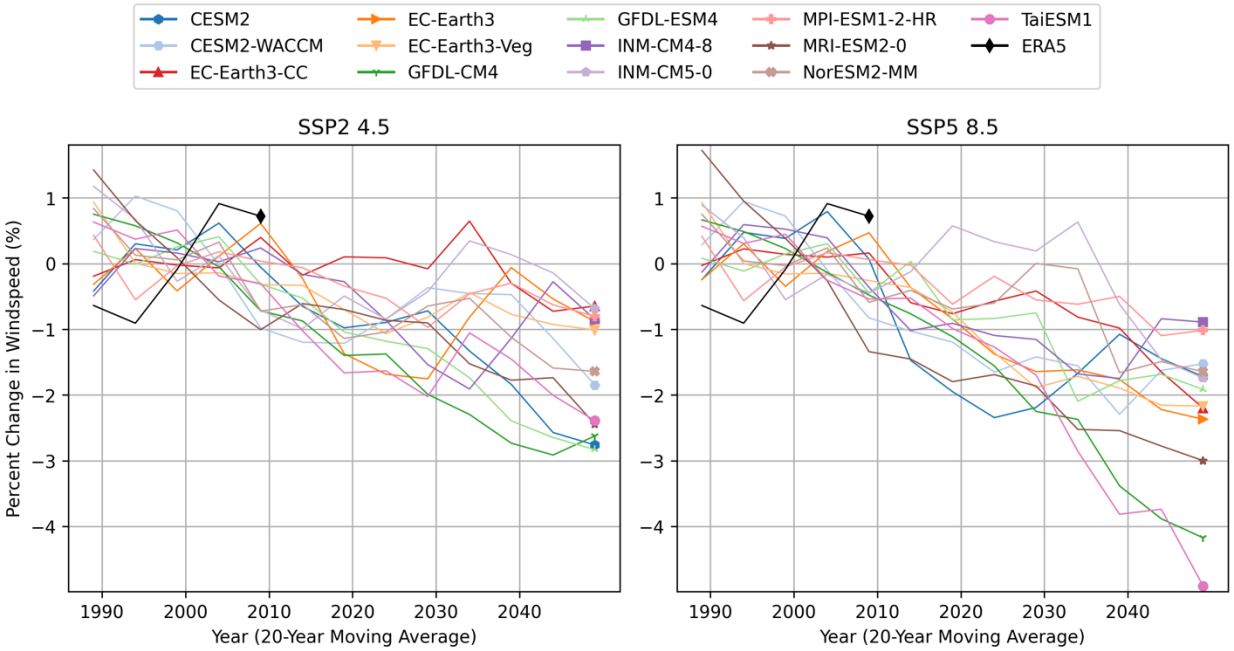

Figure 61. Comparison of GCM trends in changes to daily average 100-meter windspeed for WECC.

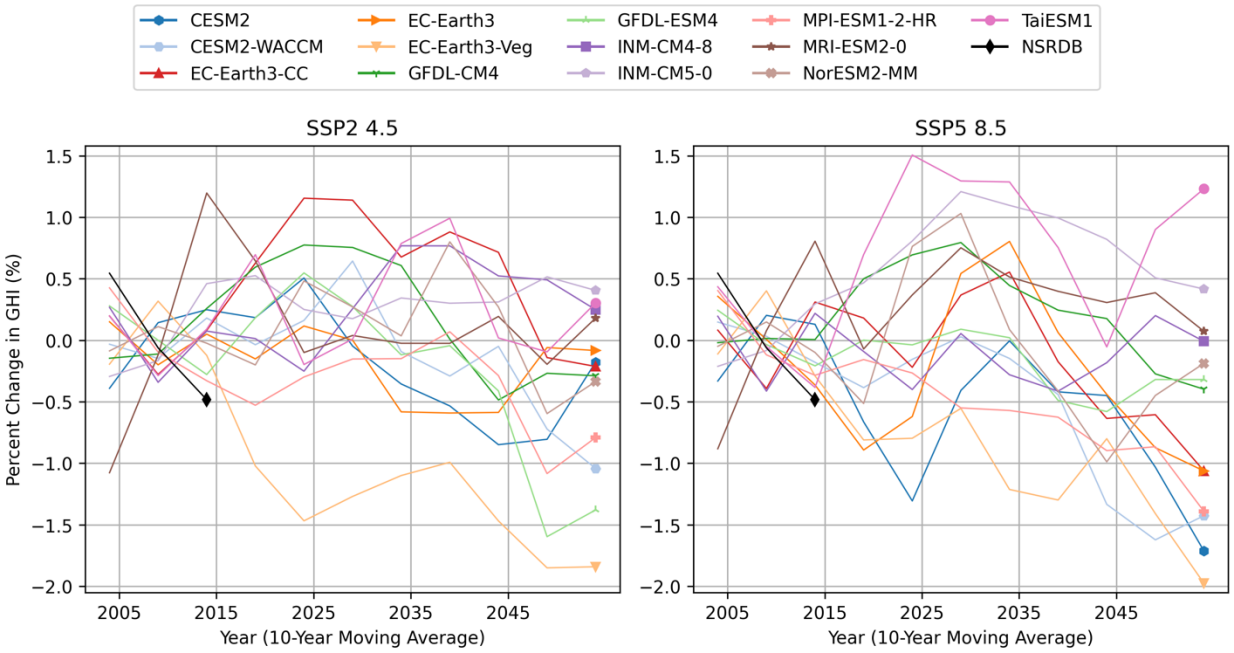

Figure 62. Comparison of GCM trends in changes to daily average GHI for WECC.

Appendix G. Offshore Wind Region: Atlantic

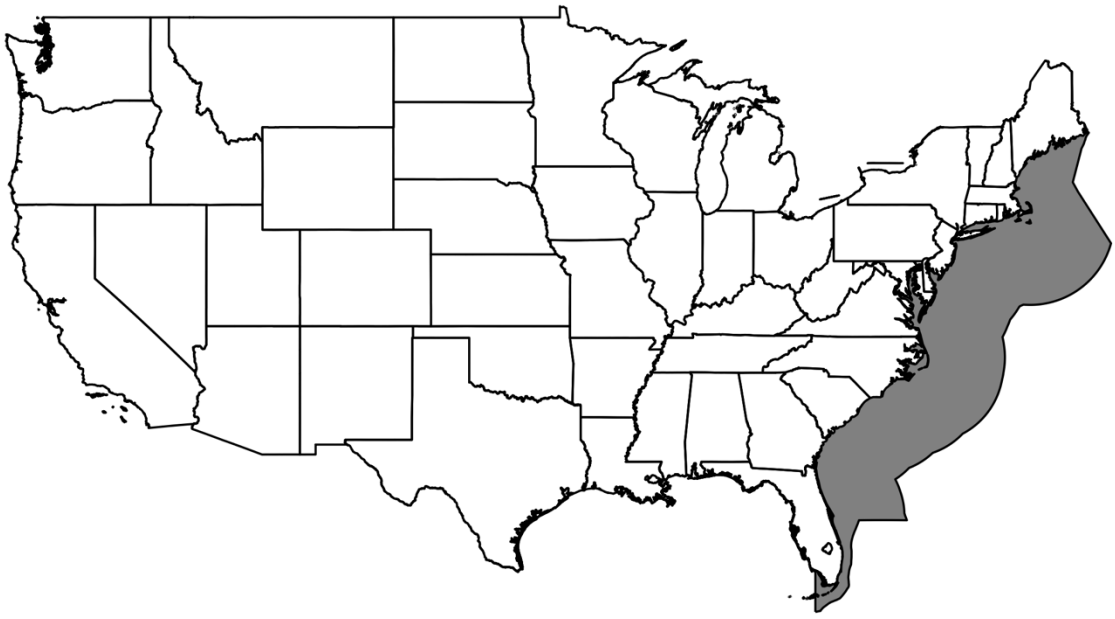

Figure 63. Offshore Wind Region: Atlantic (included area shaded in grey).

Table 10. Summary of historical GCM skill using KS statistic and bias metrics for the Atlantic Offshore Region. Values for a given metric in each row are ranked from best to worst historical skill (dark blue to dark red).

	TaiESM1	EC-Earth3	NorESM2-MM	CESM2	MPI-ESM1-2-HR	CESM2-WACCM	EC-Earth3-Veg	EC-Earth3-CC	MRI-ESM2-0	GFDL-ESM4	GFDL-CM4	INM-CM5-0	INM-CM4-8
T2M KS	0.05	0.09	0.07	0.06	0.07	0.06	0.09	0.09	0.07	0.12	0.11	0.12	0.12
T2M Bias P50 (°C)	0.50	0.71	-0.29	0.90	-0.29	1.05	0.79	1.18	1.57	0.20	0.06	-0.01	-0.75
T2M Max KS	0.05	0.09	0.08	0.09	0.08	0.06	0.09	0.10	0.08	0.12	0.11	0.13	0.13
T2M Max Bias P95 (°C)	0.09	2.22	0.14	0.30	0.10	0.65	2.40	2.87	2.54	2.02	1.65	2.11	1.26
T2M Min KS	0.05	0.09	0.07	0.08	0.07	0.08	0.09	0.09	0.06	0.12	0.10	0.10	0.10
T2M Min Bias P5 (°C)	0.05	-0.09	-0.56	0.31	-1.65	1.99	0.27	0.65	2.06	-0.96	-1.27	-0.55	-1.28
RH2M KS	0.07	0.04	0.12	0.10	0.11	0.10	0.04	0.05	0.07	0.06	0.07	0.18	0.20
RH2M Bias P50 (%)	0.70	-1.42	1.08	2.54	0.96	2.44	-1.12	-1.17	1.74	0.35	-0.64	-1.94	-1.83
RH2M Max KS		0.05			0.15		0.04	0.04	0.09		0.10	0.21	0.23
RH2M Max Bias P95 (%)		-0.43			7.10		-0.49	-0.56	3.87		2.13	5.60	5.64
RH2M Min KS		0.05			0.10		0.04	0.05	0.07		0.06	0.18	0.20
RH2M Min Bias P5 (%)		-0.5			-8.6		-0.2	0.7	-0.5		-5.2	-26.1	-29.3
PR KS	0.08	0.05	0.08	0.08	0.07	0.08	0.05	0.05	0.06	0.07	0.07	0.08	0.09
PR Bias P50 (%)	-5.62	-1.81	-4.52	-4.14	-5.72	-4.12	-1.85	-1.84	-3.30	-3.08	-5.08	-4.02	-4.74
GHI KS	0.04	0.05	0.04	0.04	0.06	0.04	0.06	0.05	0.06	0.06	0.07	0.07	0.07
GHI Bias P50 (%)	-1.7	16.0	7.2	2.1	8.0	4.0	16.5	15.7	9.4	11.3	13.9	8.2	13.2
WS 100m KS	0.06	0.03	0.04	0.05	0.05	0.05	0.09	0.09	0.04	0.09	0.10	0.13	0.13
WS 100m Bias P50 (%)	-1.8	-7.2	-2.3	-3.5	0.7	-2.6	23.7	21.9	-14.1	23.9	28.1	-28.6	-25.6
Process Skill	0.29	0.06	0.04	0.20	0.09	0.16	0.06	0.05	0.34	0.14	0.06	0.82	0.85

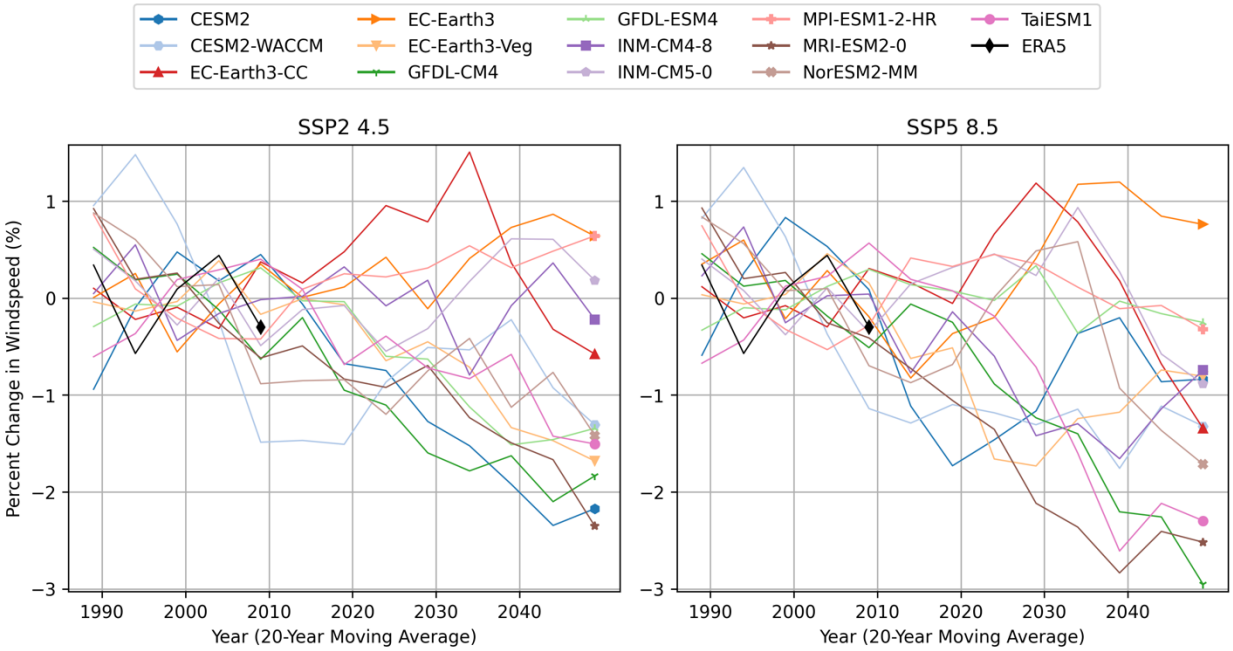

Figure 64. Comparison of GCM trends in changes to daily average 100-meter windspeed for the Atlantic Offshore Region.

Appendix H. Offshore Wind Region: Gulf

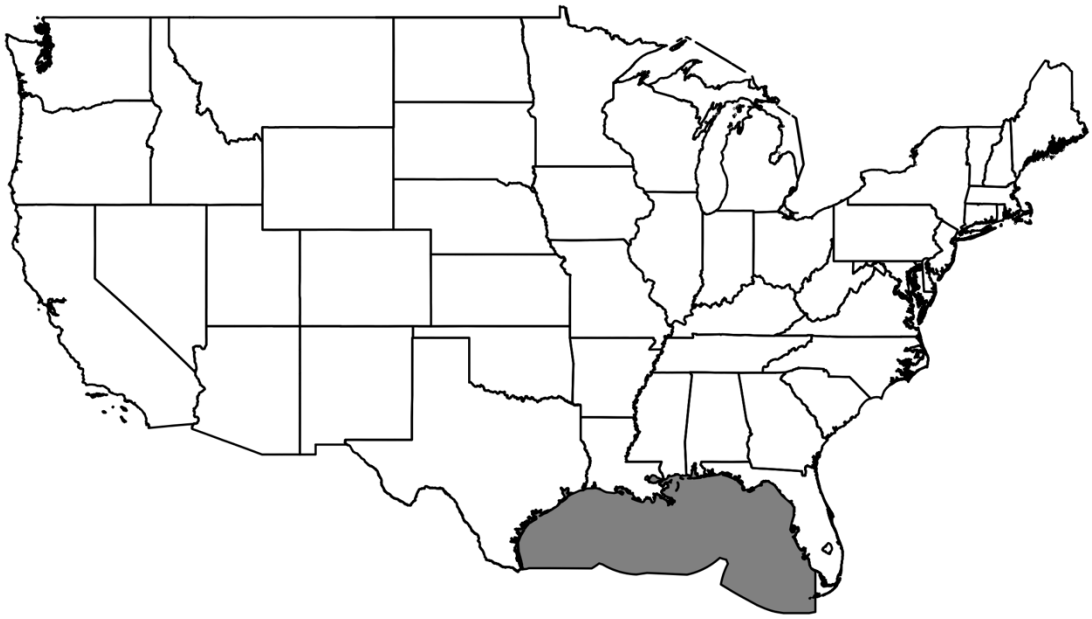

Figure 65. Offshore Wind Region: Gulf (included area shaded in grey).

Table 11. Summary of historical GCM skill using KS statistic and bias metrics for the Gulf Offshore Region. Values for a given metric in each row are ranked from best to worst historical skill (dark blue to dark red).

	EC-Earth3	EC-Earth3-Veg	NorESM2-MM	CESM2-WACCM	EC-Earth3-CC	CESM2	TaiESM1	MPI-ESM1-2-HR	MRI-ESM2-0	GFDL-CM4	GFDL-ESM4	INM-CM5-0	INM-CM4-8
T2M KS	0.05	0.04	0.03	0.05	0.05	0.05	0.04	0.08	0.12	0.13	0.12	0.18	0.16
T2M Bias P50 (°C)	-0.44	-0.30	0.53	1.05	-0.31	1.07	0.51	0.42	-0.49	-1.09	-0.60	-0.57	-0.43
T2M Max KS	0.05	0.04	0.04	0.06	0.05	0.06	0.05	0.08	0.11	0.11	0.08	0.18	0.16
T2M Max Bias P95 (°C)	-0.14	-0.13	0.43	-0.18	0.07	0.70	0.56	1.21	0.62	0.06	0.07	-2.03	-1.82
T2M Min KS	0.05	0.04	0.04	0.10	0.04	0.07	0.05	0.09	0.12	0.15	0.14	0.16	0.15
T2M Min Bias P5 (°C)	-1.28	-0.95	0.08	3.09	-0.90	1.10	0.82	0.03	-0.16	-2.09	-2.00	0.88	0.85
RH2M KS	0.05	0.04	0.05	0.05	0.05	0.05	0.06	0.10	0.09	0.09	0.10	0.07	0.07
RH2M Bias P50 (%)	-0.08	-0.17	-2.53	0.33	-0.21	0.10	-2.54	-8.71	2.03	-1.08	-0.26	-1.32	-1.10
RH2M Max KS	0.05	0.05			0.06			0.14	0.12	0.10		0.09	0.08
RH2M Max Bias P95 (%)	0.53	0.41			0.37			1.45	4.26	3.03		4.03	3.39
RH2M Min KS	0.06	0.05			0.06			0.05	0.07	0.06		0.10	0.11
RH2M Min Bias P5 (%)	4.91	4.73			4.77			-9.10	6.82	3.63		#####	#####
PR KS	0.07	0.07	0.08	0.08	0.07	0.08	0.09	0.08	0.06	0.08	0.08	0.12	0.12
PR Bias P50 (%)	0.06	0.06	0.78	1.36	0.07	1.19	1.68	0.01	0.39	0.40	0.54	9.33	9.92
GHI KS	0.03	0.03	0.05	0.04	0.03	0.04	0.04	0.04	0.03	0.04	0.04	0.04	0.05
GHI Bias P50 (%)	-3.62	-3.00	2.00	0.14	-3.90	2.28	-1.84	0.87	5.92	-2.88	-4.39	1.78	4.45
WS 100m KS	0.04	0.11	0.04	0.04	0.11	0.04	0.03	0.05	0.04	0.13	0.15	0.03	0.03
WS 100m Bias P50 (%)	-4.6	28.4	-2.0	-3.2	28.1	-3.0	-9.8	7.3	-14.1	36.0	42.7	-9.0	-11.1
Process Skill	0.06	0.06	0.04	0.16	0.05	0.20	0.29	0.09	0.34	0.06	0.14	0.82	0.85

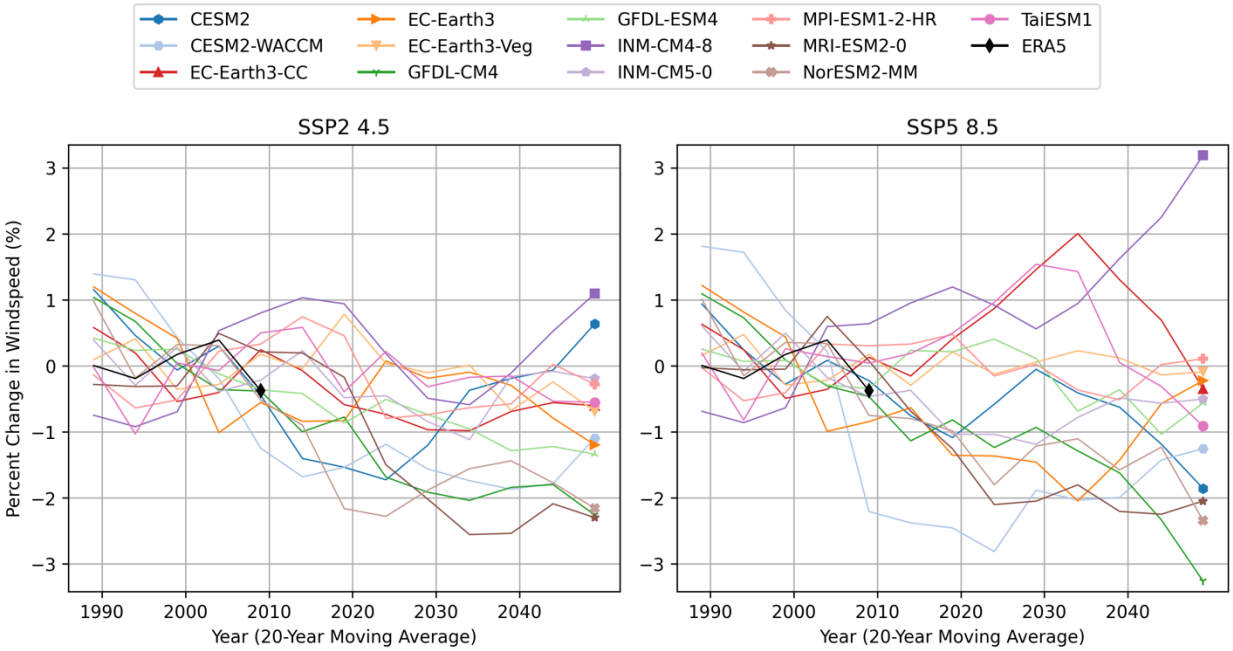

Figure 66. Comparison of GCM trends in changes to daily average 100-meter windspeed for the Gulf Offshore Region.

Appendix I. Offshore Wind Region: Pacific

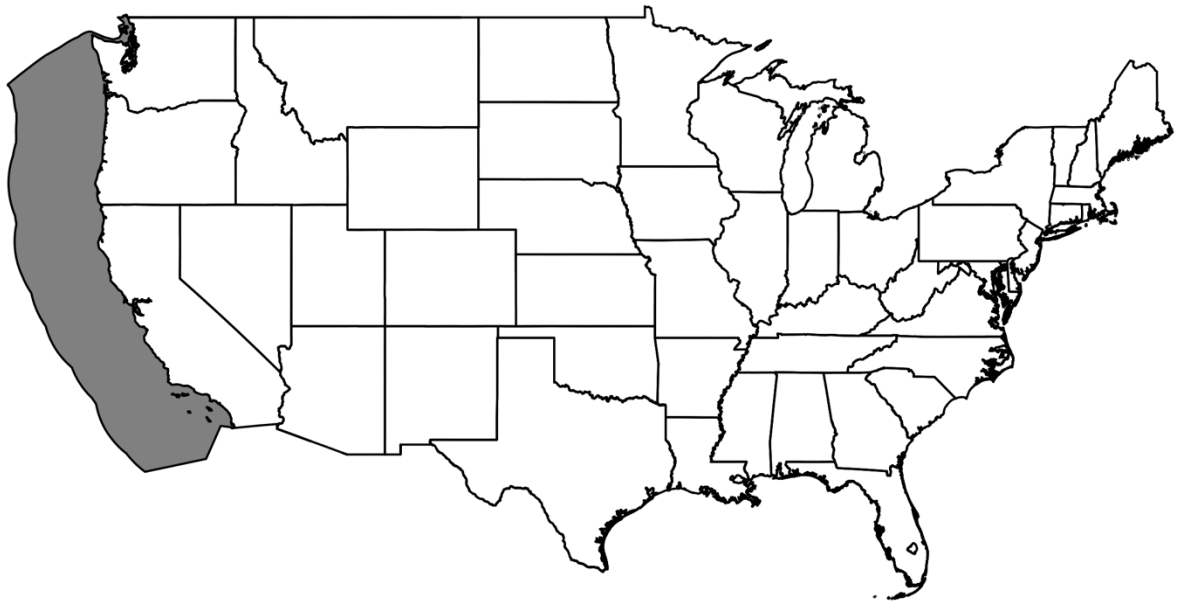

Figure 67. Offshore Wind Region: Pacific (included area shaded in grey).

Table 12. Summary of historical GCM skill using KS statistic and bias metrics for the Pacific Offshore Region. Values for a given metric in each row are ranked from best to worst historical skill (dark blue to dark red).

	EC-Earth3	MPI-ESM1-2-HR	NorESM2-MM	CESM2	EC-Earth3-Veg	EC-Earth3-CC	CESM2-WACCM	GFDL-CM4	TaiESM1	MRI-ESM2-0	GFDL-ESM4	INM-CM5-0	INM-CM4-8
T2M KS	0.05	0.06	0.04	0.05	0.05	0.05	0.05	0.07	0.07	0.06	0.08	0.10	0.11
T2M Bias P50 (°C)	0.85	0.76	1.65	2.66	1.08	1.17	2.68	-0.87	2.89	0.31	-0.44	0.60	1.57
T2M Max KS	0.05	0.05	0.05	0.06	0.05	0.05	0.06	0.06	0.07	0.05	0.07	0.11	0.12
T2M Max Bias P95 (°C)	0.37	0.92	1.53	1.80	0.59	0.82	1.11	-0.54	1.67	0.81	0.07	-1.15	-0.53
T2M Min KS	0.06	0.06	0.04	0.06	0.06	0.05	0.10	0.08	0.06	0.06	0.08	0.09	0.11
T2M Min Bias P5 (°C)	0.56	0.62	0.27	2.74	1.12	1.25	4.75	-2.14	2.03	0.06	-1.44	1.72	2.83
RH2M KS	0.04	0.09	0.05	0.05	0.04	0.04	0.05	0.07	0.07	0.11	0.10	0.09	0.09
RH2M Bias P50 (%)	-2.00	-4.92	-3.58	-1.45	-1.99	-1.86	-1.00	1.74	-3.79	4.64	2.90	-0.44	-0.01
RH2M Max KS	0.07	0.12			0.08	0.08		0.09		0.13		0.15	0.14
RH2M Max Bias P95 (%)	-0.21	1.56			-0.24	-0.21		4.04		5.80		5.20	4.77
RH2M Min KS	0.07	0.08			0.06	0.06		0.06		0.10		0.10	0.10
RH2M Min Bias P5 (%)	3.2	-3.6			3.3	3.4		2.9		10.6		-17.2	-16.3
PR KS	0.08	0.06	0.08	0.10	0.08	0.08	0.10	0.07	0.10	0.07	0.08	0.12	0.13
PR Bias P50 (%)	0.29	0.22	1.11	1.65	0.29	0.32	1.74	1.46	1.76	1.42	1.90	11.43	12.43
GHI KS	0.03	0.03	0.04	0.04	0.03	0.03	0.04	0.03	0.04	0.04	0.03	0.04	0.04
GHI Bias P50 (%)	-5.43	-1.81	3.65	-0.05	-4.90	-5.06	-0.99	-2.20	0.04	7.11	-4.64	9.15	12.11
WS 100m KS	0.04	0.06	0.04	0.06	0.13	0.13	0.06	0.11	0.04	0.03	0.12	0.04	0.04
WS 100m Bias P50 (%)	-3.2	1.3	-2.9	0.7	29.1	29.9	0.7	27.5	-4.1	-8.7	31.6	-7.5	-8.0
Process Skill	0.06	0.09	0.04	0.20	0.06	0.05	0.16	0.06	0.29	0.34	0.14	0.82	0.85

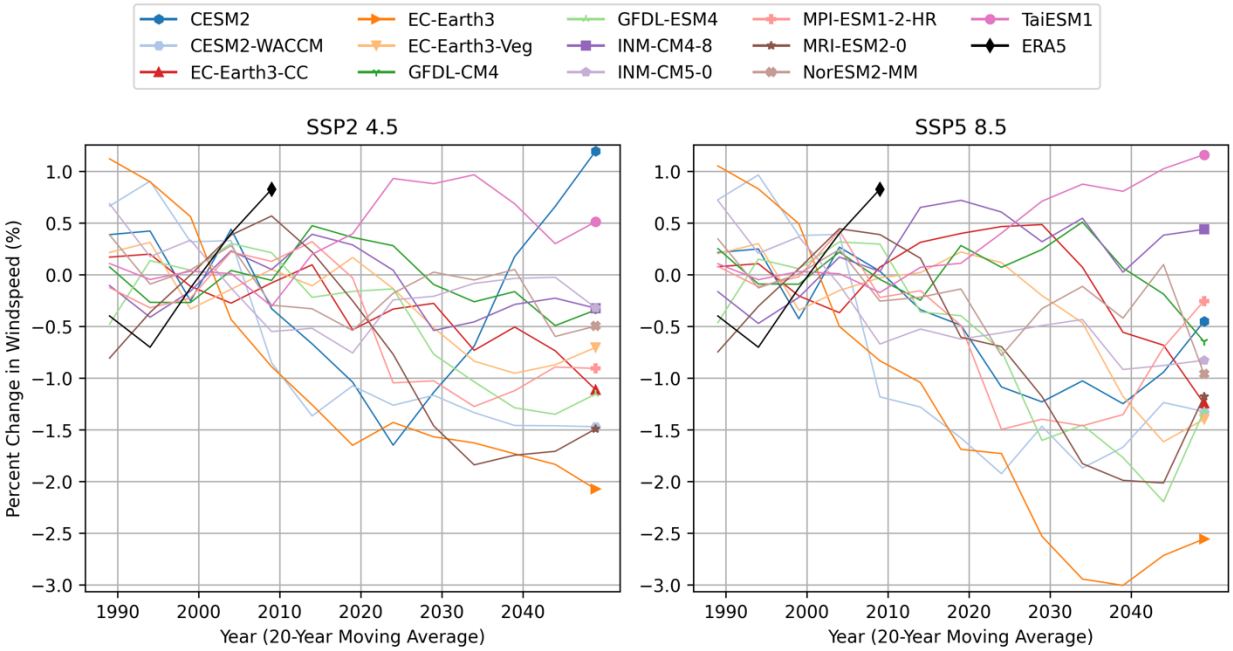

Figure 68. Comparison of GCM trends in changes to daily average 100-meter windspeed for the Pacific Offshore Region.